EXPLOITING BACTERIAL LYSIS FOR TUBERCULOSIS DRUG TARGET VALIDATION AND VACCINE DEVELOPMENT

A Dissertation

Presented to the Faculty of the Weill Cornell Graduate School

of Medical Sciences

in Partial Fulfillment of the Requirements for the Degree of

Doctor of Philosophy

by
Kan Lin
January 2018

EXPLOITING BACTERIAL LYSIS FOR TUBERCULOSIS DRUG TARGET VALIDATION AND VACCINE DEVELOPMENT

Kan Lin, Ph.D.

Cornell University 2018

Mycobacterium tuberculosis (*Mtb*) must cope with exogenous oxidative stress imposed by the host. Unlike other antioxidant enzymes, *Mtb's* thioredoxin reductase TrxB2 has been predicted to be essential not only to fight host defenses but also for *in vitro* growth. However, the specific physiological role of TrxB2 and its importance for *Mtb* pathogenesis remain undefined. Here we show that genetic inactivation of thioredoxin reductase perturbed several growth-essential processes, including sulfur and DNA metabolism and rapidly killed and lysed *Mtb*. Death was due to cidal thiol-specific oxidizing stress and prevented by a disulfide reductant. In contrast, thioredoxin reductase deficiency did not significantly increase susceptibility to oxidative and nitrosative stress. *In vivo* targeting TrxB2 eradicated *Mtb* during both acute and chronic phases of mouse infection. Deliberately leaky knockdown mutants identified the specificity of TrxB2 inhibitors and showed that partial inactivation of TrxB2 increased *Mtb's* susceptibility to rifampicin. We also screened a library of 11,000 compounds with leaky knockdown mutants and identified SKF867J as a potential novel TrxB2-specific inhibitor. These studies reveal TrxB2 as an essential thiol-reducing enzyme in *Mtb in vitro* and during infection, establish the value of targeting TrxB2, and provide tools to accelerate the development of TrxB2 inhibitors.

Ultimate control of *Mtb* is not achievable without effective vaccines. The most widely used tuberculosis (TB) vaccine, the Bacillus Calmette–Guérin (BCG) vaccine, does not provide effective protection against pulmonary TB. Current failures in TB vaccine development can be attributed in part to the lack of important virulence factors required to mediate protection in BCG-based vaccine candidates and insufficient antigen presentation at the site of infection. To overcome these limitations, we generated a novel *Mtb*-based vaccine candidate for proof-of-concept experiments, in which bacterial lysis is achieved by inducible expression of cell wall hydrolyzing enzymes, mycobacteriophage lysins. We found that lysin induction caused lytic death in both replicating and non-replicating *Mtb*. Inducible lysis restricted *Mtb* growth inside macrophages and enhanced the production of pro-inflammatory cytokines, possibly due to the release of intracellular bacterial antigens. Moreover, lysin induction impaired *Mtb* viability during mouse infection. We are now performing re-challenge experiments to determine the efficacy of the vaccine candidate against subsequent *Mtb* infection. Efforts are also underway to identify the immunological pathways activated by lysed bacteria and the bacterial components activating these pathways. In addition, we analyzed the sequences of 26 escape mutants of inducible lysis strains and showed that the tet repressor sequence is most frequently mutated. We are now designing new strains that combine other independent killing mechanisms to decrease the suppressor frequency.

BIOGRAPHICAL SKETCH

Kan Lin was born on July 27, 1987 in Quanzhou, Fujian Province, China. He spent his childhood in the army in Fuzhou, Fujian Province, where his parents served as military officers. He left the camp with his parents in 1993 when they decided to switch their careers to finance. He was happy with the move, because he thought his sleep wouldn't be interrupted by the army horn every morning any more. However, he still had to wake up early everyday in spite of no army horn, as his formal school years started. After graduating from Fuzhou No. 1 Middle School in 2005, he studied at Sun Yat-sen University in Guangzhou, China, where he majored in biochemistry and minored in finance. For the first three years in college, he spent much time in extracurricular activities and finance, barely had any lab experience and couldn't imagine himself as a scientist in the future. His formal exposure to the lab didn't start until the summer of 2008, when he attended the summer training program at the National Institute of Biological Sciences, Beijing (NIBS). During that summer, he worked with Dr. Wenhui Li on some very simple and basic molecular cloning of Hepatitis B virus (HBV), but was immediately obsessed by the charms of science and Dr. Li's personality. At the end of that summer, he chose to conduct his undergraduate thesis with Dr. Li and then worked for two years as a research technician in Dr.Li's lab on the pathogenesis of HBV and *Chlamydia*. Thanks to Dr. Li's mentorship, Kan decided to go abroad for his Ph.D. training and began his studies in the Immunology and Microbial Pathogenesis program at Weill Cornell in September 2011. He joined Dr. Sabine Ehrt's lab in the summer of 2012, pursuing his Ph.D. in tuberculosis pathogenesis and host defense.

To my grandparents

Yulin Lin and Xiuying Lin

and

parents

Ying Lin and Caifeng Huang

ACKNOWLEDGEMENTS

First and foremost, my immense gratitude is owed to my thesis advisor Sabine Ehrt. To me, her mentorship has gone far beyond that of a scientific advisor, but a trusted senior and friend who you can seek for advice on almost everything. She always encourages me to be courageous, challenge myself and reach my highest potential. She has the magic to resolve my worries with her optimism and make me energized and motivated at the end of our weekly meetings. I am also highly grateful to my co-mentor, Dirk Schnappinger, for teaching me how to critically evaluate data and tactically plan every step of the projects. The scientific rigor, strategic thinking and management skills I learnt from them will stay with me wherever I go.

I would like to acknowledge my committee members Carl Nathan and Lionel Ivashkiv for their feedback and guidance over the years. They have been great role models for me and motivated me to be better myself, with their amazing breadth of knowledge, deep scientific insight and generosity. I want to thank Aihao Ding, who attracted me to join Weill Cornell, for her encouragement and sharing her life wisdom with me. I also would like to thank my previous mentor Wenhui Li for giving me a memorable lab summer, which marked the beginning of my scientific career, and his continued guidance in the subsequent years.

Many people have contributed directly to the thesis projects presented here- Carolina Trujillo for starting the TrxB2 project; Kathryn M. O'Brien for developing the deliberately leaky expression system; Ruojun Wang for microscope analysis; Shipra Grover for TrxB2 inhibitor screening; Jennifer

McConnell, Xiuju Jiang and Natalia Betancourt for assistance with animal experiments; Joshua Wallach for constructing lysin vaccine strains and escape mutant sequencing. Thank you to Meredith Wright, Li Zhang, Weizhen Xu, Uday Ganapathy and Shipra Grover for proofreading my thesis.

I am indebted to the past and current members of Ehrt/ Schnappinger joint lab, who create such a pleasant and friendly lab environment. My special thanks go to Carolina Trujillo, who has mentored me and backed me up since my rotation. I am thankful to every member in the Nathan, Rhee and Fitzgerald labs on the BRB 11th floor for helpful weekly discussions, which provided constructive feedback on my work. I want to thank Gang Lin and Ruslana Bryk in particular for being my advisors on chemistry and biochemistry.

I am grateful to be surrounded by many wonderful friends during these years. I especially would like to thank my fellow Ehrt Lab students Uday Ganapathy, Susan Puckett, Weizhen Xu, Ruojun Wang and Meredith Wright for their accompany and moral support. I would like to thank my friend and previous roommate Pai-tseng Kuo, who left the graduate school to pursue the truth in Buddhism, for his encouragement, trust and tolerance of me. I also want to thank the fellow IMP students in my year and all my fellow students in the Chinese community for their friendship.

Finally, I would like to thank my family in China, especially my grandparents and parents, for their unconditional love. They always support my dream, even when that dream involved their only grandson or son moving halfway across the world from them. And I am highly fortunate to marry an amazing woman Mei Song and thank Mei for sharing her life with me.

TABLE OF CONTENTS

LIST OF FIGURES

LIST OF ABBREVIATIONS

atc	anhydrotetracycline
BCG	Bacillus Calmette-Guérin
BMDM	bone marrow-derived macrophages
CCL5	Chemokine (C-C motif) ligand 5
CFU	colony-forming unit
dexa	dexamethasone
doxy	doxycycline
DUC	dual control
ELISA	enzyme-linked immunosorbent assay
IFN-γ	interferon gamma
iNOS	inducible nitric oxide synthase
INH	isoniazid
KO	knockout
MIC	minimal inhibitory concentration
MDR-TB	multidrug-resistant TB
MOI	multiplicity of infection

M. smegmatis	*Mycobacterium smegmatis*
Mtb	*Mycobacterium tuberculosis*
MyD88	myeloid differentiation primary response gene 88
NADPH	nicotinamide adenine dinucleotide phosphate
NO	nitric oxide
OD	optical density
PBS	phosphate-buffered saline
PZA	pyrazinamide
RIF	rifampin
RNI	reactive nitrogen intermediates
ROS	reactive oxygen species
SOD	superoxide dismutases
TB	tuberculosis
TrxR	thioredoxin reductase
TLR	Toll-like receptors
wt	wildtype
VBNC	viable but non-culturable
XDR-TB	extensively drug-resistant TB

CHAPTER 1

1.1. Tuberculosis: Old problem and new challenge

1.1.1. A historical and global prospective of Tuberculosis

Tuberculosis (TB) is an airborne infectious disease caused by the intracellular pathogen *Mycobacterium tuberculosis* (*Mtb*). Although it primarily affects the lung, *Mtb* can cause infection throughout the body, such as the bones and the brain. The most common symptoms of active pulmonary TB include persistent cough, chest pains, weight loss, fever and night sweats (Pai et al., 2016) .

TB is an ancient scourge. *Mtb* DNA has been recovered from the lung lesions of Egyptian (200 B.C.) and pre-Columbian Peruvian (1000 A.D.) mummies (Nerlich et al., 1997; Salo et al., 1994). *Mtb* has killed more people than any other single infectious agent in history. It is believed to be responsible for 20% of the total adult death in Europe and North America between 17th and 19th centuries (Comas et al., 2013; Daniel, 2006; Wilson, 2005). The dawn of fighting TB came when Robert Koch identified *Mtb* as the causative agent of TB in 1882 and enabled later studies to look for anti-TB therapies. With the discovery of streptomycin in 1944 and isoniazid in 1952, the modern era of tuberculosis treatment began. Soon after, several other important anti-TB compounds were discovered, including pyrazinamide (1954), rifampicin (1963) and ethambutol (1961), which form the cornerstone of current TB treatment. Combination therapy was introduced soon after to overcome single drug resistant TB. Multidrug chemotherapy marked one of the greatest achievements in treating TB – for the first time, TB became a curable disease. Even Dr. Selman Waksman, the Nobel laureate known for his discovery of

streptomycin, wrote optimistically during the golden age of antibiotic discovery in 1964 that ‘the complete eradication of the disease is in sight’ (Waksman, 1964).

Despite effective chemotherapies for drug-sensitive *Mtb*, TB remains one of the top 10 causes of death worldwide. In 2015, 1.8 million people died from the disease, including 0.4 million co-infected by HIV. In fact, TB is a leading killer of HIV patients, accounting for 35% of HIV-related death. Currently, the worldwide rate of TB incidence declined by 1.5% annually, far from what is required to achieve WHO’s goal of TB eradication in 2030 (World Health Organization, 2016). Both socioeconomic and scientific factors contribute to the slow progress in TB control. Among the later, the limitation of current TB therapy and the emergence of drug-resistant *Mtb* have been two major barriers to eradicating TB.

1.1.2. Challenges of current TB chemotherapy

The current regimen for treating active, drug-sensitive TB consists of a combination of isoniazid, rifampicin, pyrazinamide and ethambutol for two months followed by four months with isoniazid and rifampicin alone. Individuals with latent TB who have a higher risk of developing active TB (e.g., people who are HIV positive, individuals living in areas with a higher TB prevalence) are recommended for preventive therapies, which usually consist of months of isoniazid or rifampicin treatment. While the long duration of combination chemotherapies is critical to ensure the clearance of both active and latent TB, it also results in significant side-effects. As many as 23% patients have to terminate medication due to side-effects and up to 86% of

patients may develop medication side-effects when treated with second-line drugs (Leimane et al., 2005; Schaberg et al., 1996). It is therefore not surprising to observe poor adherence to treatment in TB patients, which in turns leads to drug-resistant bacteria.

Multidrug-resistant TB (MDR-TB) has been reported in almost every country surveyed (World Health Organization, 2016). MDR-TB is defined as resistance to at least isoniazid and rifampicin, the two most powerful, first-line anti-TB drugs. Appropriately 480,000 people developed MDR-TB in 2015. MDR-TB is still treatable with second-line anti-TB drugs, but the treatment can take up to two years and comes with severe side-effects as mentioned above. In some cases, extensively drug-resistant TB (XDR-TB), an even more severe form of drug-resistant TB, can develop. XDR-TB is resistant to isoniazid and rifampicin, plus any fluoroquinolone, and at least one of three second-line injectable drugs (capreomycin, kanamycin and amikacin). XDR-TB accounts for about 9.5% of MDR-TB cases in 2015. Very few treatment options are available for XDR-TB patients, resulting in a high mortality rate. Although XDR-TB is considered to be rare, 117 countries worldwide had reported at least one case by the end of 2015. Overall, only 52% of MDR-TB patients and 28% of XDR-TB worldwide are successfully treated (World Health Organization, 2016).

The long duration and side-effects of current chemotherapies impede rigorous patient adherence and lead to the development of drug resistance. The high TB prevalence and worldwide emergence of drug-resistant *Mtb* strains necessitate the development of new anti-TB drugs with better efficacy and fewer side-effects. Ideally, they should target previously unexploited pathways and have the potential to overcome drug resistance. Other desired features

include lower dosing frequency, minimal drug-drug interactions, and synergy with current regimens to shorten the treatment duration (Koul et al., 2011). With new molecular biology and genetic tools becoming available, much effort has been devoted to new target discovery. Recently, several pathways have been characterized as possible drug targets, including the respiratory chain, cell wall metabolism, protein processing and antioxidant pathways (Lamichhane, 2011; Lu et al., 2013). In light of the time and cost of finding new compounds with novel targets, exploring new applications for existing drugs (repurposing) has gained increasing interest. For example, the leprosy drug clofazimine is now being tested for treating MDR-TB in small-scale clinical trials (Tang et al., 2015; Zumla et al., 2013).

1.2. *Mtb* and oxidative stress

1.2.1. Oxidative stress as a host defense mechanism

The primary type of host cell encountered by *Mtb* in the lung is the alveolar macrophage, although *Mtb* can infect neutrophils, monocytes and dendritic cells (DCs) as well. These innate immune cells, in particular macrophages and neutrophils, engulf pathogens, induce inflammation and clear infection. One of the preeminent mechanisms to eradicate *Mtb* is the production of reactive oxygen species (ROS) and reactive nitrogen intermediates (RNI) (Bhat et al., 2012; Kumar et al., 2011; Trivedi et al., 2012).

The ROS, including superoxide, hydrogen peroxide, and the hydroxyl radical, are generated by a series of enzymatic reactions. NADPH oxidase (NOX2) is a membrane-bound multiprotein enzyme complex found in both the plasma membrane and the membranes of phagosomes. NADPH oxidase generates superoxide by extracting electrons from NADPH and transferring them to

molecular oxygen. Superoxide can be converted by dismutase to hydrogen peroxide, which leads to the generation of other ROS, such as hypochlorite and hydroxyl radicals. The ROS generated by these host enzymes cast devastating effects on pathogens by destroying microbial iron-dependent enzymes, lipids and DNA (Imlay, 2013). Besides direct antimycobacterial activity, ROS may mediate the activation of inflammatory responses in macrophages. For example, NOX2 interaction with TLR2 is required for the expression of an antimicrobial peptide cathelicidin upon *Mtb* infection (Yang et al., 2009). Patients with germline mutations in phagocyte NADPH oxidase are predisposed to mycobacterial diseases (Bustamante et al., 2011). In contrast, *Mtb* is relatively resistant to ROS-mediated killing *in vitro* and mice lacking NADPH oxidase subunits are only slightly susceptible to *Mtb* infection (Chan et al., 1992; Cooper et al., 2000; Jung et al., 2002). The discrepancy may reflect the different reliance of mouse and human immune systems on this pathway. Nevertheless, the human genetics data clearly indicates that the respiratory burst in human macrophages is a crucial protective mechanism against *Mtb*. Additionally, *Mtb* catalase–peroxidases (*katG*) mutant is markedly attenuated in wild-type C57Bl/6 mice, and the attenuation of *katG* mutant is reversed in NADPH oxidase deficient mice, indicating that antioxidant defense contributes to virulence of *Mtb* (Ng et al., 2004).

The production of RNI is another important host defense mechanism against *Mtb* (Bhat et al., 2012). Nitric oxide (NO) is formed from the enzymatic action of the nitric oxide synthases 2 (NOS2 or iNOS) using L-arginine as a substrate (Zahrt and Deretic, 2002). NOS2 can produce superoxide under some circumstances, such as when the electron transfer between NAD(P)H in iNOS and arginine becomes ‘uncoupled’. A stepwise oxidation of nitric oxide

with oxygen results in the production of other forms of intermediates, like nitrogen dioxide radical ($^{\bullet}NO_2$) and nitrite (NO_2^-). NO oxidizes cysteine sulfhydryls, generates nitrosothiols and sulfenic acids and destroys iron-sulfur clusters (Nathan and Ding, 2010). The reaction of nitric oxide with superoxide can further generate peroxynitrite ($OONO_2^-$), which is chemically unstable under physiological conditions and can react with all major classes of biomolecules.

Similar to ROS, exposure to RNI damages biomolecules and inhibits *Mtb* growth and survival. It is generally thought that the physiological range of NO generated by the nitric oxide synthases is between 20 nM to 2 μM (Moncada et al., 1991; Patel et al., 1999). Moderate concentrations of NO have bacteriostatic effects on *Mtb in vitro*, although high concentrations of NO can kill *Mtb* (Chan et al., 1992; Firmani and Riley, 2002). The significance of NO in TB pathogenesis in the murine model has been well-documented. Activated murine macrophages produce bactericidal levels of NO that are important for the control of TB (Chan et al., 1992). Mice lacking iNOS succumb to *Mtb* infection much faster than their wild type littermates (MacMicking et al., 1997). Administration of an iNOS inhibitor to *Mtb*-infected mice exerted a similar effect as the genetic deficiency (Chan et al., 1995; MacMicking et al., 1997). NO also possesses immunoregulatory functions; NO controls lung immunopathology by repressing neutrophil recruitment and inhibiting inflammasome activation via thiol nitrosylation (Mishra et al., 2017; Mishra et al., 2013).

In contrast to its widely accepted importance in the murine TB model, the role of NO in human pulmonary TB is less conclusive. This is mainly due to the

lack of appropriate reagents and experimental models, such as an iNOS-expressing human alveolar macrophage cell line or a protocol to isolate precursors for tissue macrophages (Nathan, 2002; Nathan and Barry, 2015). Nevertheless, a significant body of evidence implies a potentially important role of NO in controlling human TB. Active iNOS was detected in the macrophages isolated from active TB patients, but not those from normal subjects (Nicholson et al., 1996). iNOS and nitrotyrosine (a form of tyrosine nitrosated by peroxynitrite) were also found in the granulomas from surgically resected lungs of TB patients (Choi et al., 2002). Patients with impaired pulmonary NO bioavailability are associated with delayed clearance of infection and more severe disease progression (Ralph et al., 2013b). These results have encouraged some groups to consider arginine as an adjuvant to TB chemotherapy, with the intention of promoting NO production. However, the clinical benefits are not conclusive thus far (Ralph et al., 2013a; Schon et al., 2003).

1.2.2. *Mtb* antioxidant machinery

Mtb must cope with endogenous and exogenous oxidative stress to replicate and survive within its host. Not unexpectedly, *Mtb* is armed with a number of dedicated antioxidant systems to ensure replication and survival within its host, including catalase, alkyl hydroperoxidase, superoxide dismutase, mycothiol, ergothioneine, thiol peroxidase, thioredoxin reductase and a recently identified membrane-associated oxidoreductase complex (Bryk et al., 2000; Bryk et al., 2002; Carmel-Harel and Storz, 2000; Dussurget et al., 2001; Jaeger et al., 2004; Nambi et al., 2015; Newton et al., 1996; Ng et al., 2004; Piddington et

al., 2001; Saini et al., 2016). We will discuss some of the notable members here.

Catalase–peroxidases (Kat) are common enzyme systems found in almost all living organisms to detoxify hydrogen peroxide. *Mtb* encodes one catalase, KatG, which also shows peroxynitritase activity (Wengenack et al., 1999). KatG is best known for its role in activating the prodrug isoniazid, one of the most effective anti-TB drugs (Heym et al., 1995; Zhang et al., 1992). Various point mutations as well as missense mutations in KatG can lead to resistance to isoniazid. Although KatG is not required for *Mtb* growth *in vitro*, Δ*katG Mtb* is markedly attenuated in mice due to the reduced ability to withstand oxidative stress (Ng et al., 2004).

Superoxide dismutases (SODs) are metalloproteins that detoxify superoxide radicals. SOD catalyzes the dismutation of the superoxide radical into molecular oxygen or hydrogen peroxide, which is further detoxified by other enzymes like catalases. *Mtb* harbors two SODs, an iron-containing SOD called SodA and a Cu/Zn-containing SOD called SodC. SodA is constitutively expressed by *Mtb* and secreted in a SecA2-depedent manner (Andersen et al., 1991; Braunstein et al., 2003; Zhang et al., 1991). Diminishing SodA expression by the antisense approach confirmed its role in protecting *Mtb* against superoxide *in vitro* (Edwards et al., 2001). This SodA underexpressor is highly attenuated in C57BL/6 mice (Edwards et al., 2001). Deletion of *secA2* also attenuated *Mtb* in SCID and C57BL/6 mice, partially due to reduced secretion of SodA (Braunstein et al., 2003). While *sodC* null mutants are sensitive to killing by superoxides and hydrogen peroxide, there is less unanimity on its contribution to TB pathogenesis. Different results have been

observed depending on the experimental models used (Dussurget et al., 2001; Piddington et al., 2001).

Alkyl hydroperoxides, a highly reactive form of organic peroxides, are generated when peroxide reacts with cellular components, in particular lipids. *Mtb* alkyl hydroperoxide reductase (AhpC), a member of the peroxiredoxin family of nonheme peroxidases, detoxifies the organic peroxide and peroxynitrite to alcohol and nitrite respectively (Chen et al., 1998; Hillas et al., 2000). Mechanistically, AhpC is linked by AhpD to metabolic enzymes Lpd and SucB, forming a four-component antioxidant system (Bryk et al., 2000; Bryk et al., 2002). Consistent with the biochemistry data, genetic inactivation of AhpC increased *Mtb* sensitivity to organic peroxide cumene hydroperoxide, but not to hydrogen peroxide. However, the *ahpC* knockout is not attenuated during mouse infection, suggesting its role in *Mtb* pathogenesis may be redundant (Springer et al., 2001).

The low-molecular-weight thiol thioredoxin and glutathione are produced by living cells to combat disulfide stress and maintain redox hemostasis. Unlike many Gram-negative bacteria, *Mtb* lacks the glutathione system (Newton et al., 1996). Instead, mycothiol has been suggested as substitute for glutathione in actinobacteria, including *Mtb*. Mycothiol consists of an N-acetylcysteine amide conjugated to glucosamine, which is then linked to inositol. *Mtb* contains millimolar quantities of mycothiol in oxidized and reduced forms (Newton et al., 1996). Oxidized mycothiol is reduced by the mycothione reductase using electrons from NADPH. Mycothiol acts as a major buffering system to protect mycobacteria against ROS and RNI (Rawat et al., 2002; Ung and Av-Gay, 2006).

There are five enzymatic steps in mycothiol biosynthesis, catalyzed by MshA1, MshA2, MshB, MshC and MshD respectively. The *mshA* deletion mutants are defective in producing mycothiol and require catalase to grow, but are otherwise normal (Vilcheze et al., 2008). Mycothiol and mycothione reductase have been proposed to be drug targets for developing new antimycobacterial compounds, because this pathway is unique to actinobacteria. However, only MshC is essential in *Mtb*, while deletion of the other mycothiol biosynthesis enzymes have little impact on *Mtb* survival (Buchmeier et al., 2006; Vilcheze et al., 2008). There are two copies of mycothione reductase, *msrA* and *msrB*, neither of which alone is essential. Furthermore, *msh* mutations cause *Mtb* resistance to ethionamide, a second-line drug to treat drug-resistant TB, raising questions about the suitability of mycothiol pathway as a drug target (Vilcheze et al., 2008).

1.2.3. The thioredoxin system in *Mtb* and other bacteria

The thioredoxin system, which is composed of thioredoxin (Trx), thioredoxin reductase (TrxR) and NADPH, represents one of the most important antioxidant systems in almost all living organisms. Thioredoxins are small redox proteins (typically 12 kDa) that catalyze protein disulfide/dithiol exchange through the two active cysteine residues. The reduction of protein targets is accompanied by the formation of oxidized thioredoxin, which will then be reduced by the thioredoxin reductase with electrons extracted from NADPH (Lu and Holmgren, 2014).

Although the thioredoxin system is highly conserved from mammalian cells to bacteria, the mammalian and bacterial TrxRs are vastly different in structures

and catalytic mechanisms. Mammalian TrxRs belong to the high molecular weight TrxR family with 55 kDa for each subunit, while the bacterial TrxRs are of low molecular weight, typically around 35 kDa (Williams et al., 2000). Mammalian TrxRs possess one active site at each terminus of the proteins, which enables them to act on a broad spectrum of substrates, including thioredoxin, protein disulfide isomerase and even small molecules. For example, mammalian TrxRs can directly reduce hydrogen peroxide and act as an antioxidant. In contrast, the low molecular weight TrxRs of bacteria contain only one active site, resulting in narrow substrate specificity. It is generally thought that bacterial TrxRs interact with Trxs and then Trxs provide direct reducing power to other proteins (Lu and Holmgren, 2014).

Most of the knowledge on bacterial TrxR was derived from studies using *E.coli*, a gram-negative bacterium, as a model organism. Most gram-negative bacteria, possess both Trx and glutathione (GSH) systems like mammalian cells. *E.coli* deficient in Trx production become even more resistant to oxidative stress, which may be due to the compensatory upregulation of other antioxidant systems like the GSH system (Ritz et al., 2000). Deleting both Trx and GSH systems in *E.coli* rendered it highly susceptible to thiol-oxidizing stress. The double mutant required supplementation of a disulfide reductant in the medium to grow well aerobically (Prinz et al., 1997). Besides its antioxidant function, another particularly important role of *E.coli* Trx system is to provide reducing power to the ribonucleotide reductase (RNR), which is essential to generate deoxyribonucleotide for DNA biosynthesis (Nordlund and Reichard, 2006).

The GSH system is absent in many gram-positive bacteria and *Mtb*, suggesting that they may completely rely on the Trx system for antioxidant and redox buffering. *Mtb* encodes three copies of thioredoxin, *trxA*, *trxB* and *trxC*. Interestingly, TrxA cannot receive electrons from TrxR and its transcripts are undetectable under different growth conditions, suggesting that only TrxB and TrxC are biologically active Trxs (Akif et al., 2008). *Mtb* also contains other Trx-like proteins, such as ThiX, a hypothetical thioredoxin. In contrast, there is only one copy of TrxR in the *Mtb* genome, encoded by *trxB2*. Purified TrxB2 has been shown to mediate detoxification of hydrogen peroxide, organic peroxide, and dinitrobenzene *in vitro* (Akif et al., 2005; Jaeger et al., 2004; Zhang et al., 1999). Transposon mutagenesis analysis predicted that TrxB2 is essential for *Mtb in vitro* growth, which was confirmed by genetic study using replacement transformation (Harbut et al., 2015; Zhang et al., 2012). Overexpression of Trx and TrxR from virulent mycobacteria enhanced the survival of avirulent *M. smegmatis* in macrophages, suggesting the importance of the thioredoxin system in TB pathogenesis (Wieles et al., 1997). Although TrxR is present in human, the catalytic mechanism of *Mtb* TrxB2 differs greatly from that of mammalian TrxR and enables selective targeting TrxB2. Furthermore, the crystal structure of TrxB2 has been solved (Akif et al., 2005). Therefore, TrxRs may represent valuable drug targets for the development of inhibitors against bacteria lacking a GSH system, including *Mtb*.

1.3. TB vaccine development

1.3.1. A brief overview of TB immunology

It is estimated that one-third of the world's population is infected with *Mtb*, however, the majority are latently infected and remain asymptomatic throughout their lifetime. The likelihood to progress into active disease significantly increases in the HIV-positive population or patients receiving immunosuppressive treatments, highlighting the importance of the immune system in controlling TB. Recent progress in bacterial genetics, immunology, and human genetics has significantly advanced our understanding of TB immunology. However, a large knowledge gap still exists and limits the development of prophylactic and therapeutic interventions for this deadly disease. Here I briefly summarize current knowledge on protective immunity during *Mtb* infection, with a focus on adaptive immune responses and the implications for vaccine development.

TB infection is initiated when patients inhale bacilli-containing droplets coughed by an individual with an active disease. The initial stage of the immune responses is characterized by the recruitment of inflammatory phagocytes, such as resident alveolar macrophages, neutrophils and dendritic cells, which constitute the first-line of defense against *Mtb* infection. Macrophages and neutrophils possess a wide range of antimicrobial mechanisms, such as inducing phagosome acidification, producing ROS, RNI and antimicrobial peptides, and recruiting other immune cells. Despite the widely appreciated protective role, macrophages can also be manipulated by *Mtb* for disease dissemination. Depletion of macrophages protected mice from a lethal *Mtb* infection (Leemans et al., 2001). Studies in zebrafish revealed that

Mtb induced recruitment of new macrophages via the ESX1/RD1 virulence factor to disseminate infection (Davis and Ramakrishnan, 2009). *Mtb* preferentially recruits and infects permissive macrophages while evading microbicidal ones by using *Mtb* lipid phthiocerol dimycoceroserate (Cambier et al., 2014). Neutrophils also play a dual role in TB infection. The likelihood of getting TB infection is lower in individuals with high blood neutrophil counts at the time of exposure (Martineau et al., 2007). In contrast to the protective role of early recruited neutrophils, the accumulation of neutrophils at a late stage of infection acerbates lung inflammation (Kimmey et al., 2015; Mishra et al., 2017; Nandi and Behar, 2011). Transcriptomics analysis of peripheral blood also found a neutrophil-driven signature is associated with progression to active TB, which is further supported by the observation of infected neutrophils in the airways of active TB patients (Berry et al., 2010; Eum et al., 2010). Other types of innate immune cells, such as mucosal associated invariant T (MAIT) cells and invariant natural killer T (iNKT), have been implicated in the early response to TB infection as well (Gold et al., 2010; Rothchild et al., 2014).

Although innate immunity efficiently curbs *Mtb* growth, bacterial load will keep increasing until the onset of adaptive immune responses. During *Mtb* infection, the priming of antigen-specific CD4 T cells is significantly delayed due to the long lag between initial infection and the migration of infected $CCR2^{+}$, MHCII-expressing DCs from the lungs to local lymph nodes (Gallegos et al., 2008; Reiley et al., 2008; Samstein et al., 2013; Wolf et al., 2008). Multiple pathways may be involved in activating CD8 T cells during TB infection. Leakage of *Mtb* antigen through damaged membranes or direct *Mtb* phagosomal escape may generate antigens for the classical cytosolic MHC I

presentation pathway (van der Wel et al., 2007). Uninfected DCs can take up apoptotic vesicles from infected cells that undergo apoptosis and thereby cross-present antigens to CD8 T cells (Schaible et al., 2003; Winau et al., 2006). For example, enhancing apoptosis of *Mtb*-infected cells by manipulating eicosanoid pathways resulted in more robust cross-priming and activation of CD8 T cells in mice (Divangahi et al., 2010).

CD4 T cells are crucial to TB control in both mice and humans. Mice deficient in CD4 T cells, either by deleting the MHC II molecule or antibody depletion, failed to control bacterial growth and quickly succumbed to infection (Mogues et al., 2001). Epidemiologic analysis found HIV patients are 5 to 10-fold more likely to progress from latent to active TB due to the low CD4 T cell count (Pai et al., 2016).

Of all the cells involved in the immune response to *Mtb*, the protective role of Th1 cells is the best characterized. Th1 cells depend on IL-12 and transcription factor T-bet for differentiation and maintenance, and produce interferon gamma (IFN-γ) and tumor necrosis factor (TNF) as signature cytokines. IL-12-deficient mice have delayed T cell activation and reduced IFN-γproduction, and cannot control *Mtb* growth (Cooper et al., 1997). Mice lacking IFN-γ and TNF are unable to restrict bacilli growth as well (Cooper et al., 1993; Flynn et al., 1993; Flynn et al., 1995). More importantly, mutations in the IL-12/IFN-γ axis in children predispose them to disseminated infection caused by the vaccine strain BCG and environmental mycobacteria (Casanova et al., 2013). Rheumatoid arthritis patients receiving TNF blocking antibodies are at a higher risk for TB reactivation, supporting TNF as an important mediator of resistance to infection in human. Intriguingly, transfer of

antigen specific CD4 T cells conferred protection to mice, even when these T cells were not able to produce IFN-γ and TNF, although different results have been observed depending on the models used (Gallegos et al., 2011; Green et al., 2013). Furthermore, other studies found a poor correlation between CD4 T cell IFN-γ production and protection against TB in humans (Kagina et al., 2010). These studies highlight the need to revisit the central dogma of TB immunology. CD4 T cells must have other mechanisms of controlling *Mtb in vivo*, independent of IFN-γ and TNF production. What are the major cellular sources of IFN-γ? Although the protective roles of CD4 T cells, IFN-γ and TNF are well-established, we are just beginning to understand their exact contributions to resistance.

Considering the importance of Th1 responses in protection, it is not surprising that Th2 responses, which impede Th1 cell development, are detrimental to TB control. TB and helminthic co-infection occurs in many parts of the world where TB is endemic. A hallmark of helminthic infections is the generation of Th2 responses, which can potentially inhibit Th1 responses against *Mtb*. Indeed, worm infection is associated with poor BCG-induced immunity and reduced Th1 responses in both active and latent TB (Babu et al., 2009; Resende Co et al., 2007; Stewart et al., 1999). Mechanistically, that may be in part caused by the alternative activation of macrophages via the IL-4Rα signaling pathway (Potian et al., 2011).

Th17 cells produce IL-17A and IL-17F as signature cytokines and mediate anti-microbial immunity against extracellular bacteria and fungi. Their contribution to TB immunity has recently been recognized. Transfer of antigen–dependent Th17 cells only partially inhibits *Mtb* growth, suggesting

that Th17 cells may not be required for TB control (Gallegos et al., 2011). However, Th17 cells augment BCG-induced responses after vaccination and are essential for mature granuloma formation (Khader et al., 2007; Okamoto Yoshida et al., 2010). Individuals carrying loss-of-function mutations in RORC, which encodes the lineage-specific transcription factors for Th17 cells, exhibit impaired immunity to both chronic candidiasis and *Mtb*. Surprisingly, the hypersusceptiblity is due to defective IFN-γ production by circulating γδ T cells and $CD4^{+}CCR6^{+}CXCR3^{+}$ αβ T cells in RORγ- and RORγT-deficient individuals, highlighting the complicated immunological network in mediating resistance to TB (Okada et al., 2015). Furthermore, IL-17 can cause pathogenic responses and lung tissue damage in mice that received multiple BCG vaccinations (Cruz et al., 2010). To complicate matters, the major cellular source of IL-17 during infection may be γδ T cells, rather than Th17 cells (Okamoto Yoshida et al., 2010)

CD8 T cells are another important contributor to anti-TB immunity, although CD4 T cells may play a more crucial role (Lin and Flynn, 2015; Mogues et al., 2001). The early observation that MHC I, TAP, or CD1d deficient mice show increased susceptibility to TB suggested that CD8 T cells are necessary to control the infection (Behar et al., 1999; Flynn et al., 1992; Sousa et al., 2000). However, these genetic knockout mice may have profound unexpected phenotypes in cellular compartments other than CD8 T cells. Later studies using CD8 T cell depletion antibodies further confirmed their non-redundant and important role in mediating protection (Mogues et al., 2001; van Pinxteren et al., 2000). In addition to producing IL2, IFN-γ, and TNF like CD4 T cells, CD8 T cells are able to directly kill infected cells via cytotoxic granule functions

(via perforin, granzymes, and granulysin) or Fas-Fas ligand interaction to induce apoptosis (Lin and Flynn, 2015). Interestingly, rapid accumulation of antigen-specific CD8 T cells, rather than CD4 T cells, is correlated with BCG vaccination-induced protection in challenged mice. The poly-functional signature of CD8 T cells (simultaneous production of IL2 and IFN-γ) is associated with a protective immune response following treatment (Caccamo et al., 2009). However, unlike CD4 T cells, the requirement for CD8 T cells in controlling TB infection has not been definitely proven in humans, although human CD8 T cells can directly kill *Mtb* via granulysin *in vitro* (Stenger et al., 1998).

1.3.2. Bacillus Calmette–Guérin (BCG) vaccine

The BCG vaccine has been administrated more than 4 billion times worldwide and remains the only available TB vaccine. BCG is an attenuated form of *Mycobacterium bovis* (*M. bovis*), a close relative of *Mtb* commonly found in cows, and is usually well-tolerated in healthy individuals. However, children with genetic deficiencies in key immune genes, such as the IL-12/IFN-γ axis, or with active HIV infection are likely to develop disseminated BCG infection. In 2007, WHO stopped recommending BCG vaccine for HIV-positive children even in TB endemic areas.

Although BCG provides a cost-effective way to prevent tuberculous meningitis, a severe form of extrapulmonary TB infection, its protection against pulmonary TB infection appears to be highly variable (Trunz et al., 2006). The efficacy ranged from no protection to 50% reduction in the risk of getting TB, depending on the populations and methods used in the studies (Colditz et al.,

1995; Colditz et al., 1994; Nguipdop-Djomo et al., 2016; Roy et al., 2014). The duration of protection is under debate as well. Some studies showed BCG-induced protection waned in adolescence, while other studies found the efficacy persisted for 50 to 60 years (Aronson et al., 2004; Nguipdop-Djomo et al., 2016). The wide variation of BCG performance may be due to a number of reasons, such as genetic variation in BCG strains, genetic variation in host populations, environmental mycobacteria that induce immune regulation and helminthic co-infection (Brandt et al., 2002; Brosch et al., 2007; Moliva et al., 2017).

Whatever the explanation for the variations, BCG is at best 50% effective against the development of pulmonary TB in adults. Therefore, current BCG clearly does not satisfy the need for global TB control. A lot of efforts are underway to improve, boost or replace BCG. For example, genomic comparison revealed the absence of immunodominant *Mtb*-specific antigens from BCG, such as RD-1 locus-encoded virulence factors ESAT6 and CFP10 (Behr et al., 1999). Recombinant BCG exporting ESAT-6 demonstrated better protection against TB (Pym et al., 2003). Other strategies to increase BCG immunogenicity include overexpressing Antigen 85B (Ag85B), an immunodominant antigen shared by BCG and *Mtb* (Tullius et al., 2008). Some modified or genetically engineered BCG variants, such as the rBCGΔUreC:Hly+, have already entered the pipeline and will be discussed in the following section.

1.3.3. TB vaccine candidates in the pipeline

Both the slow decline in global TB incidence and the spread of MDR-TB highlight the critical need for new TB vaccines that are more effective than BCG. The past two decades have witnessed tremendous progress in TB vaccine development. Currently, there are five vaccines in Phase I and eight vaccines in Phase II or Phase III trials (Figure 1.1). I will discuss the major vaccine strategies and several notable candidates in each category.

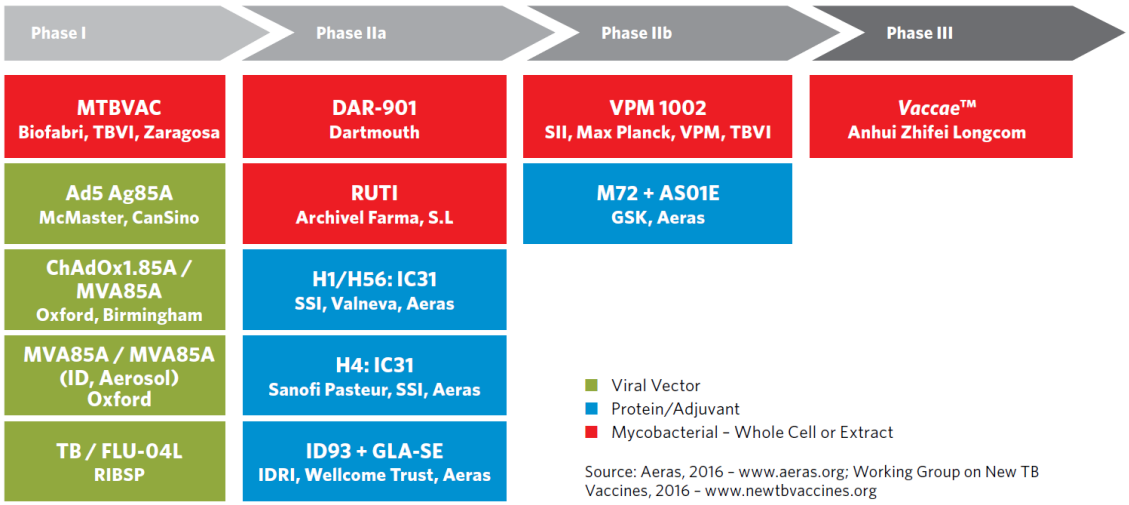

Figure 1.1 The development pipeline of new TB vaccines, August 2015

Source: WHO Global tuberculosis report 2016

A major focus of TB vaccine development is to generate live vaccines, with the goal of replacing BCG with either improved recombinant BCG or attenuated *Mtb*. The improved BCG vaccines are expected to a) be safer, not causing diseases even in immunocompromised individuals; b) be more immunogenic;

c) induce longer protection; d) induce protection against highly virulent strains and MDR-TB (Ottenhoff and Kaufmann, 2012). One stategy to improve BCG is to introduce immunodominant antigens that are absent from BCG, such as RD-1 locus encoded virulence factors ESAT6 and CFP10 (Pym et al., 2003). A similar way is to overexpress immunodominant antigens that are already expressed by BCG but probably not at a sufficiently high level, such as the antigen 85 complex (Ag85) (Horwitz et al., 2000). Another approach is to modify the way the immune system recognizes BCG by enhancing cross-presentation or inhibiting BCG's ability to block phagosomal maturation. For example, the candidate VPM 1002 (rBCGΔUreC:Hly+) expresses a membrane perforating enzyme listeriolysin and contains a deletion in urease C (*ureC*), which abolishes its ability to neutralize phagosome and is required for listeriolysin to function (Grode et al., 2005). Membrane perforation allows BCG antigens to gain cytosolic access, increase host cell apoptosis and enhance immune activation. This candidate has shown better protection in animal models and is now in the Phase IIb trial (Desel et al., 2011; Farinacci et al., 2012). A major drawback of BCG-based vaccine design is that BCG was derived from *M. bovis,* an animal-adapted mycobacterium species, while the natural host of *Mtb* is human. Furthermore, genomic analysis revealed that more than 100 genes are missing in the BCG genome, compared to *Mtb* clinical isolates (Behr et al., 1999; Brosch et al., 2007). Considering the co-evolution of pathogens with their natural hosts, it is likely that some of the factors that mediate protection against human TB are missing in BCG.

To substitute BCG with attenuated recombinant *Mtb*, at least two independent gene deletions or killing mechanisms are required to prevent escape mutants

and virulence reversion. An early example is the r*Mtb*ΔRD1ΔpanCD, which has deletions in RD-1 locus and two genes required for the synthesis of pantothenate (Sambandamurthy et al., 2002). This strain underwent limited replication in mice and was more attenuated than BCG in immunocompromised mice. r*Mtb*ΔRD1ΔpanCD provided similar protection as BCG in mice and guinea pigs, but failed to protect in calves and cynomolgus macaques (Larsen et al., 2009; Sambandamurthy et al., 2006; Waters et al., 2007). Several other attenuated r*Mtb* vaccine candidates are constructed based on similar principles. Recently, the first live-attenuated *Mtb*-based vaccine, *MTB*VAC, entered clinical trials, which contains two independent deletions of the *phoP* and *fadD26* genes (Arbues et al., 2013). PhoP is a part of the two-component system that regulates the transcription of *Mtb* virulence factors and its mutant is even more attenuated than BCG (Martin et al., 2006). Fad26 is an enzyme critical for glycolipid cell-wall synthesis. *MTB*VAC had a comparable safety profile as the current BCG and showed slightly better protection than BCG in mice (Arbues et al., 2013).

Another major category are subunit vaccines, which are delivered as a mixture of recombinant *Mtb* antigens and adjuvants. GSK M72 contains a fusion of *Mtb* antigens 32A (Rv0125) and 39A (Rv1196) mixed with a GSK adjuvant AS01E, which has favorable clinical properties (Garcon and Van Mechelen, 2011). This candidate induced a high frequency of M72-specific CD4 T cells expressing multiple combinations of Th1 cytokines. GSK and Aeras are now recruiting patients for the Phase IIb trial of M72/AS01E (Penn-Nicholson et al., 2015). H1:IC31 consists of a fusion protein Hybrid 1 (H1, containing immunodominant antigens Ag85B and ESAT6) and an adjuvant IC3, which

binds TLR9 and enhances DC activation (Ottenhoff et al., 2010). H1:IC31 boosted the antigen-specific T cell responses induced by BCG (van Dissel et al., 2011). In another candidate H56:IC31, the latent TB antigen Rv2660c was incorporated into the backbone of H1:IC3, based on its strong upregulation during latent infection. H56:IC31 represents a significant advance in subunit vaccine design for TB. When administrated alone, H56 provided a similar extent of protection to BCG during the acute phase and even more efficient than BCG and H1 during the chronic phase (Aagaard et al., 2011). Boosting with H56:IC31after BCG vaccination reduced disease severity in a non-human primate model and even prevented TB reactivation after TNF neutralizing antibody treatment (Lin et al., 2012). Subunit vaccines are generally safe and well-tolerated, compared to viable BCG or TB vaccines. However, the antigen selection is largely empirical, although gene expression profiling is now employed to assist rational design, like in the case of H56:IC3.

Viral-vector based vaccines deliver TB antigens through a replication-deficient viral vector system and raised a lot of interest a decade ago. Recombinant modified vaccinia virus Ankara expressing antigen 85A (MVA85A) induced a strong Ag85-specific CD4 T cell response in preclinical animal models and humans (McShane et al., 2004). However, MVA85A failed to show efficacy in infants as a BCG booster in a randomized and placebo-controlled Phase 2b trial (Tameris et al., 2013). Many explanations have been proposed for the late stage failure of MVA85. Some researchers argued that aerosol delivery of this vaccine might offer immunological advantages and MVA85A is now in clinical trial for delivery through a different route (Satti et al., 2014). A retrospective examination of published *in vivo* data in animal models of MVA85A raised

concerns on the quality of the data to support its preclinical efficacy, such as reproducibility, improper randomization and baseline comparability (Kashangura et al., 2015). Currently, there are several other candidates based on a highly similar strategy in the pipeline, such as Ad5 Ag85A and ChAdOx1.85A. More rigorous preclinical research is required before investing valuable resources and time on large-scale clinical trials. There are also doubts about our current model of TB vaccine development. Are we oversimplifying the problem by designing vaccines based on already abundantly expressed TB antigen?

1.4. Thesis research aims

1.4.1. Early antimycobacterial drug target validation focusing on TrxB2

Mtb encounters intensive endogenous and exogenous oxidative stress during its life cycle. Not surprisingly, *Mtb* is armed with complicated antioxidant machineries to cope with the stress. There is a high degree of redundancy among these machineries, most of which are dispensable for *Mtb* survival and growth. In contrast, *Mtb's* thioredoxin reductase TrxB2 has been predicted to be essential not only to fight host defenses but also for *in vitro* growth. However, its biological evaluation has not advanced beyond the prediction of its essentiality for growth of *Mtb* on standard agar plates. I focused on addressing the specific physiological role of TrxB2 and its importance for *Mtb* pathogenesis. I generated a TrxB2 conditional knockdown mutant, evaluated the suitability of TrxB2 as an antimycobacterial drug target, and developed novel genetic tools - deliberately leaky knockdown mutants- to facilitate target-specific drug discovery. A collaboration with GlaxoSmithKline (GSK) to screen for novel TrxB2 inhibitors is ongoing.

1.4.2. Early TB vaccine development by exploiting bacterial lysis

Both the slow decline in global TB incidence and the spread of drug-resistant TB necessitate the development of new TB vaccines that are more effective than BCG. The inadequacy of BCG-mediated protection is in part due to the absence of important virulence factors required to confer protection from BCG genome and insufficient antigen presentation at the site of infection. To overcome these limitations, we generated a novel *Mtb*-based vaccine candidate for proof-of-concept experiments, in which bacterial lysis is achieved by inducible expression of cell wall hydrolyzing enzymes. I characterized the inducible lysis *Mtb* strains in different growth and physiological conditions. I also addressed the impact of induced bacterial lysis on the host immune system, with the ultimate goal of generating the knowledge required for development of more effective vaccines for TB and other infectious diseases.

CHAPTER 2

ANTIOXIDANT AND BEYOND: TARGETING THIOREDOXIN REDUCTASE LYSES *MYCOBACTERIUM TUBERCULOSIS* *

2.1. Introduction

Mycobacterium tuberculosis (*Mtb*) must cope with exogenous oxidative stress imposed by the host. Unlike other antioxidant enzymes, *Mtb's* thioredoxin reductase TrxB2 has been predicted to be essential not only to fight host defenses but also for *in vitro* growth. However, the specific physiological role of TrxB2 and its importance for *Mtb* pathogenesis remain undefined. Here we show that genetic inactivation of thioredoxin reductase perturbed several growth-essential processes, including sulfur and DNA metabolism and rapidly killed and lysed *Mtb*. Death was due to cidal thiol-specific oxidizing stress and prevented by a disulfide reductant. In contrast, thioredoxin reductase deficiency did not significantly increase susceptibility to oxidative and nitrosative stress. *In vivo* targeting TrxB2 eradicated *Mtb* during both acute and chronic phases of mouse infection. Deliberately leaky knockdown mutants identified the specificity of TrxB2 inhibitors and showed that partial inactivation of TrxB2 increased *Mtb's* susceptibility to rifampicin. We also screened a library of 11,000 compounds with leaky knockdown mutants and identified SKF867J as a potential novel TrxB2-specific inhibitor. These studies reveal TrxB2 as an essential thiol-reducing enzyme in *Mtb in vitro* and during infection, establish the value of targeting TrxB2, and provide tools to accelerate the development of TrxB2 inhibitors.

* This chapter contains published work from Lin, K., O'Brien, K.M., Trujillo, C., Wang, R., Wallach, J.B., Schnappinger, D., and Ehrt, S. (2016). Mycobacterium tuberculosis Thioredoxin Reductase Is Essential for Thiol Redox Homeostasis but Plays a Minor Role in Antioxidant Defense. PLoS Pathog *12*, e1005675.

2.2. Background

Endogenous oxidative stress represents an inevitable challenge for microbes adapted to an aerobic lifestyle (Imlay, 2013). In addition, pathogens like *Mycobacterium tuberculosis* (*Mtb*) are continuously exposed to exogenous reactive oxygen and nitrogen species generated by the host immune system. Not unexpectedly, *Mtb* is armed with a number of dedicated antioxidant systems to ensure replication and survival within its host. Notable members include catalase, alkyl hydroperoxidase, superoxide dismutase, mycothiol, ergothioneine, thiol peroxidase, thioredoxin reductase and a recently identified membrane-associated oxidoreductase complex (Bryk et al., 2000; Bryk et al., 2002; Carmel-Harel and Storz, 2000; Dussurget et al., 2001; Jaeger et al., 2004; Nambi et al., 2015; Newton et al., 1996; Ng et al., 2004; Piddington et al., 2001; Saini et al., 2016). The thioredoxin system, together with the glutathione system, regulates many important cellular processes, such as antioxidant pathways, DNA and protein repair enzymes, and the activation of redox-sensitive transcription factors (Carmel-Harel and Storz, 2000; Lu and Holmgren, 2014). Unlike many Gram-negative bacteria, which possess both systems, *Mtb* lacks the glutathione system (Lu and Holmgren, 2014; Newton et al., 1996). Instead, mycothiol has been suggested as substitute for glutathione in *Mtb* (Newton et al., 1996). Mycothiol-deficient *Mtb* requires addition of catalase for growth *in vitro*, but is not significantly attenuated in mice (Vilcheze et al., 2008). In contrast, there is evidence that thioredoxin reductase (TrxB2) is essential for growth *in vitro*, implying a unique role for TrxB2 (Harbut et al., 2015; Sassetti et al., 2003; Zhang et al., 2012). Although purified TrxB2 has been shown to mediate

detoxification of H_2O_2, peroxide, and dinitrobenzene *in vitro* (Akif et al., 2005; Jaeger et al., 2004; Zhang et al., 1999), its role in oxidative stress defense in physiological conditions and its specific biological functions in *Mtb* physiology are poorly understood. Bacterial thioredoxin reductases have recently been demonstrated to be druggable targets (Harbut et al., 2015; Lu et al., 2013), however, it has not been determined whether inactivating TrxB2 *in vivo*, in acute and chronic infections, attenuates *Mtb*.

To address these questions, we applied a tunable dual-control genetic switch (Kim et al., 2013) to generate a conditional TrxB2 knockdown mutant and evaluated the impact of TrxB2 depletion. Unexpectedly, depleting TrxB2 not only rapidly killed *Mtb*, but also led to bacterial lysis. TrxB2 depletion perturbed growth-essential processes, including sulfur and DNA metabolism and death could be prevented by addition of a strong disulfide reductant. *In vivo* depletion of TrxB2 resulted in clearance of *Mtb* during both the acute and chronic phases of infection. We generated deliberately leaky knockdown mutants to dissect the contribution of TrxB2 to oxidative stress detoxification and found *Mtb* with partially depleted TrxB2 highly susceptible to thiol-specific oxidizing stress, but, surprisingly, not to peroxide and reactive nitrogen species. The leaky knockdown mutants were used to evaluate the specificity of two TrxB2 inhibitors and revealed that targeting TrxB2 results in hypersusceptibility to the frontline anti-tuberculosis drug rifampicin.

2.3. Results

2.3.1. TrxB2 is essential for growth and survival of *Mtb in vitro*

We first established that TrxB2 is indeed required for growth of *Mtb* under standard laboratory conditions (Figure 2.1). Because a deletion mutant could not be isolated, we generated a TrxB2 dual-control (DUC) strain (Figure 2.2). In TrxB2-DUC expression of TrxB2 is controlled by both transcriptional silencing and inducible proteolytic degradation, while TrxC is constitutively expressed from its native promoter (Kim et al., 2013). Upon addition of anhydrotetracycline (atc) TrxB2 protein was rapidly depleted and below the limit of detection after 6 hours, which corresponds to less than 5% of TrxB2 amount in wild type (wt) H37Rv (Figure 2.3 A and Figure 2.4). TrxB2 depletion not only inhibited *Mtb* growth in nutrition-rich 7H9 medium, but also led to rapid killing (Figure 2.3 B and C). Bacterial viability declined by 2.7 log after 24 hours, and 3.4 log after 4 days of atc treatment, indicating that TrxB2 is required for bacterial growth and survival in replicating conditions. We also assessed the impact of inactivating TrxB2 on non-replicating *Mtb*, which is known to be tolerant to anti-TB drugs and, in part, responsible for the long duration of anti-TB chemotherapy (Barry et al., 2009). TrxB2 depletion was induced with atc after 10 days of incubation in PBS. Remarkably, TrxB2 depletion killed ~90% of the bacilli after 48 h and 99.9% within two weeks of PBS starvation, highlighting that starvation-induced non-replicating *Mtb* depends on TrxB2 for survival as well (Figure 2.3 D and E).

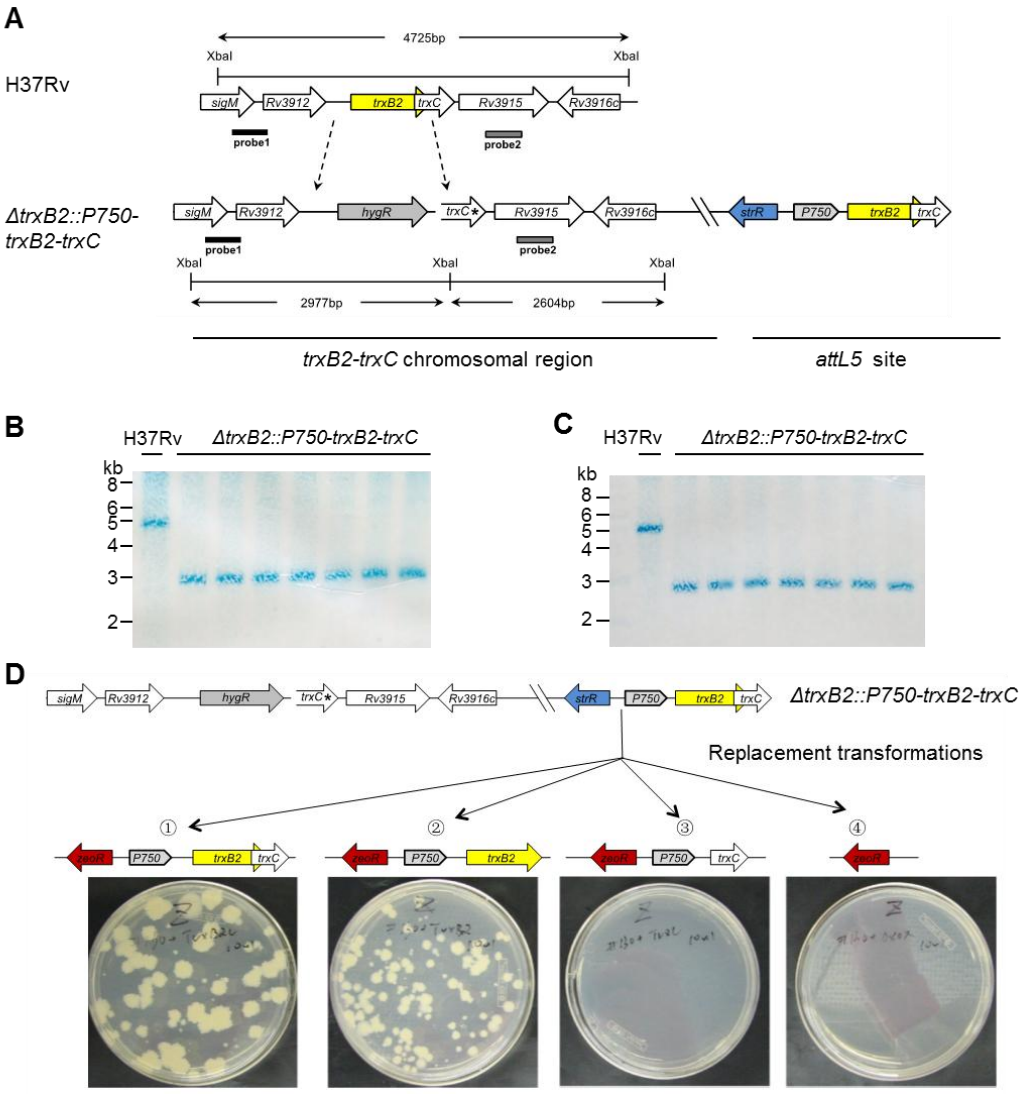

Figure 2.1 TrxB2 is required for growth of *Mtb*.

(A) Map of the *trxB2-trxC* genomic region in H37Rv and Δ*trxB2*::P750-*trxB2-trxC*. To construct Δ*trxB2*::P750-*trxB2-trxC*, we first generated a merodiploid strain by integrating a second copy of the *trxB2-trxC* operon into the attL5 site. Then *trxB2* and the first 4 bps of*trxC*, which overlap with *trxB2*, were replaced with a hygromycin cassette by homologous recombination. Inactivated *trxC* lacking the first 4 bps is marked with an asterisk. (B and C) Southern blot of *Xba*I-digested genomic DNA from H37Rv and seven Δ*trxB2*::P750-*trxB2-trxC* candidates probed with probes 1 (B) and 2 (C) as indicated in (A). (D) To test essentiality of *trxB2* and *trxC*, Δ*trxB2*::P750-*trxB2-trxC* was transformed with integrative plasmids expressing *trxB2-trxC*, *trxB2*, *trxC* or vector control to replace the *trxB2-trxC*copy in the attL5 site. Only plasmids containing *trxB2* yielded colonies demonstrating that *trxB2* but not *trxC* is required for growth.

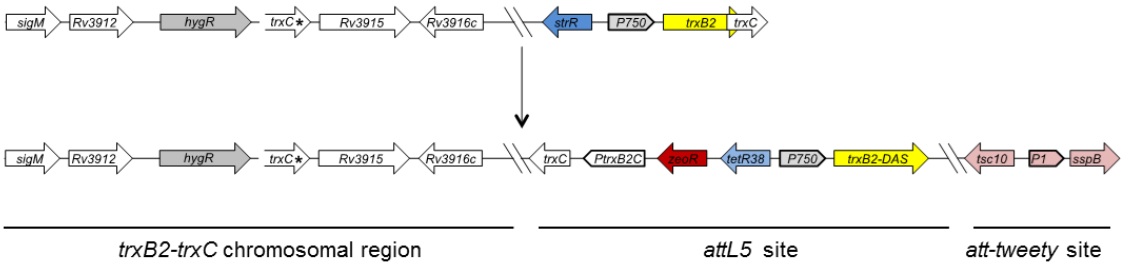

Figure 2.2 Construction of TrxB2-DUC.

To generate the dual control (DUC) mutant, the *trxB2-trxC* plasmid located in the attL5 site of Δ*trxB2*::P750-*trxB2-trxC* was replaced with a plasmid containing DAS-tagged *trxB2*expressed from the tet-operator containing promoter P750, *trxC* with its native promoter, and reverse tet repressor with a constitutive promoter. In addition the mutant was transformed with a plasmid that integrates in the tweety phage attachment site and expresses the SspB adaptor protein under control of wt tet repressor.

Figure 2.3 TrxB2 is essential for *Mtb* survival in replicating and non-replicating conditions.

(A-C) Impact of TrxB2 depletion on replicating *Mtb*. (A) Immunoblot of protein extracts from H37Rv and TrxB2-DUC grown with and without atc. Blot was probed with TrxB2-specific and Eno-specific (loading control) antisera. TrxB2 in the TrxB2-DUC mutant is of increased molecular weight due to the C-terminal DAS tag. (B) Growth of individual*Mtb* strains quantified by optical density in nutrient-rich medium with or without atc. Starting density of the cultures was OD_{580} ~ 0.01. (C) Survival of *Mtb* strains quantified by CFU in 7H9 medium with or without atc (n = 6 per group). (D and E) Impact of TrxB2 depletion on non-replicating *Mtb*. (D) Immunoblot of protein extracts from *Mtb* cultures during starvation in PBS with or without atc. H37Rv and TrxB2-DUC were suspended in PBS for 10 days to obtain a non-replicating state. Where indicated, atc was added to the cultures on day 10. (E) Quantification of CFU from cultures in (D) at the indicated time points (n = 3 per group). (F) Appearance of the atc-treated TrxB2-DUC culture in 7H9 medium on day 4 and on day12. (G) Growth of TrxB2-DUC in 7H9 medium, treated with atc or meropenem–clavulanate (MCA). Starting density of the cultures was OD_{580}~ 0.1. (H) Immunoblot analysis of dihydrolipoamide acyltransferase (DlaT), enolase (Eno), proteasome beta subunit (PrcB) and secreted protein antigen 85B (Ag85B) from culture supernatants in (G) at the indicated times. (I) Quantification of cell length by microscopy of indicated *Mtb* strains treated or not with atc for 4 days. Mean cell lengths (n = 100) are indicated. **** $p<0.0001$ by one-way ANOVA. All results are representative of at least three independent experiments. Data in (C) and (E) are means ± SD. In some panels, error bars are too small to be seen.

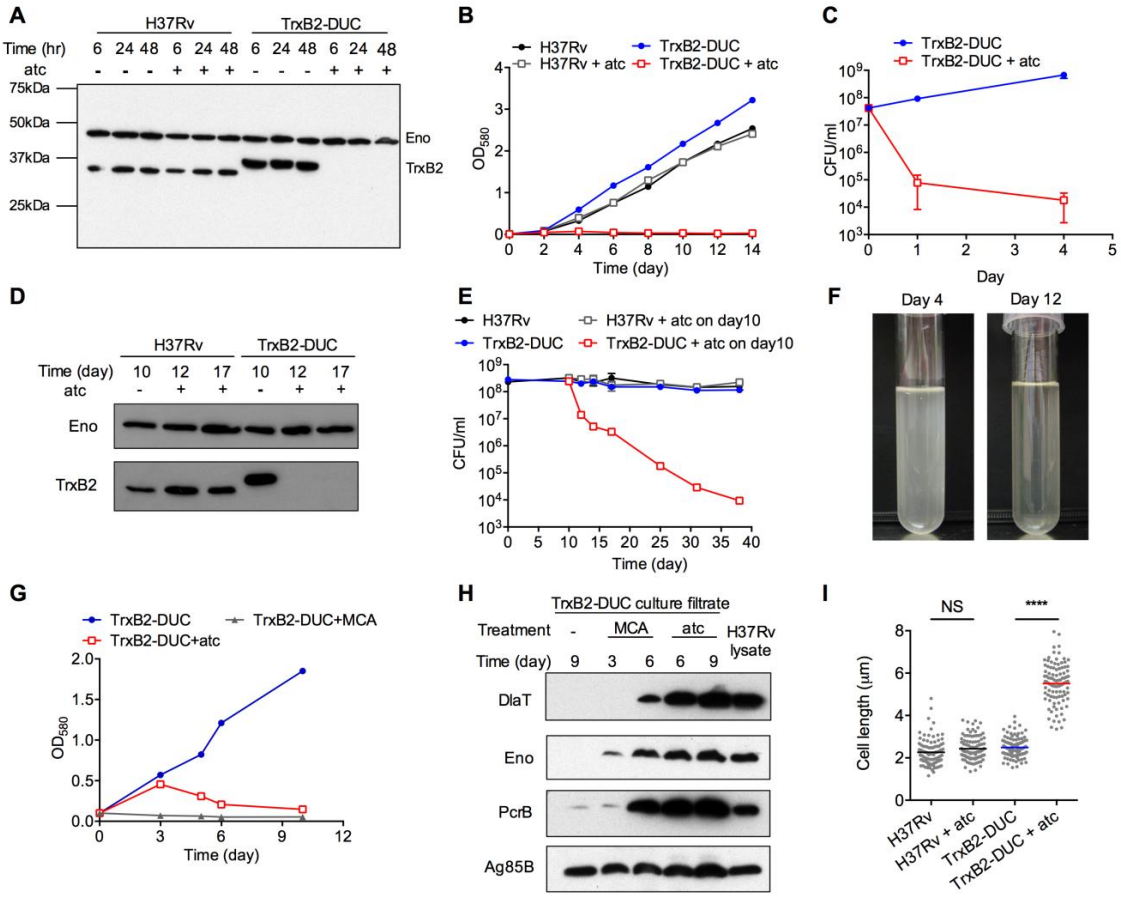
A
H37Rv
TrxB2-DUC
Time (hr) 6 24 48 6 24 48 6 24 48 6 24 48
atc - - - + + + - - - + + +
75kDa
50kDa
37kDa
25kDa
Eno
TrxB2
B
H37Rv
H37Rv + atc
TrxB2-DUC
TrxB2-DUC + atc
OD580
Time (day)
C
TrxB2-DUC
TrxB2-DUC + atc
CFU/ml
Day
D
H37Rv
TrxB2-DUC
Time (day) 10 12 17 10 12 17
atc - + + - + +
Eno
TrxB2
E
H37Rv
H37Rv + atc on day10
TrxB2-DUC
TrxB2-DUC + atc on day10
CFU/ml
Time (day)
F
Day 4
Day 12
G
TrxB2-DUC
TrxB2-DUC+MCA
TrxB2-DUC+atc
OD580
Time (day)
H
TrxB2-DUC culture filtrate
Treatment - MCA atc H37Rv lysate
Time (day) 9 3 6 6 9
DlaT
Eno
PcrB
Ag85B
I
NS
****
Cell length (μm)
H37Rv
H37Rv + atc
TrxB2-DUC
TrxB2-DUC + atc

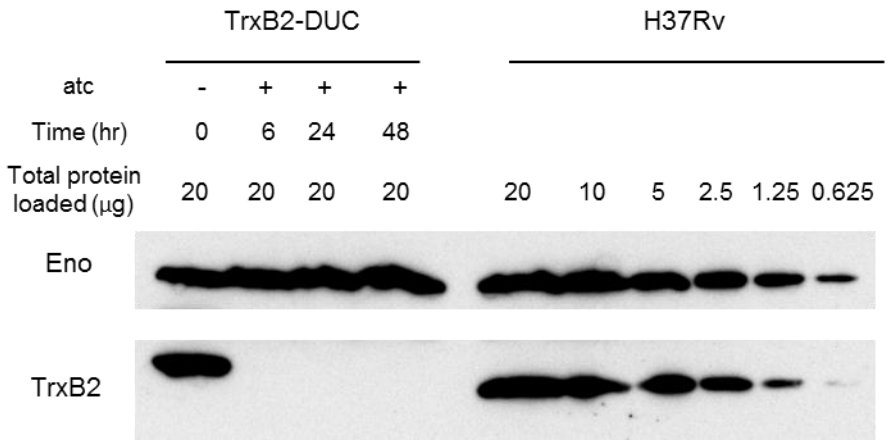

Figure 2.4 Semiquantitative immunoblot analysis of TrxB2 in TrxB2-DUC.

Immunoblot of protein extracts from TrxB2-DUC treated with atc for 6, 24 and 48 hrs. Serially diluted H37Rv lysate was used to determine the limit of detection of TrxB2. Eno serves as loading control.

2.3.2. Depleting TrxB2 caused lytic death of *Mtb*

While culturing TrxB2-depleted *Mtb* in liquid growth medium, we observed that the culture gradually declined in optical density and turned clear (Figure 2.3 F and G). This motivated us to ask whether TrxB2 depletion caused lysis of *Mtb*. Notably, mycobacterial death is not always accompanied by lysis. So far, only a small number of cell-wall targeting compounds have been shown to induce lytic death (Kumar et al., 2012). To further investigate whether lysis occurred upon TrxB2 depletion, we monitored the release of the cytoplasmic enzymes enolase (Eno), dihydrolipoamide acyltransferase (DlaT) and the proteasome beta subunit (PrcB) into the culture supernatant. Because Eno, DlaT and PrcB are generally not detected in the culture supernatant of intact mycobacterial cells, we consider their release as an indicator of bacterial lysis. Consistent with a previous report that meropenem-clavulanate caused *Mtb* lysis (Kumar et al., 2012), we found Eno, DlaT and PrcB in the culture filtrate 6 days after exposure to meropenem-clavulanate (Figure 2.3 H). There was no detectable lysis of TrxB2-DUC in the absence of antibiotic or atc, even after 9 days of incubation. In contrast, cytoplasmic proteins were readily detectable in the supernatant of TrxB2-DUC treated with atc for 6 or 9 days, confirming our hypothesis that TrxB2 depletion caused lytic death (Figure 2.3 H). In contrast, depletion of nicotinamide adenine dinucleotide synthetase (NadE) which also rapidly kills *Mtb* (Kim et al., 2013), did not result in detectable lysis of NadE-DUC (not shown). Microscopic analysis revealed that lysis of TrxB2-depleted *Mtb* was preceded by significant cell elongation (Figure 2.3 I and Figure 2.5). The majority of TrxB2-depleted bacteria were twice as long

as those expressing TrxB2, suggesting that TrxB2 depletion affects processes required for cell division.

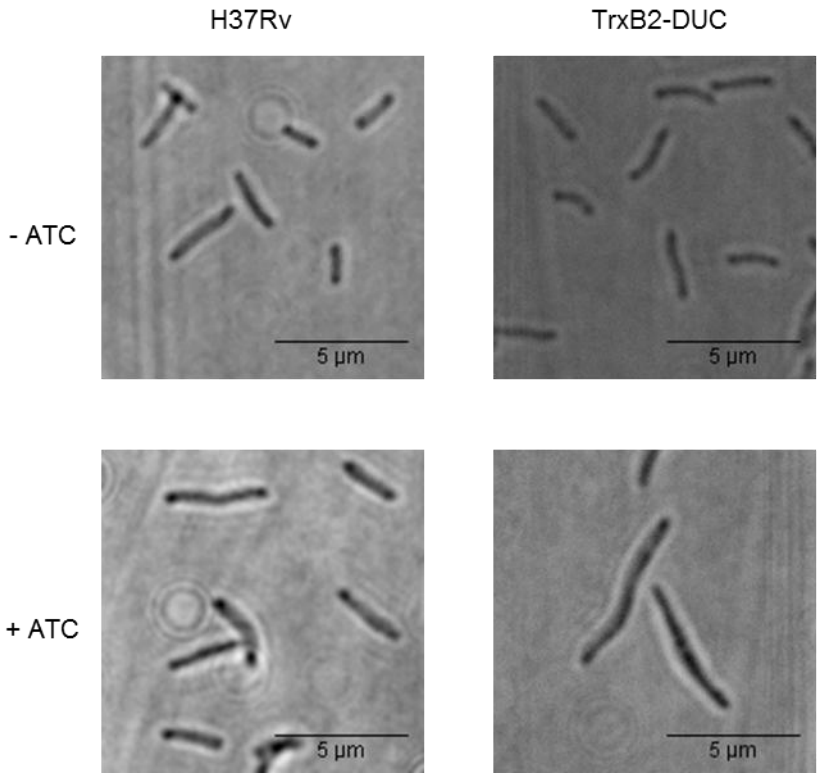

Figure 2.5 TrxB2 depletion in *Mtb* causes cell elongation.

Representative images of H37Rv and TrxB2-DUC treated with atc or not for 4 days. Samples were examined with bright-field microscopy. Data processing was performed with ImageJ.

2.3.3. TrxB2 is essential for *Mtb* to establish and maintain infection in mice

To evaluate the importance of TrxB2 for virulence of *Mtb*, mice were infected with TrxB2-DUC and fed doxycycline (doxy) containing food to inactivate TrxB2 at selected time points. The infection was rapidly cleared in mice given doxy food from the time of infection or during the acute phase of infection on day 10 (Figure 2.6 A and B). No pulmonary pathology was observed in these mice (not shown). Even when TrxB2 depletion was initiated during the chronic phase of infection on day 35, colony forming units (CFU) declined rapidly and no bacteria could be isolated from both lungs and spleens on day 160 (Figure 2.6 A and B). The decline of CFU was accompanied by progressive healing of lesions in the lungs (Figure 2.6 C and D). These results establish that TrxB2 is required for growth and persistence of *Mtb* in mice and point to the value of targeting TrxB2 to treat TB.

2.3.4. Reactivation of infection after *Mtb* is cleared by TrxB2 depletion

Reactivation of latent infection represents a major problem in treating human tuberculosis and accounts for a significant proportion of active TB cases (Pai et al., 2016). Disease relapse has been reported in several murine models to study the latency and reactivation of tuberculosis, even after combination chemotherapies have reduced the number of viable bacilli to an undetectable level (Botha and Ryffel, 2002, 2003; McCune et al., 1966a; McCune et al., 1966b; McCune et al., 1956; McCune and Tompsett, 1956) .

To determine whether TrxB2 depletion completely eradicates *Mtb* infection, especially the latent bacilli, we infected the mice with TrxB2-DUC, fed them

with doxy containing food starting on day 28 and maintained the treatment until day 140 post infection. TrxB2 inactivation rapidly cleared the infection and no viable colonies were detected in lungs, spleens, livers, kidneys or bones since day 112 (Figure 2.7 A and B, and data not shown). However, 23 weeks after the cessation of doxy treatment, 62.5% (10/16) of the mice spontaneously relapsed with active tuberculosis in the lungs and 25% (4/16) in the spleens (Figure 2.7 A and B). A more significant proportion of reactivation was observed in the mice rendered immunocompromised by dexamethasone treatment. 81.25% (13/16) of the mice had disease reactivation in the lungs and 43.75% (7/16) in the spleens (Figure 2.7 C and D). The bacterial load in the spleen was slightly higher in the mice receiving dexamethasone treatment compared to that in the immunocompetent host. We also tested the response of these reactivated bacteria to atc regulation. Their growth was completely inhibited by atc treatment, indicating that they were not escape mutants of tet-regulated system (data now shown). Although TrxB2 depletion quickly reduced infection to an undetectable level, a substantial proportion of the mice reactivated with active disease spontaneously or upon immunosuppression, suggesting that viable bacteria were still present in the host after TrxB2 inactivation.

Figure 2.6 TrxB2 is essential for *Mtb* to establish and maintain infection in mice.

(A and B) Quantification of bacterial loads in lungs (A) and spleens (B) of C56BL/6 mice infected with TrxB2-DUC. Mice received doxy-containing food starting at the indicated time points or not at all. Data are means ± SD of four mice per group. The limit of detection was 4 CFU per organ and is indicated by the dashed line. (C) Gross pathology of lungs from infected mice receiving doxy-containing food starting on day 35 or not at all. Lungs were isolated on day 56, 119 and 160 post infection. (D) Haematoxylin/eosin-stained lung tissue sections from mice infected with TrxB2-DUC not treated or treated with doxy-containing food starting on day 35 post infection. Images are representative of the histopathology of the four mice from each group. Scale bar, 1.0 mm. Results are representative of two independent experiments.

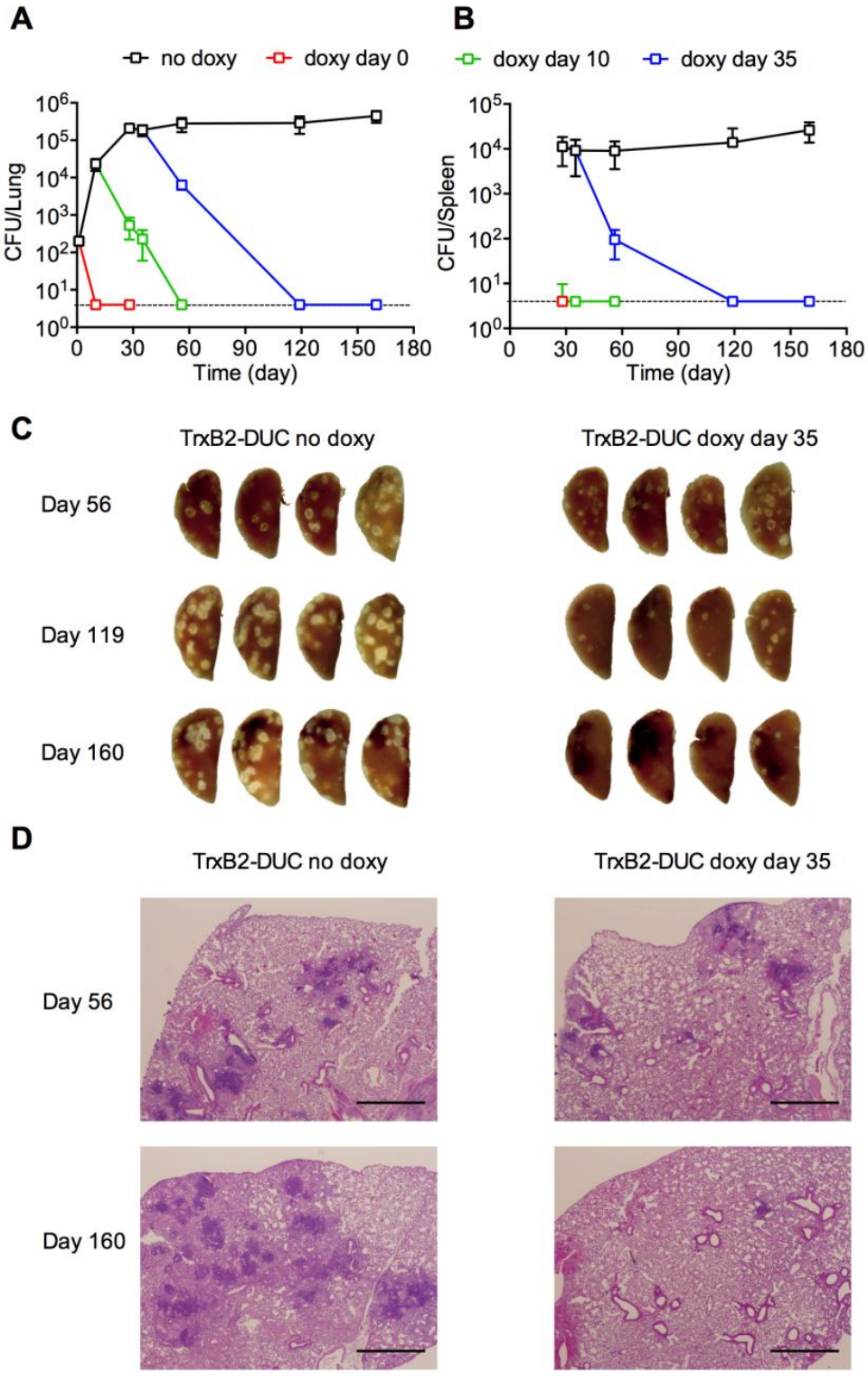
A
no doxy
doxy day 0
CFU/Lung
Time (day)
B
doxy day 10
doxy day 35
CFU/Spleen
Time (day)
C
TrxB2-DUC no doxy
TrxB2-DUC doxy day 35
Day 56
Day 119
Day 160
D
TrxB2-DUC no doxy
TrxB2-DUC doxy day 35
Day 56
Day 160

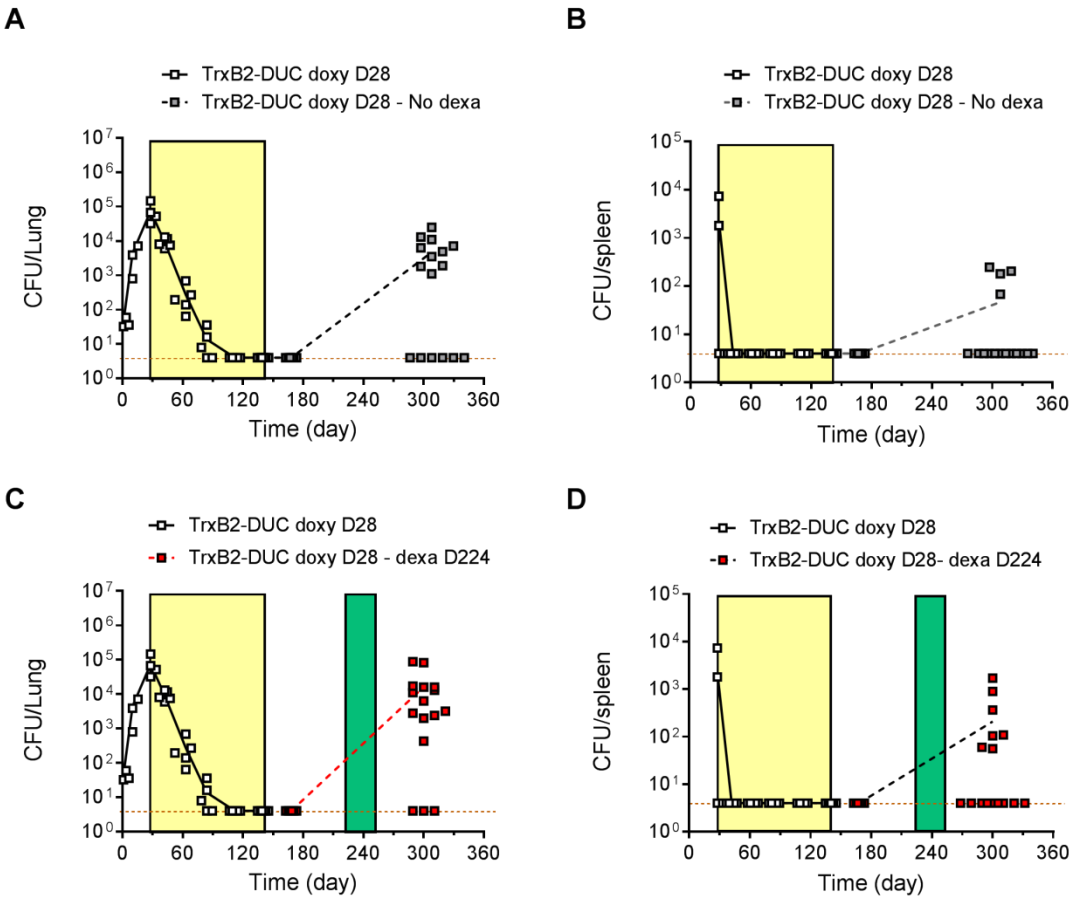

Figure 2.7 Reactivation of infection after *Mtb* is cleared by TrxB2 depletion.

(A and B) Quantification of bacterial loads in lungs (A) and spleens (B) of C56BL/6 mice infected with TrxB2-DUC. Mice received doxy-containing food for 16 weeks, starting day 28 post infection. (C and D) Quantification of bacterial loads in lungs (C) and spleens (D) of C56BL/6 mice infected with TrxB2-DUC. Mice received doxy-containing food from day 28 to day 140 post infection. Then mice were treated with dexamethasone in drinking water for 4 weeks, starting on day 224 post infection. Each dot represents data obtained from one mouse. The limit of detection was 4 CFU per organ and is indicated by the dashed line.

2.3.5. Leaky TrxB2-TetON mutants reveal a specific role for TrxB2 in preventing thiol-oxidizing stress

Although purified TrxB2 has been shown to reduce H_2O_2 and other peroxides, little is known about the detoxification function of TrxB2 in a physiological setting (Jaeger et al., 2004; Zhang et al., 1999). Therefore, we sought to evaluate the impact of partial TrxB2 depletion on the susceptibility of *Mtb* to oxidative stress. Achieving partial TrxB2 depletion to an extent that does not affect viability but significantly reduces the intracellular TrxB2 protein amount is technically challenging with a DUC strain because of the steep atc dose response curve of this regulatory switch (Kim et al., 2013). To circumvent this problem, we generated a panel of TrxB2-TetON mutants that contain point mutations in the operator of the tet promoter resulting in different degrees of constitutive, leaky transcription upon atc removal. Transcription from the mutated tet promoters is similar without TetR, however leaky repression results in a range of promoter activities without atc (Figure 2.8 A). Two of the leaky TrxB2-TetON mutants, TrxB2-tetON-WT and TrxB2-tetON-1C, showed growth defects in the absence of atc (Figure 2.8 B). Their growth defects correlated well with the protein depletion kinetics of TrxB2 (Figure 2.8 C). These mutants thus achieved a phenotypically significant level of TrxB2 depletion yet retained enough TrxB2 to support growth. The moderate impact on growth of TrxB2-tetON-1C permitted the use of standard minimal inhibitory concentration (MIC) assays to measure how inhibition of TrxB2 affects susceptibility of *Mtb* to different chemical stresses.

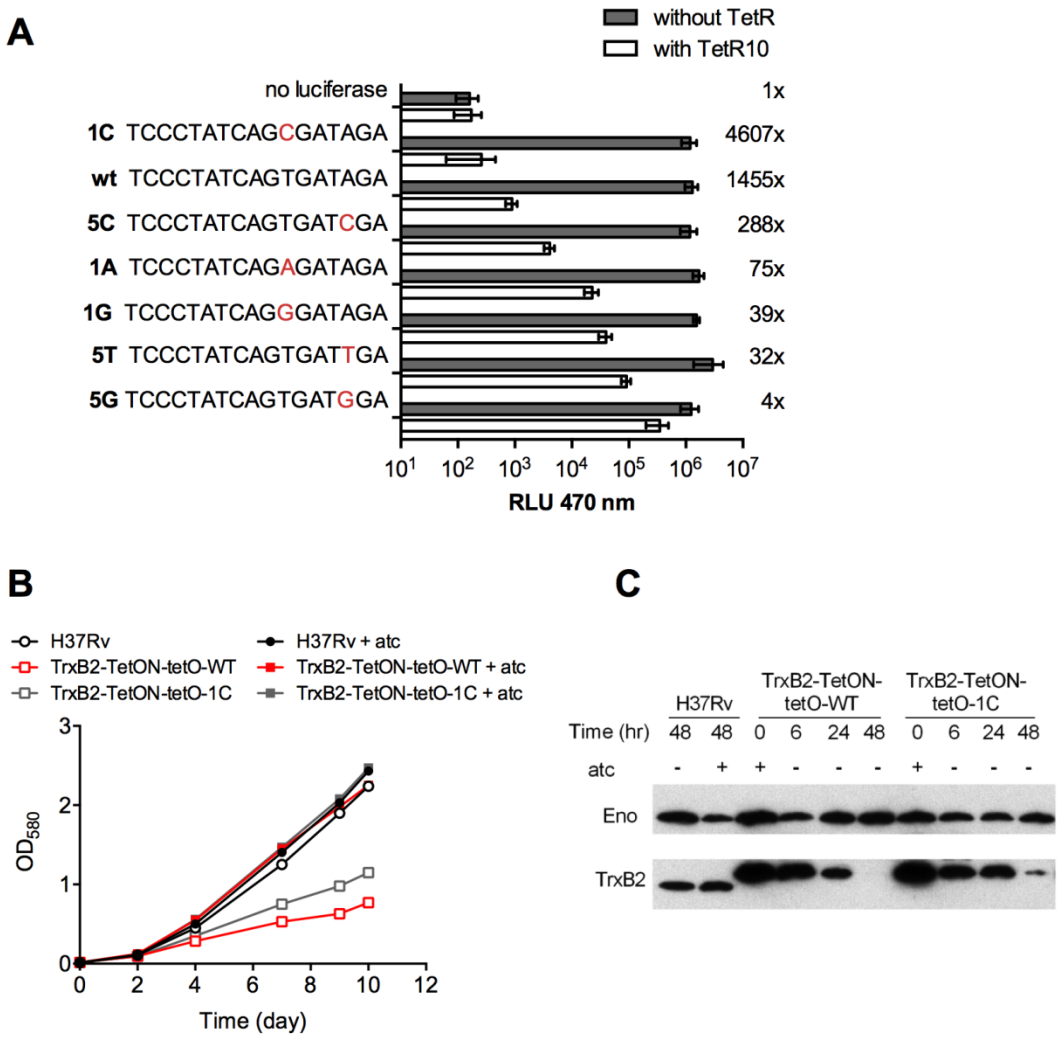

Figure 2.8 Design and characterization of leaky TrxB2-TetON mutants.

(A) Repression of luciferase activity of leaky tet promoters by TetR in *M*. *smegmatis*. The x-axis specifies the promoter that was used to express luciferase and its tetO. Mutated nucleotides are shown in red. The *kanR* luciferase and *hygR* TetR plasmids were integrated into the *M*. *smegmatis* chromosome at the att-L5 and att-Tweety sites, respectively. Integers on the right indicate fold change in RLUs between bacteria without (gray bars) and with TetR (white bars). Data are means ± SD of eight replicates from at least two independent experiments. (B) Growth of H37Rv and TrxB2-TetON-tetO mutants in 7H9 medium in the presence or absence of atc. (C) Kinetics of TrxB2 depletion in TrxB2-TetON-tetO mutants in the absence of atc. TrxB2 in TrxB2-TetON-tetO mutants is of increased molecular weight due to the C-terminal DAS tag. Results in (B) and (C) are representative of three independent experiments.

Surprisingly, partial inhibition of TrxB2 did not affect *Mtb's* susceptibility to growth inhibition or killing by plumbagin, a superoxide generator (Figure 2.9 A and Fig 2.10). TrxB2 silencing only caused a 2-fold shift of the MIC of H_2O_2, and we did not detect significant survival differences between wild type H37Rv and the TrxB2-tetON mutant following H_2O_2 exposure (Figure 2.9 B and Fig 2.10). Additionally, we measured *Mtb's* susceptibility to reactive nitrogen species and found that TrxB2-silenced *Mtb* was only slightly less resistant to acidified nitrite at a high concentration (Figure 2.9 C). In contrast, TrxB2-silenced *Mtb* was 8–16 fold more susceptible to growth inhibition by diamide, a thiol-specific oxidant (Figure 2.9 D). This hypersusceptibility suggested a specific role for TrxB2 in detoxifying thiol-oxidizing stress.

To determine if thiol-specific oxidizing stress was responsible for the lethality caused by TrxB2 depletion, we tested if supplementation with the strong thiol-reducing agent dithiothreitol (DTT) could prevent death of TrxB2-depleted *Mtb*. Indeed, DTT rescued viability of TrxB2-DUC in a dose-dependent manner (Figure 2.9 E). In contrast, neither glutathione nor catalase provided any survival benefit (Figure 2.9 F). These results indicate that the primary function of TrxB2 in *Mtb* is to detoxify thiol-specific oxidative stress and that TrxB2 is the dominant thiol-reducing enzyme in *Mtb*.

Figure 2.9 TrxB2 protects *Mtb* from thiol-specific oxidizing stress and contributes less to defense against oxidative and nitrosative stress.

(A and B) Susceptibility of partially TrxB2-depleted *Mtb* to plumbagin (A) and H_2O_2 (B). TrxB2-TetON-tetO-1C was cultured in 7H9 medium without atc for 3 days to decrease TrxB2 expression before treatment with plumbagin and H_2O_2. OD_{580} was recorded and normalized to the corresponding strains without drug treatment. (C) Survival of *Mtb* strains after 4 days exposure to increasing concentrations of $NaNO_2$ at pH 5.5. Data are means ± SD (n = 3 per group) and are representative of two independent experiments. (* $p<0.05$, one way ANOVA was used for group comparison). (D) Susceptibility of partially TrxB2-depleted *Mtb* to diamide. (E) Impact of dithiothreitol (DTT) on TrxB2 depletion-induced death in the TrxB2-DUC strain. *$p<0.05$, **$p<0.01$ and ***$p<0.001$ by unpaired Student's t test. (F) Impact of extracellular glutathione (GSH) and catalase on TrxB2 depletion-induced death in the TrxB2-DUC strain. Data shown means ± SD (n = 3 per group) and are representative of two to three independent experiments.

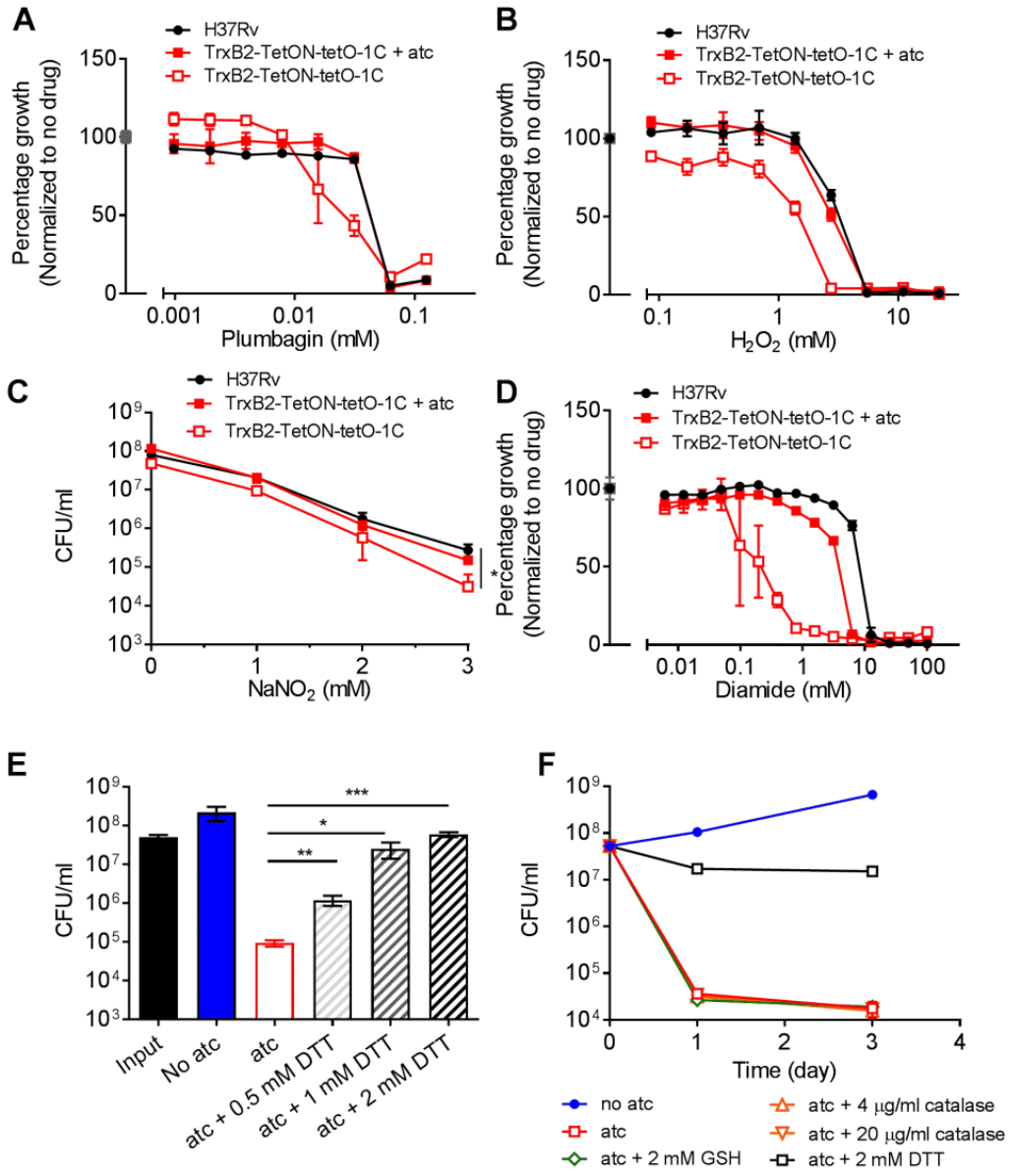
A
H37Rv
TrxB2-TetON-tetO-1C + atc
TrxB2-TetON-tetO-1C
Percentage growth (Normalized to no drug)
Plumbagin (mM)
B
H37Rv
TrxB2-TetON-tetO-1C + atc
TrxB2-TetON-tetO-1C
Percentage growth (Normalized to no drug)
H2O2 (mM)
C
H37Rv
TrxB2-TetON-tetO-1C + atc
TrxB2-TetON-tetO-1C
CFU/ml
NaNO2 (mM)
D
H37Rv
TrxB2-TetON-tetO-1C + atc
TrxB2-TetON-tetO-1C
Percentage growth (Normalized to no drug)
Diamide (mM)
E
CFU/ml
Input
No atc
atc
atc + 0.5 mM DTT
atc + 1 mM DTT
atc + 2 mM DTT
F
CFU/ml
Time (day)
no atc
atc
atc + 2 mM GSH
atc + 4 μg/ml catalase
atc + 20 μg/ml catalase
atc + 2 mM DTT

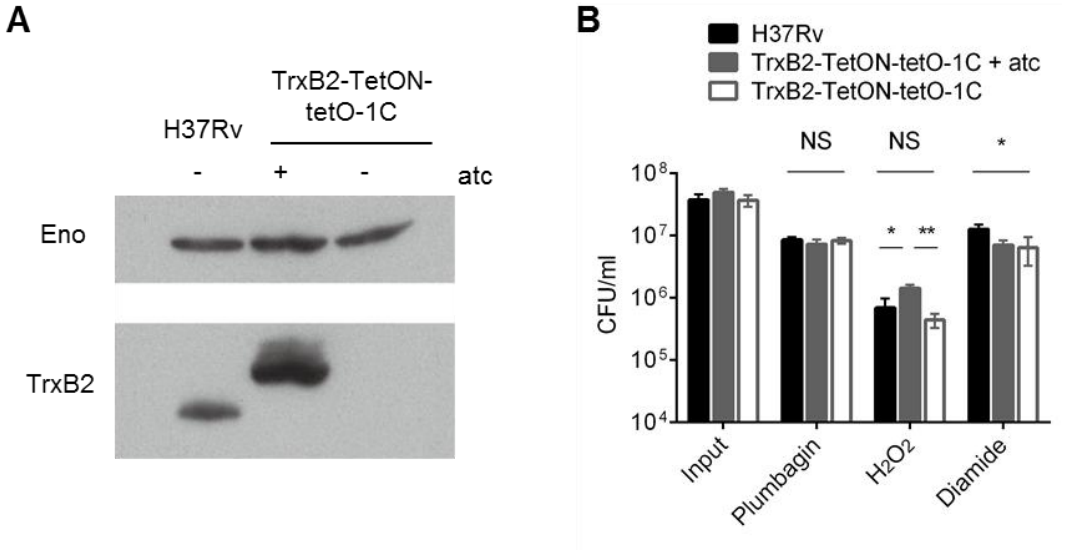

Figure 2.10 Susceptibility of partially TrxB2-depleted *Mtb* to oxidative stress.

(A) Immunoblot analysis of TrxB2 in protein extracts prepared from cultures used in (B). (B) TrxB2-TetON-tetO-1C mutant was cultured in the absence of atc for 3 days to decrease TrxB2 expression. *Mtb* strains were then exposed to 0.25 mM plumbagin for 5 h, to 5.4 mM H_2O_2 for 4 h or to 50 mM diamide for 8 h and bacterial survival was determined by CFU. * $p<0.05$, ** $p<0.01$, one way ANOVA was used for group comparison. Results are representative of three independent experiments.

2.3.6. TrxB2 depletion perturbs growth-essential pathways

We sought to investigate the pathways affected in TrxB2-depleted *Mtb* and analyzed the transcriptome changes associated with TrxB2 depletion. We found an early induction of 61 genes after 6 hours of atc treatment (fold change >2, p<0.02), 12 of which belong to sulfur metabolism pathways (Figure 2.11 A). *Mtb* converts imported inorganic sulfate into adenosine 5'-phosposulfate (APS), which can be used for metabolite sulfation (Hatzios and Bertozzi, 2011; Paritala and Carroll, 2013). Alternatively, APS can be sequentially reduced for the biosynthesis of essential sulfur-containing metabolites, including cysteine, methionine and mycothiol. The first committed step in this reductive branch, the conversion of sulfate to sulfide by APS reductase (*cysH*), requires reducing potential supplied by the thioredoxin system (Paritala and Carroll, 2013). We observed extensive up-regulation of sulfate importer genes (*cysT*, *cysW*, *cysA1* and *subI*) and genes in the reductive branch, including *cysH* and the O-acetylserine sulfhydrylase encoding *cysK1* and *cysK2*, which indicates a response to compensate for a defect in sulfur assimilation. Consistent with that, TrxB2 depletion also resulted in increased expression of *cysE*, encoding a serine acetyl transferase, which is required for *de novo* cysteine biosynthesis (Figure 2.11 A). The expression of sulfur metabolism genes remained induced at 24 hrs post atc treatment (Figure 2.11 B) and we asked whether death could be prevented or delayed by addition of reduced sulfur metabolites. A *cysH* deletion mutant was viable and had no growth defect, as long as it was supplemented with either 2 mM cysteine or methionine (Senaratne et al., 2006). However, neither cysteine nor methionine protected TrxB2-depleted *Mtb* from death, indicating that TrxB2 is

required for other essential pathways besides sulfur metabolism (Figure 2.11 C).

Indeed, among the most highly up-regulated genes after 24 h of TrxB2 depletion were those involved in DNA metabolism (Figure 2.11 B). We observed extensive up-regulation of genes involved in three DNA repair pathways, including base excision repair (*nei*, *alkA*, *ung*, *ogt* and *xthA*,), nucleotide excision repair (*ercc3*, *uvrA* and *uvrD2*), and homologous recombination (*recA*, *ruvA*and *ruvC*), suggesting that inhibition of TrxB2 was associated with DNA damaging stress. In support of this, we found that partial TrxB2 depletion decreased *Mtb's* tolerance to genotoxic stress caused by mitomycin C, a potent DNA crosslinker (Figure 2.11 D).

Of note, several genes involved in cell division were significantly down regulated in TrxB2-depleted *Mtb* (Figure 2.11 B) consistent with the observed cell elongation (Figure 2.5). The induction of antioxidant genes (*trxB1*, *trxC*, *thiX*, *ahpC*, *ahpD* and *mshA*) and *whiB3* encoding an intracellular redox sensor and regulator (Singh et al., 2009) further supports that TrxB2 depletion induces thiol-oxidizing stress.

Because DTT rescued survival of TrxB2-depleted *Mtb* (Figure 2.9 E and F) we investigated its impact on the transcriptional changes caused by TrxB2 depletion. DTT treatment alleviated most of the mRNA changes associated with TrxB2 depletion without affecting atc-mediated transcriptional silencing and proteolytic degradation of TrxB2 (Figure 2.12 and Figure 2.13). It reduced the expression of most antioxidant genes to basal levels, suppressed the induction of sulfur metabolism genes, reduced suppression of cell division

genes and decreased the activation of genes involved in DNA repair (Figure 2.13).

Together, these data demonstrate that death following TrxB2 depletion was caused by pleiotropic effects on a number of growth-essential pathways, including sulfur and DNA metabolism, and was mediated primarily through exhaustion of thiol-reducing power (Figure 2.14).

Figure 2.11 TrxB2 depletion perturbs growth-essential pathways.

(A) Heat-map representation of selected genes with mean expression fold changes >2 in TrxB2-DUC at 6 h post atc treatment (adjusted p<0.02 by one-way ANOVA). (B) Heat-map representation of selected genes with mean expression fold change >3 in TrxB2-DUC at 24 h post atc treatment (adjusted p<0.02 by one-way ANOVA). (C) Impact of extracellular cysteine and methionine on TrxB2 depletion-induced death. Atc-treated TrxB2-DUC cultures were supplemented with 2 mM cysteine, 2 mM methionine or both. CFU were determined at the indicated time points. (D) Impact of partial TrxB2 depletion on susceptibility of *Mtb* to mitomycin C. TrxB2-TetON-tetO-1C was cultured in 7H9 medium without atc for 3 days to decrease TrxB2 expression before treatment with mitomycin C. Data in (C) and (D) are means ± SD (n = 3 per group) and are representative of three independent experiments.

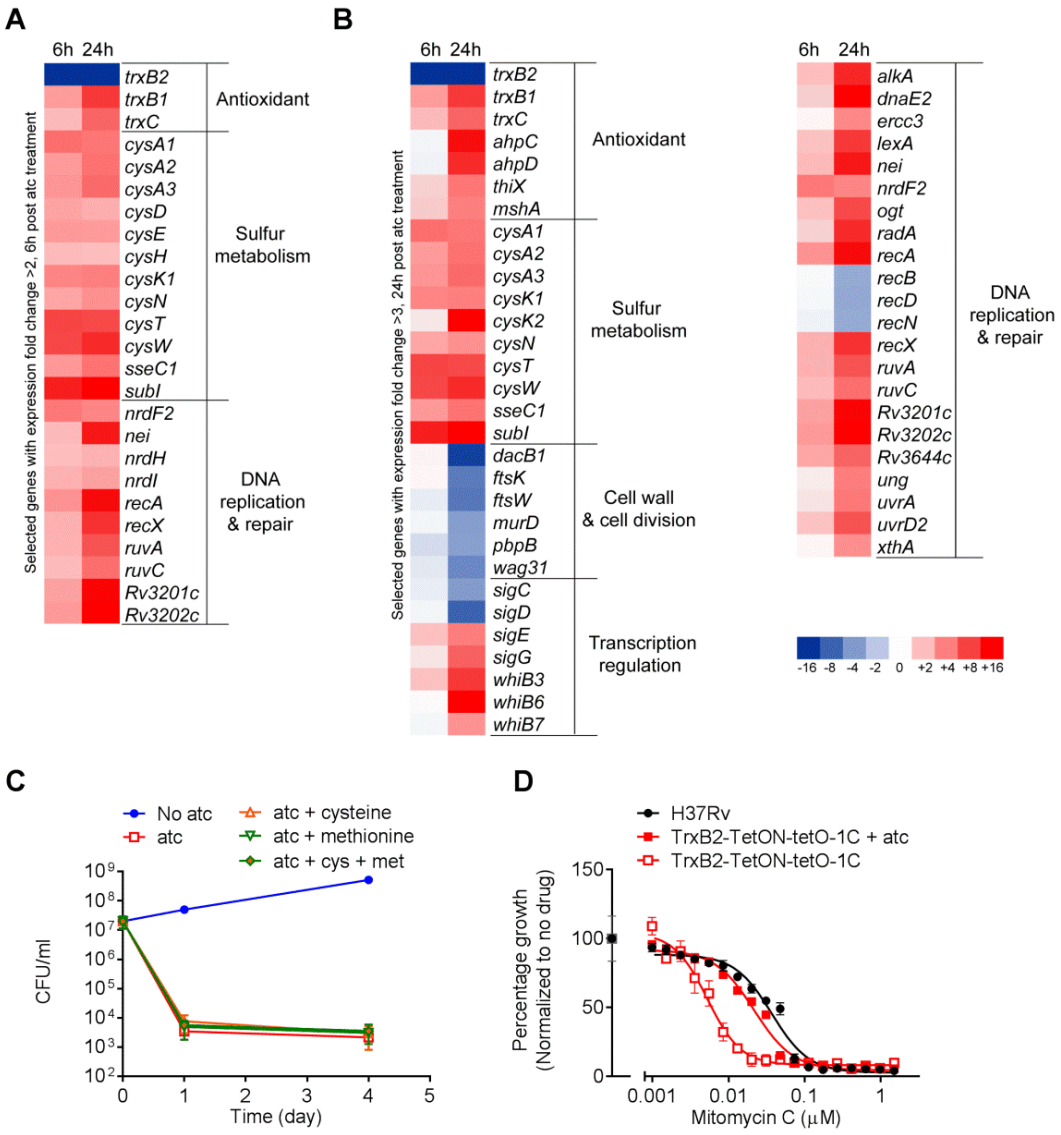
A
6h 24h
Selected genes with expression fold change >2, 6h post atc treatment
trxB2
trxB1
trxC
Antioxidant
cysA1
cysA2
cysA3
cysD
cysE
cysH
cysK1
cysN
cysT
cysW
sseC1
subI
Sulfur metabolism
nrdF2
nei
nrdH
nrdI
recA
recX
ruvA
ruvC
Rv3201c
Rv3202c
DNA replication & repair
B
6h 24h
Selected genes with expression fold change >3, 24h post atc treatment
trxB2
trxB1
trxC
ahpC
ahpD
thiX
mshA
Antioxidant
cysA1
cysA2
cysA3
cysK1
cysK2
cysN
cysT
cysW
sseC1
subI
Sulfur metabolism
dacB1
ftsK
ftsW
murD
pbpB
wag31
Cell wall & cell division
sigC
sigD
sigE
sigG
whiB3
whiB6
whiB7
Transcription regulation
6h 24h
alkA
dnaE2
ercc3
lexA
nei
nrdF2
ogt
radA
recA
recB
recD
recN
recX
ruvA
ruvC
Rv3201c
Rv3202c
Rv3644c
ung
uvrA
uvrD2
xthA
DNA replication & repair
-16 -8 -4 -2 0 +2 +4 +8 +16
C
No atc
atc
atc + cysteine
atc + methionine
atc + cys + met
CFU/ml
Time (day)
D
H37Rv
TrxB2-TetON-tetO-1C + atc
TrxB2-TetON-tetO-1C
Percentage growth (Normalized to no drug)
Mitomycin C (μM)

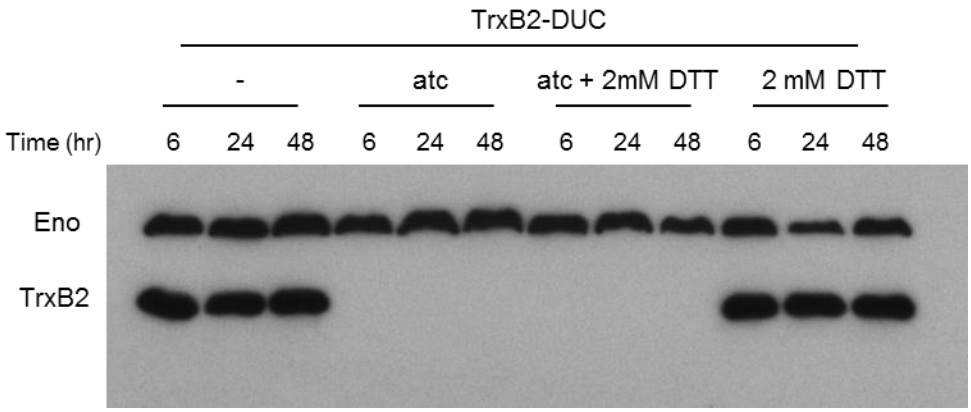

Figure 2.12 DTT treatment does not affect atc-mediated TrxB2 depletion in TrxB2-DUC.

Immunoblot of protein extracts from TrxB2-DUC with different treatment as indicated. Blot was probed with TrxB2-specific and Eno-specific (loading control) antisera.

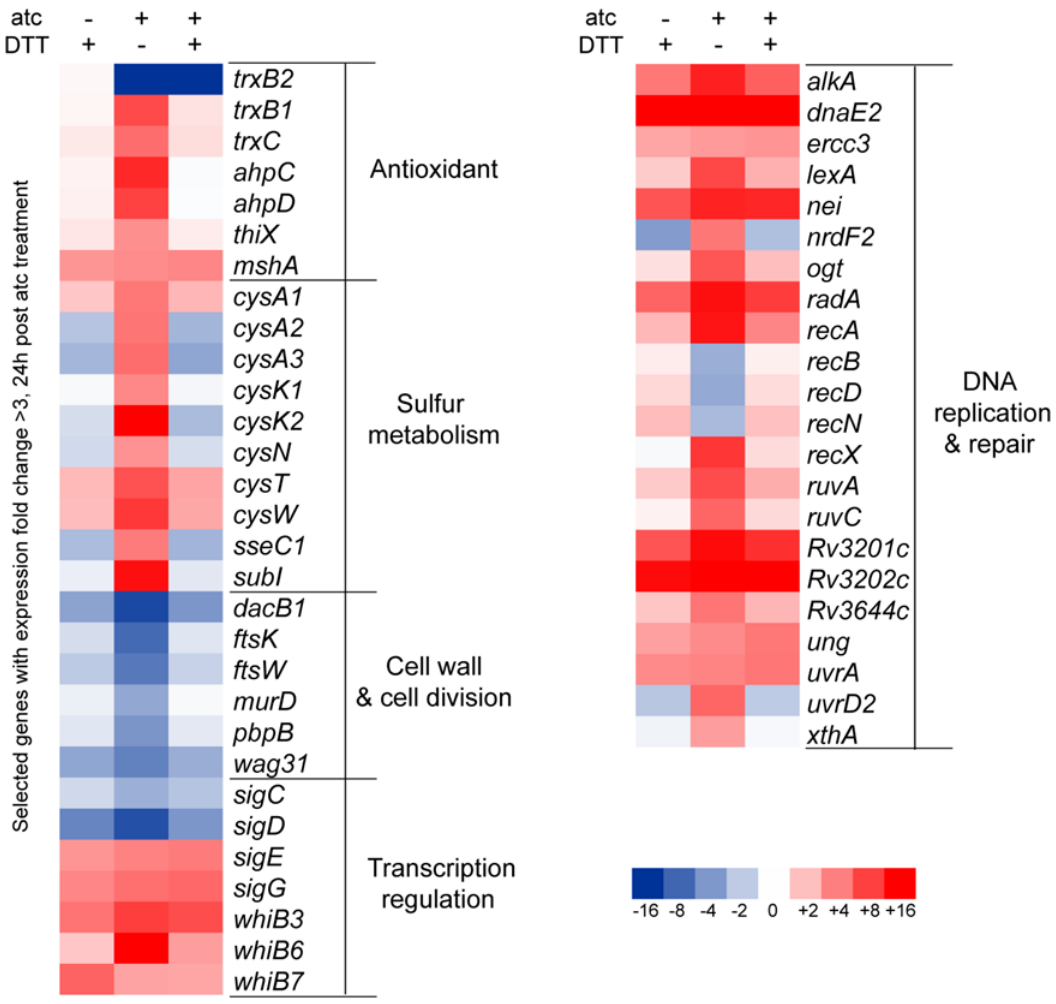

Figure 2.13 DTT mitigates the transcriptional impact of TrxB2 depletion.

Heat-map representation of expression level of fold-changes of selected genes in response to atc and DTT treatment. mRNA abundances in TrxB2-DUC treated with atc, DTT or both were compared to those in untreated TrxB2-DUC. One-way ANOVA was used for group comparison (n=3 per group), with Benjamini–Hochberg correction for multiple hypothesis testing. Selected genes with mean expression fold change >3 at 24 h post atc treatment are shown (adjusted $p<0.02$).

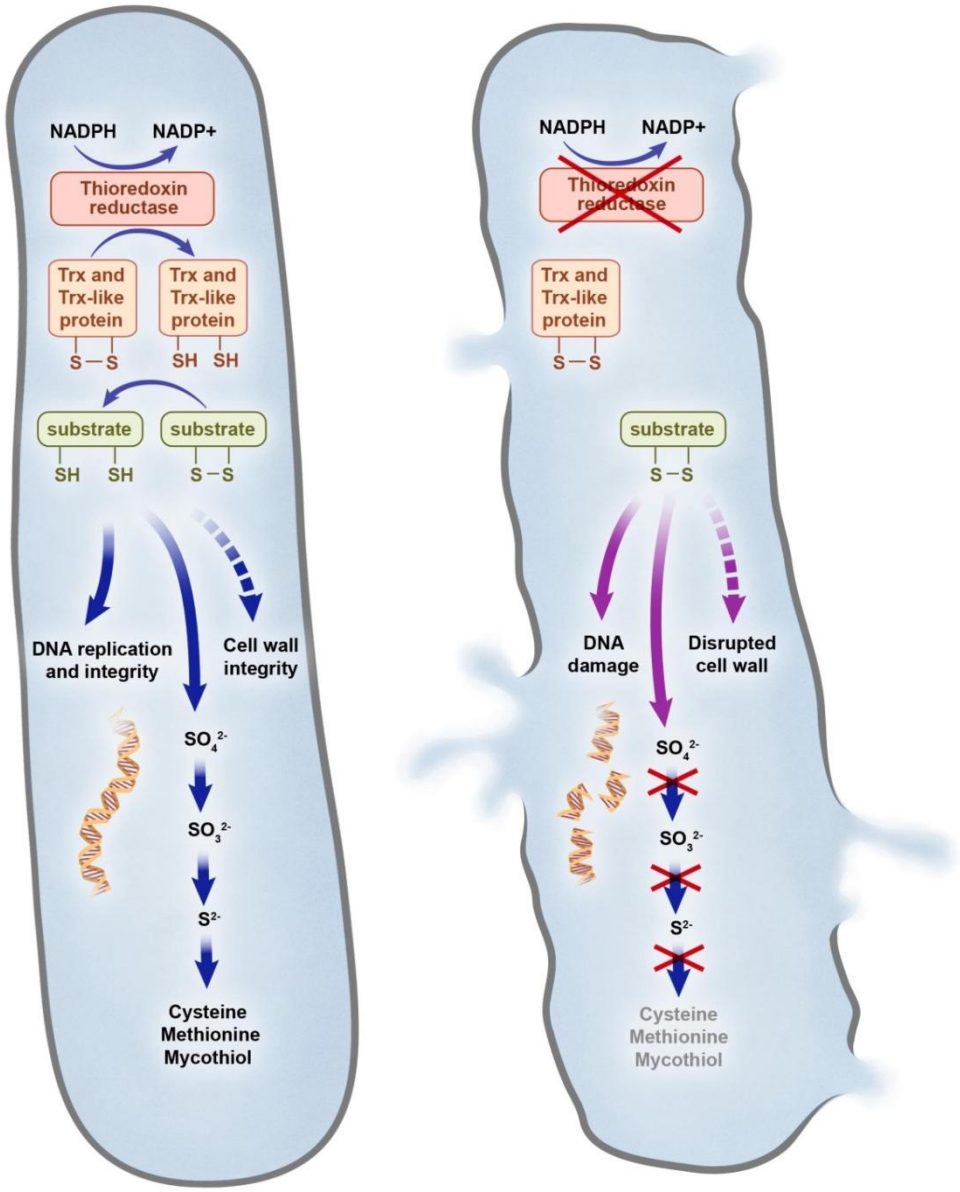

Figure 2.14 Proposed model for the activities of thioredoxin reductase in *Mtb*.

Mtb's thioredoxin system is composed of thioredoxin reductase (encoded by *trxB2*), thioredoxin (Trx) and NADPH. TrxB2 catalyzes the disulfide-thiol exchange of thioredoxins and thioredoxin-like proteins using electrons from NADPH. Thioredoxins and thioredoxin-like proteins are then able to reduce their substrates and maintain essential biological pathways, such as DNA replication, genome integrity, sulfur metabolism and cell wall processes. Loss of TrxB2 activity results in thiol-oxidizing stress, which damages DNA, perturbs sulfur metabolism, affects cell wall processes and leads to lysis of *Mtb*.

2.3.7. Impact of partial TrxB2 depletion on susceptibility of *Mtb* to antimicrobial compounds

We utilized the leaky TrxB2 knockdown mutants to evaluate the specificity of two thioredoxin reductase inhibitors, ebselen and auranofin. Ebselen is a substrate of mammalian thioredoxin reductase, a competitive inhibitor of thioredoxin reductase from *E. coli*, and inhibits growth of *Mtb* (Lu et al., 2013). *Mtb's* susceptibility to ebselen was, however, not altered by partial TrxB2 depletion suggesting that ebselen inhibits *Mtb* growth by affecting other targets (Figure 2.15 A). Auranofin, a gold-containing compound, was recently found to inhibit the enzymatic activity of *Mtb's* TrxB2 *in vitro* and to kill *Mtb* (Harbut et al., 2015). Partial depletion of TrxB2 caused a 3.6-fold shift of the MIC of auranofin and sensitized *Mtb* to killing by 0.65 µg/ml auranofin, a concentration that did not affect viability of wt *Mtb* (Figure 2.15 B and C). However, wt and mutant were killed similarly in the presence of a higher concentration of auranofin (Figure 2.15 C). Our data suggest that TrxB2 is one of the major targets of auranofin, although auranofin likely inhibits multiple enzymes with reactive cysteine residues in *Mtb*, such as mycothione reductase (Harbut et al., 2015).

To determine whether targeting TrxB2 sensitizes *Mtb* to other antimicrobial compounds, we screened the leaky TrxB2-TetON-1C mutant against a panel of antibiotics, including most of the first and second line anti-TB drugs. We found TrxB2-depleted *Mtb* highly susceptible to the cell wall biosynthesis inhibitors vancomycin and moenomycin (Figure 2.15 D and F). Moenomycin directly inhibits bacterial peptidoglycan glycosyltransferases, while vancomycin can block both transglycosylation and transpeptidation by binding to the

terminal D-Ala-D-Ala residues of the peptide stem (Ostash and Walker, 2005). Other inhibitors of peptidoglycan transpeptidation such as ampicillin, did not affect TrxB2-depleted *Mtb* more than wt *Mtb* (Figure 2.15 F). Thus inhibiting TrxB2 may impair transglycosylation, which could contribute to the lysis phenotype we observed. Unexpectedly, depleting TrxB2 decreased the MIC of rifampicin by 5.6 fold, suggesting that a compound that inhibits TrxB2 may synergize with this important first line anti-TB drug (Figure 2.15 E).

Figure 2.15 Impact of partial TrxB2 depletion on susceptibility of *Mtb* to antimicrobial compounds.

(A and B) Impact of partial TrxB2 depletion on susceptibility of *Mtb* to TrxB2 inhibitors ebselen (A) and auranofin (B). TrxB2-TetON-tetO-1C was washed and suspended in 7H9 medium without atc, then cultured for 3 days to decrease TrxB2 expression before treatment with ebselen or auranofin. OD_{580} was recorded and normalized to the corresponding strain without drug treatment. (C) Survival of strains after exposure to 0.65 μg/ml or 1.5 μg/ml auranofin. (D and E) Impact of partial TrxB2 depletion on susceptibility of *Mtb* to vancomycin (D) and rifampicin (E). (F) Heat-map representation of MIC_{90} shift of partially TrxB2 depleted *Mtb* to antimicrobial compounds. The MIC_{90}shifts are shown as the ratio of the MIC_{90} for H37Rv to the MIC_{90} for TrxB2-TetON-tetO-1C in the absence of atc. Data in (A) to (E) are means ± SD of three replicates and are representative of three independent experiments. Data shown in (F) are representative of at least two independent experiments.

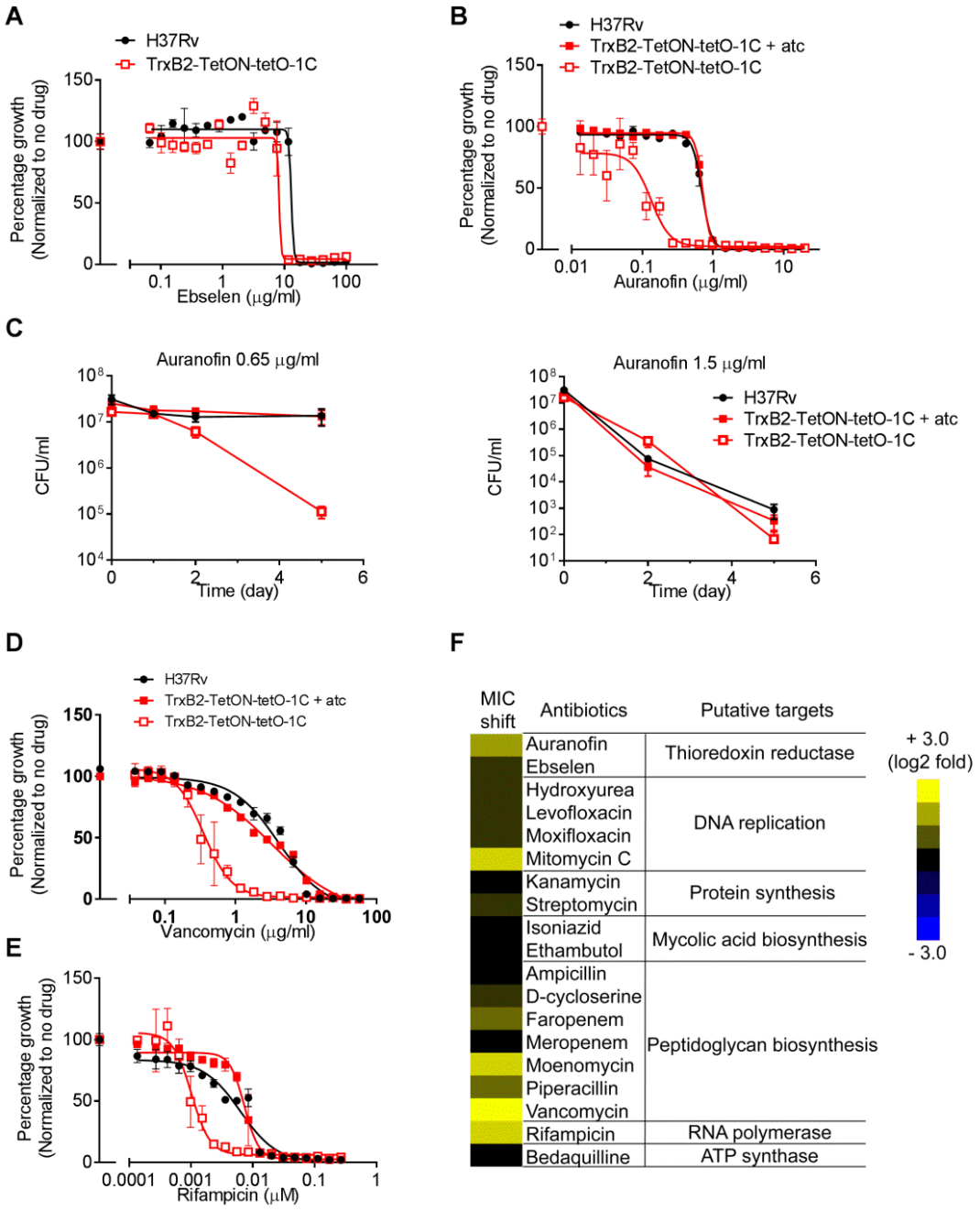
A
H37Rv
TrxB2-TetON-tetO-1C
Percentage growth (Normalized to no drug)
Ebselen (μg/ml)
B
H37Rv
TrxB2-TetON-tetO-1C + atc
TrxB2-TetON-tetO-1C
Auranofin (μg/ml)
C
Auranofin 0.65 μg/ml
CFU/ml
Time (day)
Auranofin 1.5 μg/ml
D
Vancomycin (μg/ml)
E
Rifampicin (μM)
F
MIC shift
Antibiotics
Putative targets
Auranofin
Ebselen
Thioredoxin reductase
Hydroxyurea
Levofloxacin
Moxifloxacin
Mitomycin C
DNA replication
Kanamycin
Streptomycin
Protein synthesis
Isoniazid
Ethambutol
Mycolic acid biosynthesis
Ampicillin
D-cycloserine
Faropenem
Meropenem
Moenomycin
Piperacillin
Vancomycin
Peptidoglycan biosynthesis
Rifampicin
RNA polymerase
Bedaquilline
ATP synthase
+ 3.0 (log2 fold)
- 3.0

2.3.8. High-throughput screening with leaky TrxB2-TetON mutants identified SKF867J as a potential TrxB2-specific inhibitor

To discover novel TrxB2-specific inhibitors, we collaborated with GlaxoSmithKline (Tres Cantos, Spain) to perform a high-throughput screening with TB Box, a focused library containing around 11,000 compounds that exhibit whole cell activity against *Mtb* (Figure 2.16). The cell-based screening identified 127 lead hits that were hyperactive against the leaky TrxB2-TetON-5C mutant. These hits were then tested for their potential 'on target' activity at a single concentration of 50 μM against the purified TrxB2 enzyme. In the enzymatic assay, TrxB2 catalyzes reduction of the substrate DTNB (5, 5'-dithiobis (2-nitrobenzoic) acid) to TNB (5-thio-2-nitrobenzoic acid) in presence of NADPH and TrxC. The product TNB generates a strong yellow color that can be detected at 412 nm. Six compounds (SKF867J, GSK602A, GW723X, GSK840A, GSK430A and GSK121A) exhibited modest to strong inhibition of TrxB2 enzymatic activity. Two of them (SKF867J and GSK602A) almost completely inhibited the reaction, and the other four compounds (GW723X, GSK840A, GSK430A and GSK121A) reduced the enzymatic activity by more than 40% at 50 μM concentration (Figure 2.17).

We next performed dose-response analysis for these six compounds and found four compounds (SKF867J, GSK602A, GW723X, and GSK430A) that inhibited TrxB2 enzymatic activity in a dose-dependent manner (Figure 2.18 A-E). SKF867J emerged as the best candidate among the four compounds, with an IC_{50} of 0.68 μM and an IC_{90} of 6.25 μM. We further confirmed the hyperactivity of SKF867J against TrxB2-silenced *Mtb*. Indeed, silencing TrxB2 decreased the MIC of SKF867J by 5.6 to 8.4 fold, confirming that SKF867J

inhibits *Mtb* growth by targeting TrxB2 (Figure 2.18 F). Through a combination of chemical genomics approach and biochemistry approach, we identified SKF867J as a potentially novel TrxB2-specific inhibitor. SKF867J potently inhibits TrxB2 enzymatic activity, with IC_{50} and IC_{90} values well below the levels needed to achieve its cellular effects (MIC_{50} values of 7.5 μM and MIC_{90} values of 15.15 μM).

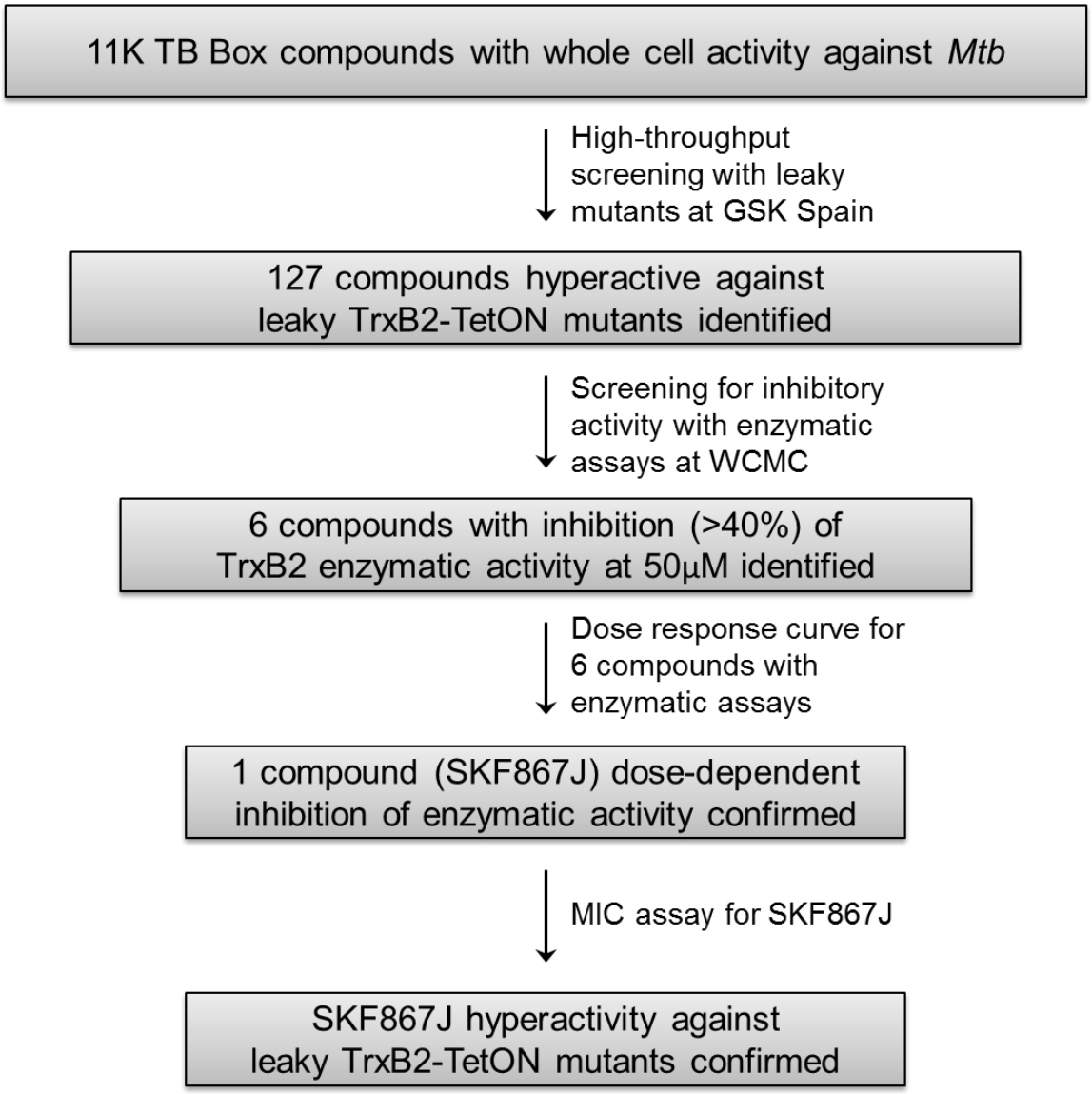

Figure 2.16 Workflow for the high-throughput screening to identify TrxB2-specific inhibitors

The high-throughput screening was performed by Shipra Grover at GlaxoSmithKline, Spain.

GSK697A	GSK215A	GSK902A	GSK257A	GSK636A	GSK114A	GSK595A	GSK038A
0.0%	12.7%	0.0%	0.0%	4.6%	0.0%	1.9%	19.7%
SKF867J	GSK831A	GSK362A	GSK808A	GSK632A	GSK289A	GSK581A	GSK602A
97.4%	35.2%	0.0%	10.8%	23.7%	0.0%	5.4%	100.0%
GSK597A	GSK547A	GSK295A	GSK027A	GW723X	GSK517A	GSK601A	GSK816A
0.0%	0.0%	0.0%	0.0%	53.7%	5.2%	0.0%	1.5%
GSK805A	GSK840A	GSK798A	GSK651A	GSK139A	GSK214A	GSK589A	GR746X
2.1%	47.5%	0.0%	0.0%	0.0%	0.0%	0.0%	16.0%
GSK517A	GSK647A	GSK846A	GSK826A	GSK197A	GSK987A	GSK765A	GSK299A
4.7%	3.6%	6.0%	0.0%	13.7%	0.0%	13.1%	1.5%
GSK037A	GSK586A	SB301	GSK028A	GSK748A	GSK475A	GSK791A	GSK959A
4.8%	3.5%	5.2%	5.9%	1.4%	0.0%	0.0%	5.3%
GSK353A	GSK773A	GSK018A	GSK891A	GSK577A	GSK361A	GSK460A	GSK180A
12.8%	5.6%	0.0%	0.0%	0.9%	11.1%	8.8%	0.0%
GSK793A	SB671	GSK804A	GSK633A	GSK766A	GSK825A	GSK376A	GSK697A
0.0%	16.6%	5.4%	2.5%	11.3%	0.0%	5.5%	0.0%
GSK141A	GSK047B	GSK326A	GSK195A	GSK560A	GSK438A	GSK769A	GSK689A
1.5%	0.0%	0.0%	0.0%	9.8%	3.3%	2.0%	1.9%
GSK991A	GSK728A	GSK877A	GSK261A	GSK862A	GSK724A	GSK206A	GSK703A
0.0%	5.4%	7.8%	0.2%	1.1%	0.0%	0.0%	0.0%
GSK659A	GSK180A	GSK388A	GSK752A	SB308	GSK789A	GSK780A	BRL002GM
5.2%	9.0%	6.5%	8.0%	0.0%	0.6%	0.0%	26.8%
GSK597A	SB119	GSK045A	GSK470A	GSK430A	GSK317A	GSK138A	GSK860A
0.0%	20.2%	0.0%	0.0%	41.6%	22.4%	0.0%	0.0%
GSK598A	GSK753A	GSK582A	GSK677A	GSK011A	GSK010A	GSK587A	GSK002A
0.0%	0.0%	0.0%	0.0%	2.1%	0.0%	0.0%	6.1%
GSK782A	GSK045A	GSK001A	GSK969A	GSK821A	GSK044A	GSK384A	GR839X
4.6%	9.0%	8.2%	0.0%	5.5%	1.9%	0.0%	0.0%
GSK655A	GSK729A	GSK710A	GSK644A	GSK908A	GSK121A	GSK892A	GSK500A
0.0%	7.7%	0.0%	0.0%	0.4%	40.2%	17.4%	1.5%
GSK932A	SB024	GSK863A	GSK886A	GSK678A	GSK048A	GSK584A	EBS
0.0%	3.9%	8.1%	0.0%	8.7%	5.7%	0.3%	100.0%

Figure 2.17 Inhibition of 127 lead compounds against TrxB2 enzymatic activity at 50 μM concentration

Purified recombinant TrxB2 was preincubated with or without inhibitors for 30 min. Reactions were initiated by the addition of mixture containing NADPH, TrxC and DTNB. The final concentration of each inhibitor in the reaction was 50 μM. The change in absorbance at 412 nm within the first 15 mins of reaction was monitored. The numbers shown depict the percentage of inhibition of the maximum rate of reaction within 15 mins by the compounds. Negative control assays (0% inhibition) were conducted in the absence of inhibitors. Ebselen was used as a positive control for the inhibition of TrxB2 enzymatic activity. Data are representative of three independent experiments.

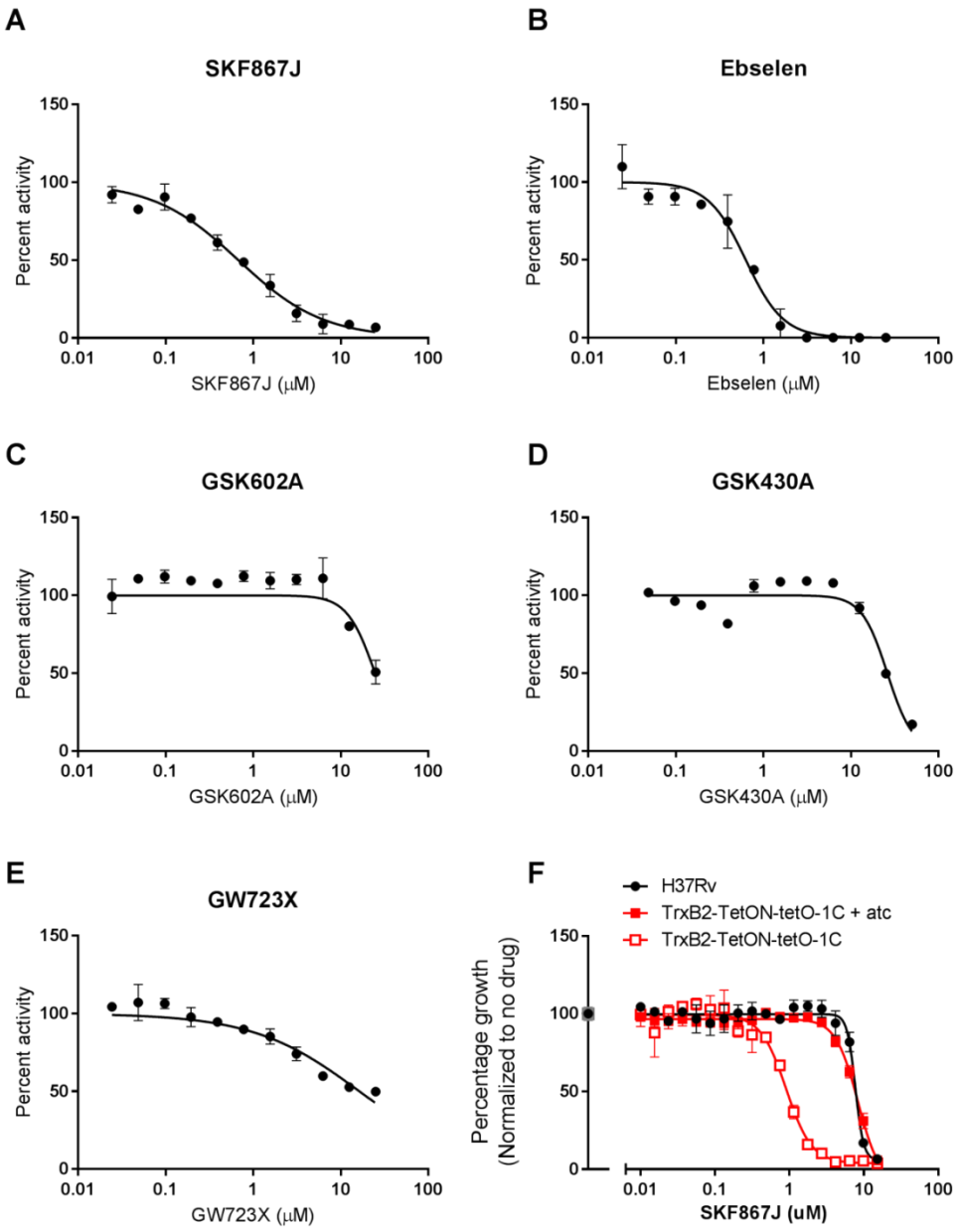

Figure 2.18 SKF867J inhibits *Mtb* growth through targeting TrxB2.

(A-E) Dose–response curves of SKF867J (A), Ebselen (B), GSK602A (C), GSK430A (D) and GW723X (E) on TrxB2 enzymatic activity. Ebselen is used as a positive control. (F) Impact of partial TrxB2 depletion on the susceptibility of *Mtb* to SKF867J. Data in (A) to (E) are means ± SD of three replicates and are representative of three independent experiments.

2.4. Discussion

2.4.1. TrxB2 is a valuable target to develop novel antimycobacterial compounds

The paucity of targets that are both biologically validated and susceptible to inhibition by drug-like small molecules, i.e. “druggable”, is a major bottleneck in antimycobacterial drug development. *Mtb*’s thioredoxin reductase TrxB2 has recently been shown to be druggable, yet its biological evaluation has not advanced beyond the prediction of its essentiality for growth of *Mtb* on standard agar plates (Harbut et al., 2015). Auranofin inactivates thioredoxin reductase *in vitro* but has multiple targets in bacteria, including in *Mtb* (Harbut et al., 2015; Thangamani et al., 2016). It was thus unknown how the specific inhibition of TrxB2 would affect *Mtb* in different environments including those encountered during acute and chronic infections. We addressed these questions using genetic strategies and found that inactivating TrxB2 quickly cleared *Mtb* during the acute and, importantly, the chronic phase of mouse infection, validating TrxB2 as a valuable target for therapeutic intervention.

It is noteworthy to point out while TrxB2 depletion quickly reduced the number of bacilli to an undetectable level in multiple organs (including lungs, spleens, kidneys and bones), a substantial proportion of the mice relapsed spontaneously or upon immunosuppression. This observation suggests that TrxB2 inactivation by treating with doxy-containing food did not completely eradicated viable bacteria in the host, despite the culture-negative state. Instead, some bacilli may enter the state of ‘viable but non-culturable’ (VBNC) and become invulnerable to TrxB2 depletion (Nathan and Barry, 2015). However, this does not preclude TrxB2 from being an attractive drug target for

several reasons. First, the relapse experiment that we performed in section 2.3.4 has not been routinely incorporated by other researchers in the studies to identify novel antimycobacterial drug targets. Therefore, it is hard to draw comparison between TrxB2 and other targets in terms of the relapse rate. Second, it remains to be determined whether there are bacterial reservoirs in the host that are not accessible to doxy treatment, as the complete profile of doxy distribution *in vivo* is still not clear. It is thus possible that culturable bacilli stayed alive in the reservoirs that were not regularly examined when we applied doxy treatment. Upon the cessation of treatment, those bacteria disseminated to lungs and spleens and caused disease relapse, even though they were still susceptible to killing by TrxB2 depletion. In this scenario, the relapse is due to incomplete doxy penetration in the tissues, rather than the bacteria that survive TrxB2 depletion. For example, *Mtb* can travel through the bloodstream to the brain and cause meningeal tuberculosis, a type of extrapulmonary TB, while brain infection is not examined in most TB models (Thwaites et al., 2013). Third, reactivation of infection has been widely observed in murine models of TB latency, even after administration of frontline anti-TB drugs. The rate of disease relapse depends on a number of factors, such as the chemotherapy regiment, duration of treatment, and host immune state. For example, a 4-week treatment with rifampicin and isoniazid reduced the bacterial load to an undetectable level, but the infection spontaneously reactivated 8 weeks after therapy (Botha and Ryffel, 2002, 2003). The therapy of isoniazid and pyrazinamide also leads to highly variable outcomes. The spontaneous reactivation rate ranged from 0 to 50%, depending on the route of infection, the treatment dosing and duration (Scanga et al., 1999). Despite the observed disease reactivation in murine models, the four first-line anti-TB

drugs (isoniazid, rifampicin, ethabutol and pyrazinamide) are highly successful in treating TB and prevent reactivation when used in combination. Therefore, the high reactivation rate based on the monotherapy by TrxB2 depletion doesn't void the value of targeting TrxB2 to treat tuberculosis.

TrxB2 depletion drastically impairs the viability of both replicating and non-replicating *Mtb* in culture. Inactivation of TrxB2 *in vivo* quickly reduces bacterial load to an undetectable level during both acute and chronic phases of infection. In addition, deliberately leaky TrxB2 knockdown mutants revealed that a TrxB2 inhibitor may synergize with rifampicin. Treatment combinations of rifampicin and a TrxB2 inhibitor could thus reduce the required drug dosage and limit the frequency of resistant mutants as shown for the synergistic action of carbapenems and rifampicin (Kaushik et al., 2015). Furthermore, the catalytic mechanisms of mammalian and bacterial thioredoxin reductases are significantly different and the crystal structure of TrxB2 has been solved (Akif et al., 2005; Lu and Holmgren, 2014). There are *in vitro* biochemistry assays to screen for inhibitors of TrxB2 enzymatic activity available and relatively easy to perform. With the construction of leaky TrxB2-TetON mutants, TrxB2 should be listed as a target with high priority, considering its importance in *Mtb* physiology and pathogenesis and the availability of tools for inhibitor development.

2.4.2. Leaky TetON mutants provide powerful tools to facilitate drug development and study essential gene functions

In addition to revealing the synergy between targeting TrxB2 and rifampicin, we used a deliberately leaky TrxB2 knockdown mutant to determine the

specificity of two TrxB2 inhibitors. The MIC of ebselen was not affected by partial TrxB2 depletion, suggesting that ebselen inhibits *Mtb* growth primarily through targets other than TrxB2. Ebselen has been shown to bind covalently to a cysteine residue located near the antigen 85 complex (Ag85C) active site and may thereby disrupt the biosynthesis of the mycobacterial cell envelope (Favrot et al., 2013; Favrot et al., 2014). Auranofin was significantly more active against TrxB2-depleted *Mtb* than wild type indicating that it exerts its antimycobacterial activity at least partially through inhibiting TrxB2. However, auranofin exhibits a higher affinity for human thioredoxin reductase than for bacterial enzymes (Gromer et al., 1998). Furthermore, auranofin, an FDA-approved anti-rheumatic drug, has immunosuppressive activities by inhibiting NF-κB signaling and decreasing the production of nitric oxide and pro-inflammatory cytokines, which are critical for anti-TB immune responses (Han et al., 2008; Jeon et al., 2000). It also has anti-tumor activity through inhibition of proteasome-associated deubiquitinases (Liu et al., 2014; Madeira et al., 2012; Mirabelli et al., 1985).

To identify inhibitors that are more specific for TrxB2 than auranofin, we utilized the leaky TrxB2 mutants to screen a library containing 11,000 compounds with whole cell activity against *Mtb* and identified 127 lead compounds. Although all these leads are hyperactive against TrxB2 hypomorph in the screen, only one compound SKF867J was confirmed to potently inhibit TrxB2 enzymatic activity in a dose-dependent manner and the other three exhibit modest inhibition. TrxB2-silenced *Mtb* are hypersusceptible to a number of compounds that do not inhibit TrxB2 activity, which may be due to the pleiotropic effect caused by TrxB2 depletion. Numerous growth-

essential pathways were affected by the lack of thiol-reducing power, including sulfur and DNA metabolism pathways and cell wall processes. In support of this, TrxB2-silenced *Mtb* becomes highly sensitive to DNA replication inhibitor mitomycin C and peptidoglycan inhibitors vancomycin. We can speculate some of these 127 compounds may actually target these essential pathways and therefore demonstrate hyperactivity.

SKF867J is a good candidate for TrxB2-specific inhibitor, with IC_{50} and IC_{90} values well below the concentrations required to achieve its whole cell activity. Its MIC_{90} (15.15 μM) falls in a reasonable starting range to further optimize this compound. We are now collaborating with GSK Spain to obtain the structure information of SKF867J, and plan to test its cidality on *Mtb*, cellular cytotoxicity and antimycobacterial activity on *Mtb* inside macrophages. To further validate SKF867J as a TrxB2-speficic inhibitor, we need to test its selectivity against human thioredoxin reductase and analyze its impact on the *Mtb* transcriptomic profiles to see whether it resembles that in TrxB2-deplete *Mtb*. We will also continue analyzing other hit analogues generated by GSK medicinal chemists to identify TrxB2 inhibitors with better potency and selectivity.

2.4.3. TrxB2 is essential for thiol redox homeostasis but plays a minor role in antioxidant defense

In addition to determining TrxB2's value as a potential target for drug development we wanted to gain insights into the physiological functions of TrxB2, especially its role in detoxifying oxidative stress. TrxB2 expression is induced upon oxidative and nitrosative stress and purified TrxB2 can mediate

the reduction of H_2O_2, peroxide, and dinitrobenzene (Jaeger et al., 2004; Zhang et al., 1999). However, TrxB2-depleted *Mtb* was hypersensitive specifically to thiol-oxidizing stress, but not to other types of oxidants, and the thiol reductant DTT prevented death caused by TrxB2 depletion. DTT did not promote growth of TrxB2-depleted *Mtb*, likely because DTT is very labile in neutral aqueous solution and it is therefore difficult to maintain a constant concentration over time. Alternatively, TrxB2 has a function beyond its enzymatic activity, which is required for optimal growth and cannot be replaced by DTT. Notwithstanding, these results indicate that the primary function of TrxB2 in *Mtb* is to detoxify thiol-specific oxidative stress. Its potential role in defending against H_2O_2, superoxide and nitrosative stress is likely redundant with other antioxidant systems.

Mycothiol, a low-molecular-weight thiol present in millimolar quantities in mycobacterial cells, is thought to function as the mycobacterial substitute for glutathione and serve as the major redox buffer system in *Mtb* (Newton et al., 1996). *Mtb* mycothiol-deficient mutants have a dramatically reduced intracellular thiol concentration, require catalase for optimal growth *in vitro* and exhibit increased sensitivity to oxidants. However, they are viable *in vitro* and only slightly attenuated in immunecompetent mice (Buchmeier et al., 2006; Vilcheze et al., 2008). In contrast, TrxB2 depletion caused rapid lytic death even in the absence of exogenous oxidative stress and death was only prevented by DTT, but not catalase, cysteine and glutathione. Furthermore, TrxB2-depleted *Mtb* was unable to establish and maintain infection in mice. These phenotypic differences between mutants of the two major mycobacterial thiol-reducing systems emphasize that the TrxB2-dependent

system provides the dominant thiol-reducing source to maintain thiol redox homeostasis. Recently, upregulation of thioredoxin genes in mycothiol deficient *Mtb* has been observed supporting that the thioredoxin system can restore mycothiol (Attarian et al., 2009; Saini et al., 2016). Some genes involved in DNA and sulfur metabolism were also differentially expressed in both mycothiol and ergothioneine deficient *Mtb* (Saini et al., 2016), however, the majority of these was down regulated, while we found them induced in response to TrxB2 depletion. Thus, while some relationships exist between ergothionine, mycothiol and the thioredoxin system, they represent to a large degree systems with distinct activities in maintaining redox balance.

Depriving thiol-reducing power via TrxB2 depletion affected numerous essential processes, including sulfur and DNA metabolism pathways. The conversion of sulfate to sulfide by APS reductase (CysH) requires reducing potential from the thioredoxin system, which may explain why TrxB2 depletion induced extensive up-regulation of the genes involved in cysteine biosynthesis (Hatzios et al., 2011; Paritala and Carroll, 2013). TrxB2 depletion also strongly induced three different mycobacterial DNA repair pathways and consistent with this caused hypersusceptibility to the genotoxic drug mitomycin C. Ribonucleotide reductase (RNR) requires reducing power from the thioredoxin system to catalyze the reduction of NTP to dNTP (Nordlund and Reichard, 2006), but TrxB2 depletion did not lead to increased sensitivity to the RNR inhibitor hydroxyurea. This is possibly due to the presence of both class I and class II RNRs in *Mtb* while hydroxyurea only inhibits class I RNR (Torrents, 2014). It is also possible that other DNA biosynthesis and repair

enzymes rely on the thioredoxin system, a hypothesis we are currently investigating.

Surprisingly, we found that TrxB2 depletion lysed replicating *Mtb*. We observed significant cell elongation preceding lytic death consistent with the observed down-regulation of cell division genes. TrxB2-depleted *Mtb* was also highly susceptible to the peptidoglycan glycosyltransferases inhibitors moenomycin and vancomycin, but not to inhibitors of peptidoglycan transpeptidation, mycolic acid synthesis and arabinogalactan synthesis. We speculate that some enzymes or regulatory proteins involved in transglycosylation may depend on the thioredoxin system to maintain their intracellular redox states and function. Inactivation of TrxB2 may impair transglycosylation and thereby contribute to bacterial lysis. This observation also suggests a connection between redox-homeostasis and cell-envelope integrity in *Mtb*. We can therefore not exclude that TrxB2 depletion caused increased permeability to the sensitized compounds, although TrxB2-depletion did not cause susceptibility to all high molecular weight antibiotics.

In summary, our work identified TrxB2 as the dominant thiol-reducing enzyme in *Mtb* and refined understanding of its physiological roles in defending against thiol-oxidative stress and maintaining growth-essential pathways. Our results establish the importance of TrxB2 in *Mtb* pathogenesis and validate the enzyme as a drug target. The leaky TetON mutants we developed will facilitate target-based whole cell screens for the identification of TrxB2 inhibitors and can help maintaining on-target activity during drug development. We expect this strategy of partial transcriptional silencing to be widely applicable and to

facilitate chemical-genetic interaction studies for other growth-essential proteins in *Mtb* and other pathogens.

2.5. Materials and Methods

Ethics statement

All animal experiments were performed following National Institutes of Health guidelines for housing and care of laboratory animals and performed in accordance with institutional regulations after protocol review and approval by the Institutional Animal Care and Use Committee of Weill Cornell Medical College (Protocol Number 0601-441A).

Strains, media and culture conditions

Wild type *Mtb* (H37Rv) and its derivative strains were grown in Middlebrook 7H9 medium supplemented with 0.2% glycerol, 0.05% Tween-80, 0.5% BSA, 0.2% dextrose and 0.085% NaCl or on Middlebrook 7H10 agar containing OADC (Becton Dickinson and Company) and 0.5% glycerol. For growth of the TrxB2 leaky mutants, the above media were supplemented with 400 ng/ml anhydrotetracycline.

Construction of mutant strains

To generate *Mtb trxB2*-DUC, we first transformed wild type *Mtb* H37Rv with an attL5-site integration plasmid expressing *trxB2* and *trxC* under the control of P750 promoter to obtain a merodiploid strain; *trxB2* and the first 4 bps

of *trxC* (the OFR of *trxB2* overlaps with the first 4 bps of *trxC* ORF) were then deleted from the merodiploid strain by allelic exchange as previously described (Puckett et al., 2014; Schnappinger et al., 2015). After confirming deletion of the native copy of *trxB2* by Southern blot, we performed replacement transformations of attL5 inserts to generate TrxB2-DUC (Kim et al., 2013). In the TrxB2-DUC mutant, TrxB2 was expressed under the control of a TetOFF promoter and with a C-terminal DAS+4 tag. We also introduced a copy of *trxC* under the control of its native promoter to the attL5 site of TrxB2-DUC. The leaky TrxB2-TetON mutants were generated by replacement transformation of *Mtb* Δ*trxB2*::P750-*trxB2-trxC* with plasmids containing *trxB2*under the control of leaky tet promoters. A copy of *trxC* under the control of its native promoter was also introduced to the attL5 site of leaky TrxB2-TetON mutants.

Essentiality test of TrxB2 and TrxC for *in vitro* growth

We transformed *Mtb ΔtrxB2*::P750-*trxB2-trxC* mutant with zeocin resistant plasmids expressing *trxB2* and *trxC*, *trxB2*, *trxC* or vector control. The transformants were selected on zeocin containing 7H10 agar. *ΔtrxC* was isolated from *Mtb ΔtrxB2*::P750-*trxB2-trxC*transformed with the plasmid expressing only *trxB2*.

Survival of *Mtb* during nonreplicating conditions

The PBS starvation assay was set up as previously described (Kim et al., 2013). Bacteria were grown in 7H9 medium to mid-log phase, washed three times with PBST, and suspended in PBST. After incubation for 10 d, atc was

added to the cultures of TrxB2-DUC, and CFU were determined by plating on 7H10 plates.

Immunoblotting analysis of cytosolic proteins

We prepared cell lysates from mid-log phase culture by bead-beating cell pellets in lysis buffer (50 mM Tris HCl pH 7.4, 150mM NaCl and 2mM EDTA) containing protease inhibitor cocktail (Roche). We then centrifuged the lysates at 13,000 rpm for 20 min and sterilized the supernatant by passing through 0.22 µm Spin-X filters (Costar). 30–60 µg total protein were separated by SDS–PAGE and transferred to nitrocellulose membranes for probing with rabbit antisera against *Mtb* TrxB2, enolase (Eno), proteasome beta subunit (PrcB) and dihydrolipoamide acyltransferase (DlaT). Recombinant full-length Eno and TrxB2 were expressed with a C-terminal His tag, purified and used as antigen for immunization of rabbits.

Analysis of bacterial lysis by immunoblotting

Culture filtrates were prepared as follows. *Mtb* strains were grown in 7H9 medium with 0.2% glycerol, 0.05% Tween-80, 0.5% BSA, 0.2% dextrose and 0.085% NaCl until the culture reached an OD of 0.6 ~ 0.8. Cultures were then washed three times with PBS to remove BSA and Tween-80. We next suspended the pellet in 7H9 medium supplemented with 0.2% glycerol, 0.2% dextrose and 0.085% NaCl. After incubation, culture supernatant was harvested by centrifugation and filtration through 0.22 µm filters. Filtrates were concentrated 100-fold by using 3K centrifugal filter units (Millipore) and analyzed by immunoblotting with antisera against DlaT, Eno, PcrB and Ag85B (Abcam, ab43019).

Mouse infections

We infected female C57BL/6 mice (Jackson Laboratory) using an inhalation exposure system (Glas-Col) with mid-log phase *Mtb* to deliver approximately 200 bacilli per mouse. Mice received doxycycline containing mouse chow (2,000 ppm; Research Diets) starting at the indicated time-points. Lungs and spleens were homogenized in PBS, serially diluted and plated on 7H10 agar to quantify CFU. Upper left lung lobes were fixed in 10% buffered formalin, embedded in paraffin and stained with hematoxylin and eosin.

Gene expression analysis by microarray

For transcriptome analysis of TrxB2-depleted *Mtb*, we grew TrxB2-DUC in 7H9 medium to an OD of 0.5~0.6 and then added 400 ng/ml atc. Samples were collected at 6 hr and 24 hr later. Each experiment was performed with at least three independent cultures. To determine the impact of DTT, TrxB2-DUC was treated with atc, DTT (2 mM) or both for 24 hrs. Microarray analysis was performed as previously described (Goodsmith et al., 2015). Cultures were mixed at a 1:1 ratio with GTC buffer containing guanidinium thiocyanate (4 M), sodium lauryl sulfate (0.5%), trisodium citrate (25 mM), and 2-mercaptoethanol (0.1 M) and pelleted by centrifugation. Bacterial RNA was isolated and labeled using a Low Input Quick Amp Labeling Kit (Agilent) according to the manufacturer's instruction. Custom-designed *Mtb* H37Rv whole genome microarray (GEO platform GPL16177) were used. Analysis and clustering were performed with Agilent GeneSpring software. One-way ANOVA was used to compare microarray data, with Benjamini–Hochberg correction for multiple hypothesis testing. All the data have been deposited in the GEO

database with the accession numbers GSE72328, GSE72329, GSE72330 and GSE78894.

Stress assays

For oxidative stress, *Mtb* strains were grown to mid-log phase and washed twice in 7H9 medium. Bacterial single cell suspension was then prepared by centrifuging the cultures at 800 g for 10 min to remove clumps. We then adjusted the OD to 0.03, treated *Mtb* strains with H_2O_2, plumbagin, diamide or acidified nitrite and determined CFU by plating.

Antibiotic sensitivity assays

Mtb was grown to mid-log phase and diluted to an OD of 0.03 in 7H9 medium. Bacteria were then exposed to 1.5-fold serial dilution of antimicrobial compounds. Optical density was recorded after 14 days and normalized to the corresponding strains without drug treatment. Minimum inhibitory concentration is defined as the lowest concentration of a drug at which bacterial growth was inhibited at least 90%, as compared to the control containing no antimicrobial compounds. Ampicillin, auranofin, D-cycloserine, ebselen, ethambutol, faropenem, hydroxyurea, isoniazid, kanamycin, levofloxacin, meropenem, mitomycin C, moxifloxacin, piperacillin, rifampicin, streptomycin and vancomycin were purchased from Sigma Aldrich, St. Louis, MO. Moenomycin was from Santa Cruz Biotechnology. Bedaquilline was received as a gift from C. Barry.

Purification of TrxB2 and TrxC

The open reading frames of TrxB2 and TrxC were amplified from *Mtb* genomic DNA and cloned into the expression vector pEN300-NT. The plasmids were transformed into Escherichia coliBL21 (DE3) cells for expression. Cultures were grown at 37 °C to an OD_{600} of 0.6 prior induction with 0.6 mM Isopropyl β-D-1-thiogalactopyranoside (IPTG). Then the culture was left to incubate overnight at 16 °C. The cells were harvested and resuspended 50mM Tris-HCl pH 7.4 300mM NaCl, 10mM imidazole, 1mg/ml lysozyme and 1mM DTT with protease inhibitor cocktail (Roche) prior to lysis by sonication. DNase I was added after sonication and incubated with the lysate for 30min at 4 °C. The lysate was by passing through 0.45 µm filters.

The cleared lysate was incubated with washed Ni-NTA agarose for one hour while shaking at 4°C. After applying the beads to a polypropylene column, non-specifically bound proteins were removed by washing with washing buffer I (50mM Tris-HCl pH 7.4, 300mM NaCl, 20mM imidazole) and washing buffer II (50mM Tris-HCl pH 7.4, 300mM NaCl, 50mM imidazole). The protein was eluted in elution buffer (50mM Tris-HCl, pH 7.4, 300mM NaCl, 500mM imidazole). Fractions of the protein were collected and analysed by SDS–PAGE before being pooled together and dialysed overnight 25mM Tris-HCl pH 7.4, 50mM NaCl, to remove the imidazole. The purified proteins were concentrated using Amicon Ultra 10 kDa and 3 kDa for TrxB2 and TrxC respectively. Purified proteins were frozen with 5% glycerol at -80 °C for long-term storage.

TrxB2 enzymatic assay

Briefly 40nM purified recombinant TrxB2 was preincubated with drugs or DMSO control at RT for 30min in the reaction buffer containing100 mM phosphate buffer, pH 7.4, 2 mM EDTA. Then reactions were initiated by the addition of mixture containing NADPH, TrxC and 5–5′-dithiobis-(2-nitrobenzoic acid) (DTNB) . The final reaction system contains 20nM TrxB2, 10 μM TrxC, 100 μM DTNB,100 μM NADPH in 100 mM phosphate buffer, pH 7.4, 2 mM EDTA. The progress of the reactions was monitored at 412 nm against a blank control for 15 min at 25°C with a final volume of 100 μl on a Spectramax M5 plate reader. TrxB2 enzymatic activity was obtained by measuring the initial rate of DTNB reduction of during the first 15min of the reaction. Other negative controls include samples missing either TrxB2 or TrxC in the final reaction system.

Statistical analysis

One-way ANOVA was used for multiple group comparisons. Two-tailed unpaired Student's t test was used for the analysis of differences between two groups. Statistical significance was defined as $P < 0.05$ unless otherwise stated. No statistical methods were used to predetermine sample size.

CHAPTER 3

EXPLOITING INDUCIBLE BACTERIAL LYSIS TO DEVELOP NOVEL TUBERCULOSIS VACCINES

3.1. Introduction

Mycobacterium tuberculosis (*Mtb*) remains a major threat to global health. Ultimate control of *Mtb* is not achievable without effective vaccines. The most widely used tuberculosis (TB) vaccine, the Bacillus Calmette–Guérin (BCG) vaccine, does not provide effective protection against pulmonary TB. Current failures in TB vaccine development can be attributed in part to the lack of important virulence factors required to mediate protection in BCG-based vaccine candidates and insufficient antigen presentation at the site of infection. To overcome these limitations, we generated a novel *Mtb*-based vaccine candidate for proof-of-concept experiments, in which bacterial lysis is achieved by inducible expression of cell wall hydrolyzing enzymes, mycobacteriophage lysins. We found that lysin induction caused lytic death in both replicating and non-replicating *Mtb*. Inducible lysis restricted *Mtb* growth inside macrophages and enhanced the production of pro-inflammatory cytokines, possibly due to the release of intracellular bacterial antigens. Moreover, lysin induction impaired *Mtb* viability during mouse infection. We are now performing re-challenge experiments to determine the efficacy of this vaccine candidate against subsequent *Mtb* infection. Efforts are also underway to identify the immunological pathways activated by lysed bacteria and the bacterial components activating these pathways. In addition, we analyzed the sequences of 26 escape mutants of inducible lysis strains and showed that the

tet repressor sequence is most frequently mutated. We are now designing new strains that combine other independent killing mechanisms to decrease the suppressor frequency.

3.2. Background

The last two decades have witnessed a significant progress in TB control; the number of annual TB death fell by 22% between 2000 and 2015. However, TB was still responsible for 1.4 million deaths in 2015, making it one of the top 10 causes of mortality worldwide (Pai et al., 2016). Moreover, the progress has slowed down. The annual decline rate in global TB incidence worldwide stays at only 1.5%, which needs to accelerate to a 4–5% reduction per year by 2020 and 10% by 2025 to reach the global target to end the TB endemic in 2030 (World Health Organization, 2016).

Although combination chemotherapies remain our best weapon against TB, antibiotics alone are far from sufficient to stop TB dissemination. An active TB patient can spread disease to 10 to 15 contacts over the course of a year (World Health Organization, 2016). Therefore, the ultimate control of TB will not be possible without effective TB vaccines. It has proven unusually challenging to develop an effective TB vaccine. The BCG vaccine, which was developed almost 100 years ago, remains the only available TB vaccine despite its inadequate protection against pulmonary TB infection. The suboptimal protection is in part due to the absence of immunodominant *Mtb*-specific antigens from BCG, such as RD-1 locus encoded antigens ESAT6 and CFP10 (Behr et al., 1999; Pym et al., 2003). A better understanding of the requirement of protective immunity and how *Mtb* manipulates immune

activation will facilitate the generation of more effective vaccines. Previous studies revealed that the priming of *Mtb*-specific T cell responses is only initiated in the mediastinal lymph nodes and does not occur until at least 1 to 2 weeks post infection (Gallegos et al., 2008; Reiley et al., 2008; Wolf et al., 2008). This may be related to limited antigen presentation at the site of infection or delayed dendritic cell (DC) activation (Egen et al., 2011; Griffiths et al., 2016). The administration of antigen at infection site or adoptive transfer of activated T cells and DC conferred better resistance to infection (Egen et al., 2011; Gallegos et al., 2008; Griffiths et al., 2016). Therefore, we reasoned that *Mtb*-based inducible lysis vaccines may represent an attractive novel vaccine strategy, because inducing bacterial lysis inside host cells can release sufficient amount of *Mtb*-specific antigens, engage immune sensors and activate the immune system.

In this study, we constructed *Mtb* inducible lysis strains by the conditional expression of cell wall hydrolyzing enzymes, mycobacteriophage lysins, via a tet-regulated system. Lysin induction caused lytic death in both replicating and non-replicating *Mtb*. We also showed that inducible lysis impaired bacterial viability in infected macrophages and mice. Moreover, inducible lysis enhanced the immune activation in macrophages. We further sequenced escape mutants of these inducible lysis strains and identified that the majority of the mutations occurred in the tet regulation system. Our work demonstrates that inducible lysis strains are promising vaccine candidates for proof-of-concept animal experiments worth further analysis and also lays the foundation for generating safer versions of inducibe lysis vaccine candidates for human use.

3.3. Results

3.3.1. Construction of inducible lysis *Mtb* strains

Lysins are cell wall hydrolyzing enzymes produced by mycobacteriophages to lyse and exit from mycobacterial hosts when they finish replication. Lysins are extensively modular and contain C-terminus cell wall targeting domains with high specificity for mycobacterial cell wall components (Payne and Hatfull, 2012). Therefore, mycobacteriophage lysins provide ideal tools to induce lysis in *Mtb* if regulated properly.

To inducibly express mycobacteriophage lysins, we cloned the D29 and L5 phage lysin genes downstream of a Tet repressor (TetR) tsc10-regulated, atc-inducible promoter Pmyc1tetO to a plasmid that encodes TetR under a constitutive promoter Ptb21 (Figure 3.1 A). All the plasmids carry antibiotic resistance genes to allow for selection. Without atc, TetR binds to tet operators (tetO) in the promoter Pmyc1tetO and represses the transcription of lysins. Atc addition causes conformational changes of TetR and alleviates the repression, so that lysins can be induced (Figure 3.1 B). The D29 or L5 single lysin strain was generated by integrating the corresponding lysin plasmid to the *Mtb* chromosome via site-specific integration. The dual lysin strain D29-L5-Lys contained two plasmids expressing D29 and L5 lysins respectively integrated at two different sites of the *Mtb* genome. All the three lysin strains grew normally on 7H10 plates in the absence of atc. Their abilities to form colonies were dramatically inhibited by applying atc on a paper disk in the center of the plate. Adding an additional copy of lysin slightly enhanced the growth inhibition caused by lysin induction, as evidenced by the more pronounced growth defect in the dual lysin strain compared to the single lysin

strains (Figure 3.1 C). Overall, these lysin strains responded well to atc regulation on agar plates.

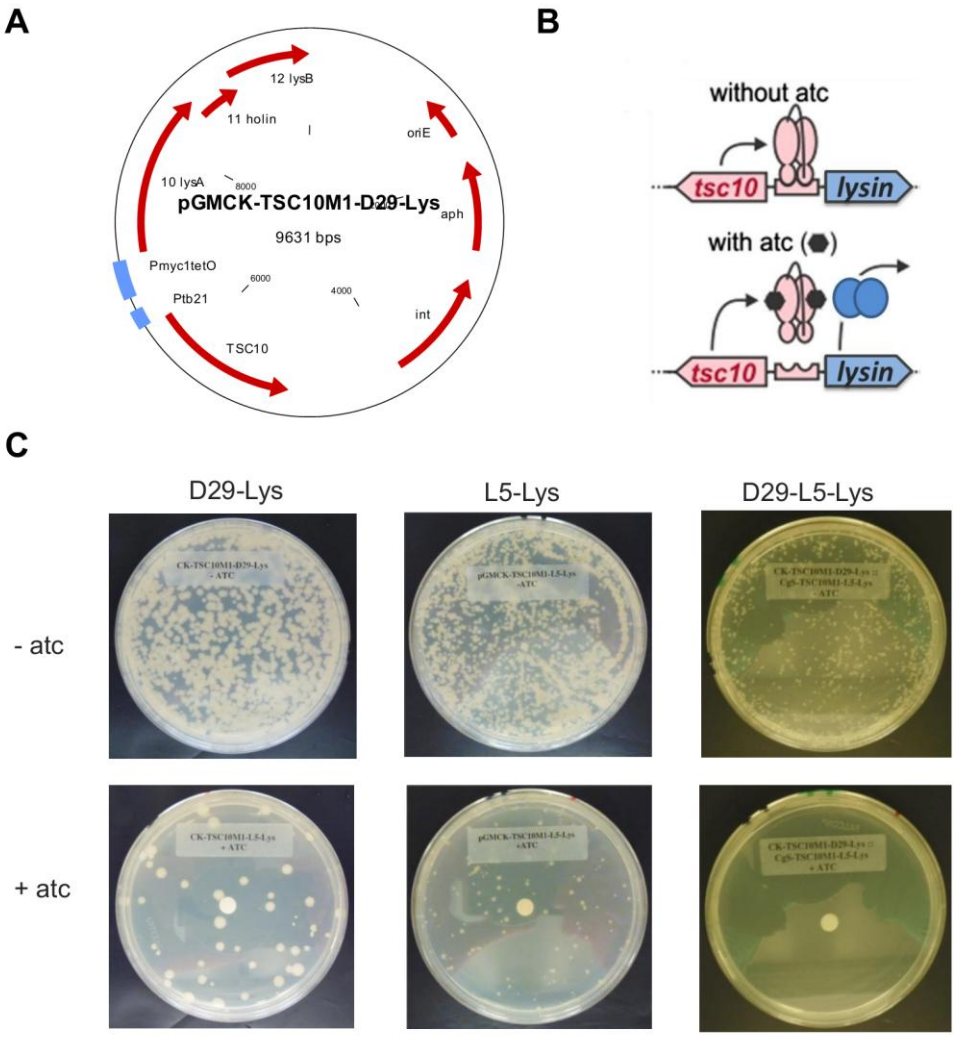

Figure 3.1 Construction of inducible lysis *Mtb* strains.

(A) Design of the integrase-containing plasmid used to inducibly express D29 phage lysin in *Mtb*. (B) Regulation of transcription of mycobacteriophage lysins by atc. Tet repressor tsc10 was transcribed constitutively; transcription of lysin cassette was repressed by TSC10 in the absence of atc. Atc addition alleviated the repression by TSC10 and allowed for lysin induction. (C) Growth of D29, L5 single lysin strains and D29-L5 dual strains on 7H10 plates, with or without atc disk, in the presence of corresponding selection antibiotics.

The inducible lysis *Mtb* strains were constructed by Joshua B. Wallach.

3.3.2. Plasmid loss is the major cause of high suppressor frequency in integrase-containing single lysin strains

Next we examined the regulation of these lysin strains in liquid culture by monitoring their growth with or without atc in 7H9 medium. Because all the lysin plasmids (including the antibiotics resistance genes) were integrated to *Mtb* chromosome, we did not add antibiotics while recording the growth curve. Lysin induction by atc suppressed *Mtb* growth in all the strains initially. However, we started observing outgrowth of D29 and L5 single lysin strains 7 days post atc treatment, while the regrowth was seen in dual lysin strains only after 13 days (Figure 3.2 A). The outgrowth of atc-treated culture is usually caused by a preexisting population of non-inducible mutants or suppressors that initially constitute only a small fraction of the whole culture (Muller et al., 1995). These non-inducible mutants have a growth advantage and gradually take up the culture, as the bacteria that respond to atc regulation are killed by lysin. The quick appearance of regrowth in the single lysin strains indicated the presence of suppressors at a high frequency.

Next we determined the suppressor frequency in these lysin strains by dividing the number of colonies recovered from atc-containing plates by that from regular 7H10 plates. Indeed, we found an extremely high suppressor frequency ~ 10^{-2} in the single lysin strains when plating on atc plates without antibiotics, while the frequency is more than 1000 fold lower in the dual lysin strain (Figure 3.2 B). Unexpectedly, adding antibiotics to the atc plate decreased the suppressor rate to 10^{-5} ~10^{-6} in the single lysin strains (Figure 3.2 B and C). In our studies, all the plasmids (including antibiotic resistance genes) were integrated into the chromosome. One advantage of the integrated

plasmid system is that these plasmids are generally stably retained in bacteria even without antibiotics selection during maintenance (Lee et al., 1991). We constructed all the strains with antibiotics selection and grew them in the presence of antibiotics during maintenance The antibiotics were only missing when we re-inoculated the bacteria to start the growth curve (Figure 3.2 A) or plated on antibiotics-free atc plates to determine the suppressor rate (Figure 3.2 B and C). Therefore, the withdrawal of antibiotics for one or two weeks was not expected to cause *Mtb* to lose the plasmids and affect their growth. Nevertheless, the striking difference between with and without antibiotics groups suggested that single lysin strains were prone to plasmid loss when lysin was induced (Figure 3.2 B and C). In contrast, plasmid loss was largely prevented in dual lysin trains, although antibiotics addition also reduced the suppressor rate for 10 fold (Figure 3.2 B and D).

To confirm that plasmid loss is responsible for the early outgrowth in single lysin strains, we repeated the growth curve in the presence of antibiotics to select for bacteria that kept the lysin plasmids. Antibiotics had no impact on the growth of lysin strains in the absence of lysin induction, but delayed the onset of outgrowth in single lysin strains from 7 days to 13 days post atc treatment (Figure 3.2 E). The plasmid integration to *Mtb* chromosome was mediated by site-specific integrases. If retaining the plasmid in *Mtb* significantly reduces bacterial fitness, the integrase can also enable the removal of plasmid via a reverse-integration reaction (Lee and Hatfull, 1993; Lee et al., 1991). Of note, all the abovementioned lysin strains (D29-Lys, L5-Lys and D29-L5-Lys) were constructed using lysin plasmids containing integrases. We reasoned that the removal of integrase can prevent plasmid

loss. Therefore, we constructed integrase-free single and dual lysin strains. They are refereed as L5-Lys-ni, D29-Lys-ni and D29-L5-Lys-ni respectively, where ‘ni’ stands for no integrase. Consistent with our hypothesis, the suppressor frequency of the integrase-free single lysins (L5-Lys-ni and D29-Lys-ni) obtained from atc plates with or without antibiotics were indistinguishable (Figure 3.2 F). In contrast, integrase removal did not further reduce the suppressors in dual lysin strains (Figure 3.2 F). Collectively, these results demonstrated the integrase-mediated plasmid loss is responsible for the high suppressor frequency in integrase-containing single lysin strains.

Figure 3.2 Plasmid loss is a major cause of escape mutants in integrase-containing single lysin strains.

(A) Growth of integrase-containing single (D29-Lys or L5-Lys) and dual lysin (D29-L5-Lys) strains in 7H9 medium in the absence of antibiotics with or without atc. (B) Suppressor frequency of integrase-containing single and dual lysin strains by quantifying the colonies on 7H10 atc plates with or without antibiotics. (C and D) Image of growth of integrase-containing D29 single lysin strain and D29-L5 dual lysin strains on 7H10 atc plates with or without antibiotics. Corresponding numbers of *Mtb* were plated on atc or atc plus antibiotics plates as indicated. (E) Growth of integrase-containing single and dual lysin strains in 7H9 medium in the presence of antibiotics. (F) Suppressor frequency of integrase-containing and integrase-free lysin strains by quantifying the colonies on 7H10 atc plates with or without antibiotics. Data in (B) and (F) are means ± SD (n = 3 per group). All results are representative of at least three independent experiments.

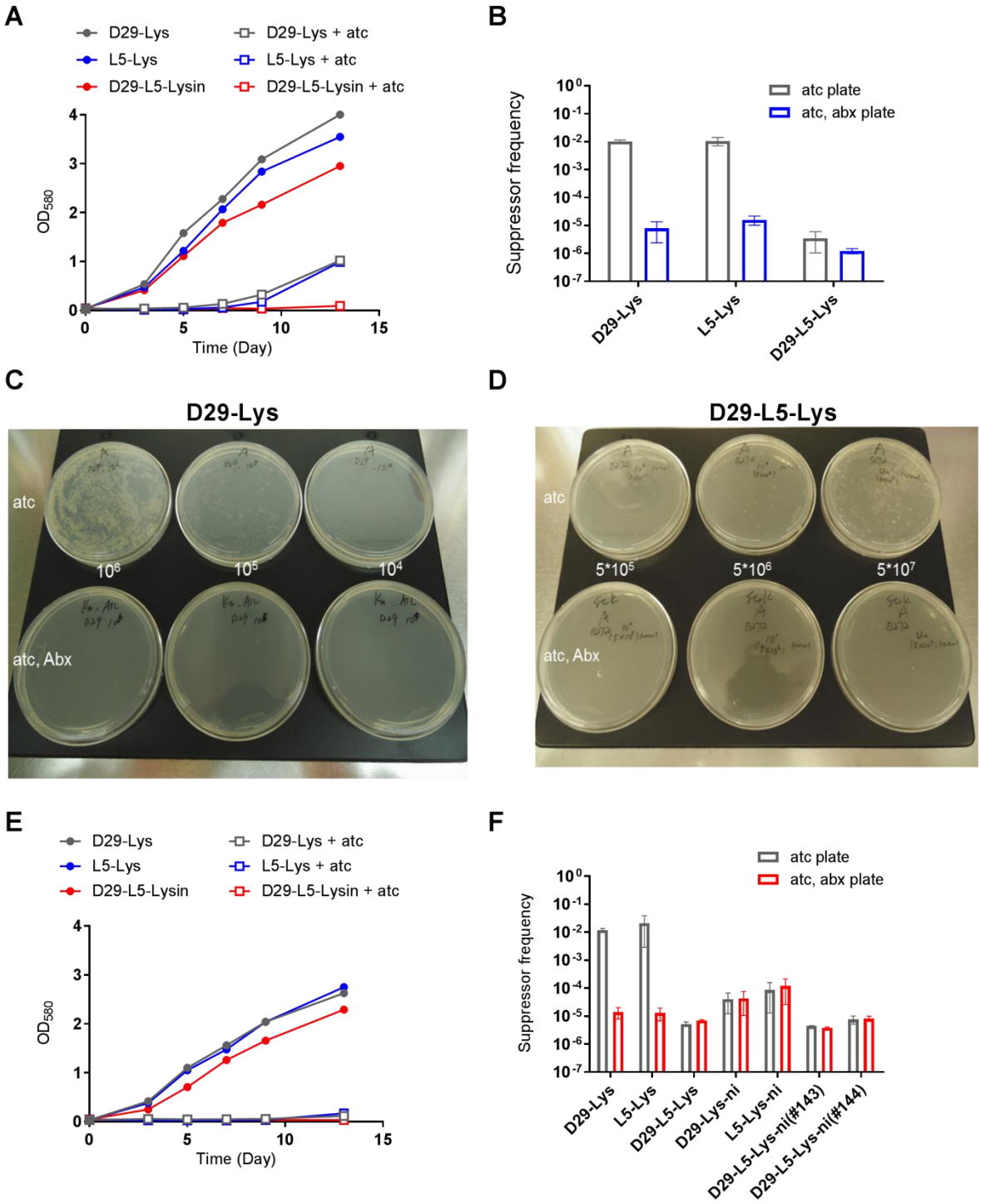
A
D29-Lys
D29-Lys + atc
L5-Lys
L5-Lys + atc
D29-L5-Lysin
D29-L5-Lysin + atc
OD580
Time (Day)
B
atc plate
atc, abx plate
Suppressor frequency
D29-Lys
L5-Lys
D29-L5-Lys
C
D29-Lys
atc
10^6
10^5
10^4
atc, Abx
D
D29-L5-Lys
atc
5*10^5
5*10^6
5*10^7
atc, Abx
E
D29-Lys
D29-Lys + atc
L5-Lys
L5-Lys + atc
D29-L5-Lysin
D29-L5-Lysin + atc
OD580
Time (Day)
F
atc plate
atc, abx plate
Suppressor frequency
D29-Lys
L5-Lys
D29-L5-Lys
D29-Lys-ni
L5-Lys-ni
D29-L5-Lys-ni(#143)
D29-L5-Lys-ni(#144)

3.3.3. Lysin induction caused bacterial lysis in replicating and non-replicating *Mtb*

To study how lysin affects replicating *Mtb*, we grew the bacteria in nutrient-rich 7H9 medium and then treated with atc to induce lysin expression. Lysin induction not only inhibited the growth of replicating *Mtb*, but also impaired bacterial viability (Figure 3.3 A and B). Exposure of the dual lysin strain to atc decreased colony-forming units (CFU) by more than 3 orders of magnitude after 7 days. We further examined the consequences of lysin induction on *Mtb* during different growth phases. The culture was first grown without atc and an aliquot of culture was taken over time to be treated with atc. Lysis was readily observed upon lysin induction at different growth stages, indicated by the decrease in culture OD (Figure 3.3 C).

Although lysin induction resulted in quick lytic death in replicating *Mtb*, it may not necessarily lyse non-replicating *Mtb*, which are known to undergo cell wall remodeling and become tolerant to most anti-TB drugs (Barry et al., 2009; Betts et al., 2002; Voskuil et al., 2004). To address the impact of lysin on non-replicating *Mtb*, we cultured the inducible lysis strain in PBS for 10 days to achieve a non-replicating state and then added atc. Bacterial viability started dropping one week after lysin induction and decreased for 4.4 log after four weeks. In addition, we detected a visible drop in culture OD after four weeks, confirming that lysin induction also caused lytic death in non-replicating *Mtb* although at relatively slower kinetics (Figure 3.3 E and F).

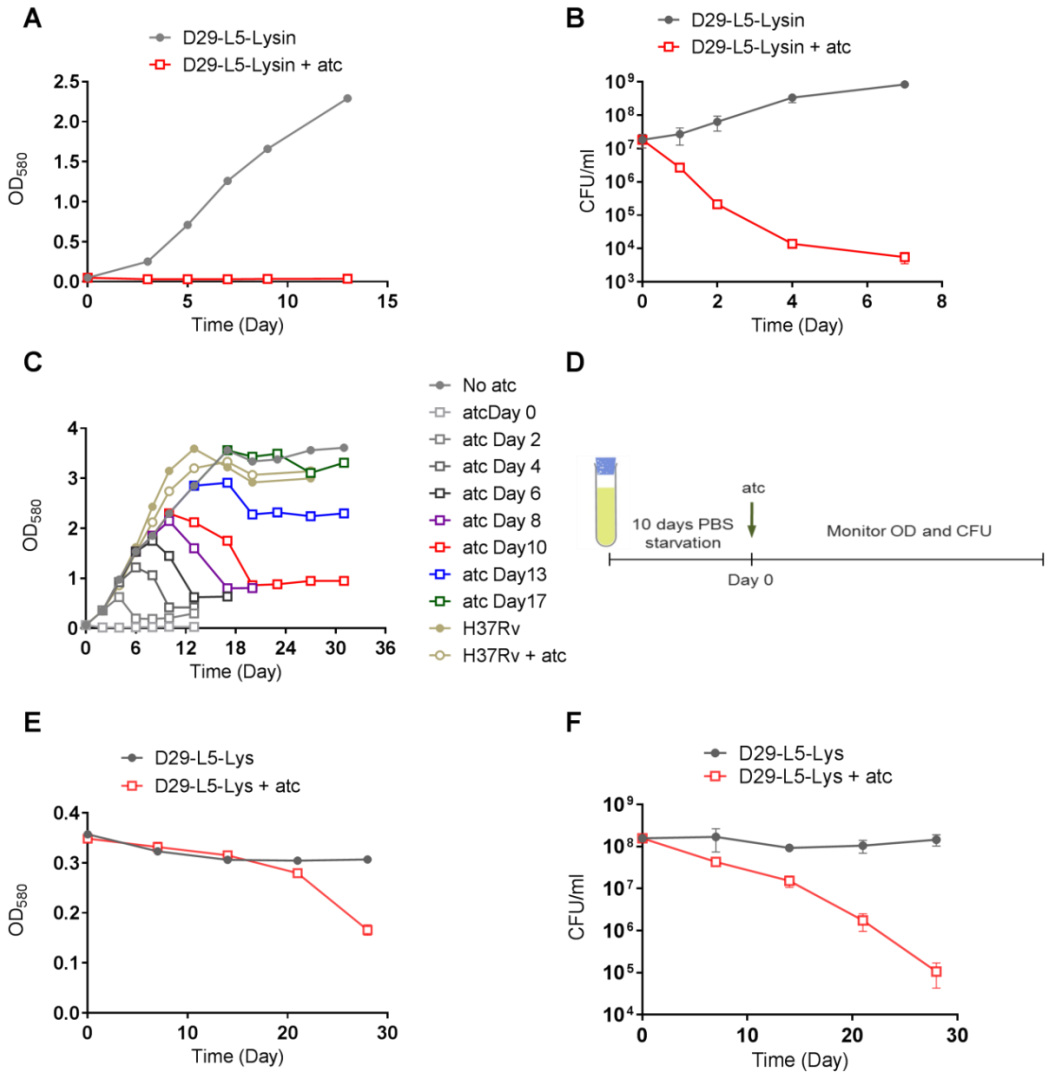

Figure 3.3 Lysin induction caused bacterial lysis in replicating and non-replicating *Mtb*.

(A) Growth of D29-L5 dual lysin strains in 7H9 medium with or without atc. (B) Survival of *Mtb* strains quantified by CFU in 7H9 medium with or without atc. (C) Impact of atc on D29-L5 dual lysin strains during different growth phases. Atc was added to wt *Mtb* H37Rv starting on day 0 and to D29-L5 dual lysin strains at indicated times. (D) Schematic of the experiment to assess the impact of lysin induction on non-replicating *Mtb*. *Mtb* was grown in PBST for 10 days to achieve a non-replicating state. Where indicated, atc was added to the cultures on day 0. (E) Optical density (OD) of *Mtb* culture in PBS starvation with or without atc. (F) Quantification of CFU from cultures in (E) at the indicated time points. Data in (B), (E)and (F) are means ± SD (n = 3 per group). All results are representative of at least two independent experiments.

3.3.4. Lysin induction restricted *Mtb* growth in macrophages and enhanced the production of pro-inflammatory cytokines

Effective host control of pathogens relies on prompt sensing of pathogen-associated molecular patterns (PAMPs), triggering innate immunity and priming the adaptive immune system. The release of *Mtb* intracellular components from lysed cells can potentially enhance immune recognition by engaging the immune sensors in macrophages or dendritic cells. To assess the impact of inducible lysis on the host immune system, we infected mouse bone marrow-derived macrophages (BMDMs) with the dual lysin strain and treated with atc or rifampicin. Lysin induction reduced *Mtb* survival in resting macrophages at both high and low multiplicity of infection (MOI). 1 μg/ml rifampicin killed *Mtb* at similar kinetics to atc treatment, allowing us to directly compare host immune responses induced by lytic death and antibiotic-mediated death (Figure 3.4 A and B). Inducible *Mtb* lysis elicited robust production of protective cytokines, whereas antibiotic-induced killing did not boost cytokine secretion from macrophages. IL-12 p40 production increased more than fivefold as a consequence of lysis and the same pattern was observed for IL-6 and TNF-a (Figure 3.4 C - E). We also included wt *Mtb* H37Rv-infected BMDMs treated with atc and rifampicin as a control, and failed to observe the boost effect, ruling out the possibility that enhanced cytokine production is merely an artifact caused by dead *Mtb* and atc (Figure 3.4 F). These results indicated that inducible lysis restricted *Mtb* growth inside macrophages and activated host immune responses, likely due to the release of intracellular bacterial contents.

Figure 3.4 Lysin induction restricted *Mtb* growth inside macrophages and enhanced the production of pro-inflammatory cytokines.

(A and B) Bacterial loads in resting mouse bone marrow derived macrophages (BMDM) infected with D29-L5 dual lysin strains at MOI 0.1 (A) and MOI 5 (B), treated with atc or 1µg/ml rifampacin four hours post infection. (C - F) Cytokine production in cell culture supernatant of BMDM infected with *Mtb* strains for 24 hours with cooresponding treatment. Cytokine concentration was measured by ELISA. Data in (A) to (E) are means ± SD of three biological replicates and representative of two independent experiments.

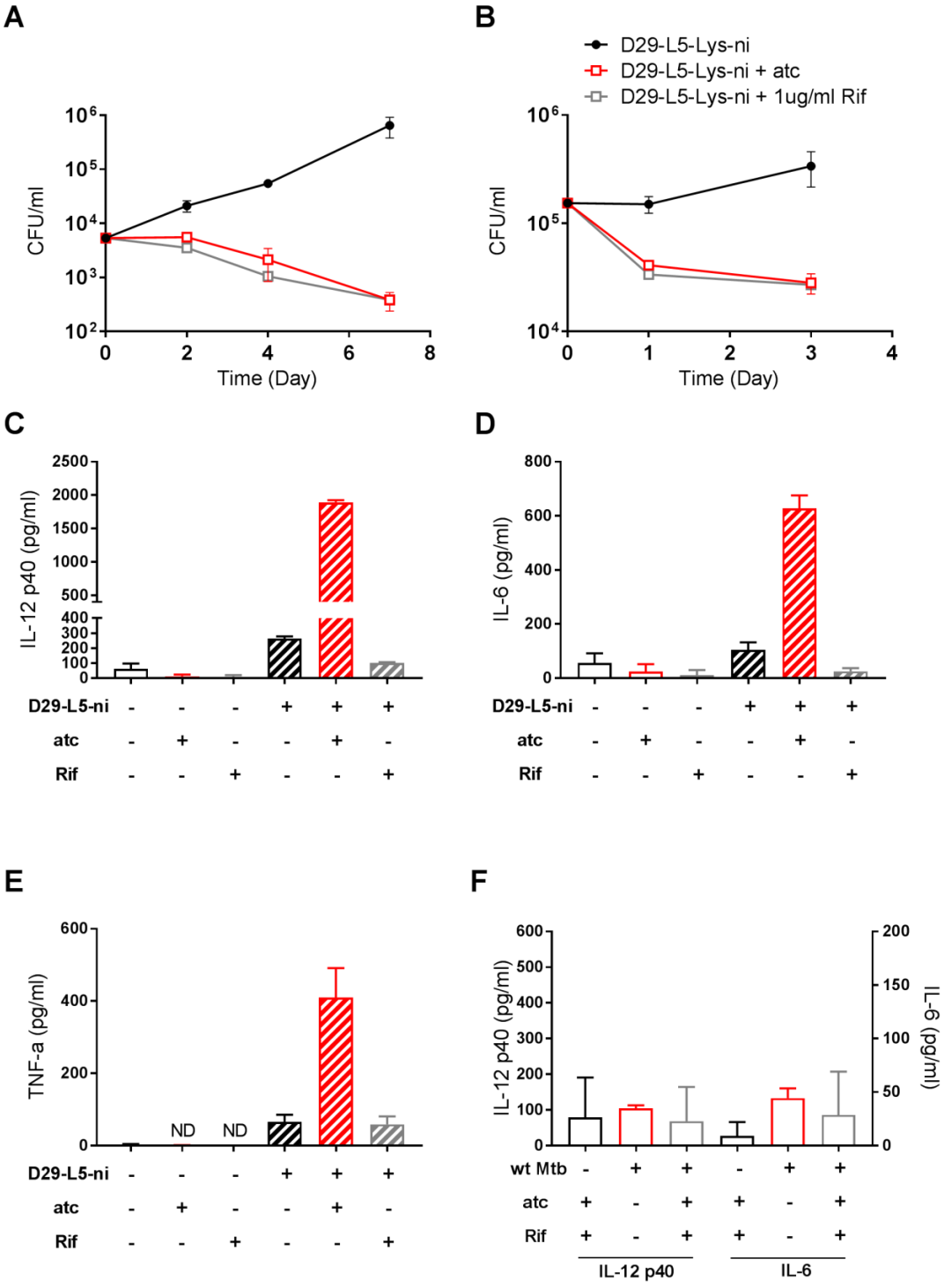
A
CFU/ml
Time (Day)
B
D29-L5-Lys-ni
D29-L5-Lys-ni + atc
D29-L5-Lys-ni + 1ug/ml Rif
CFU/ml
Time (Day)
C
IL-12 p40 (pg/ml)
D29-L5-ni
atc
Rif
D
IL-6 (pg/ml)
D29-L5-ni
atc
Rif
E
TNF-a (pg/ml)
ND
ND
D29-L5-ni
atc
Rif
F
IL-12 p40 (pg/ml)
IL-6 (pg/ml)
wt Mtb
atc
Rif
IL-12 p40
IL-6

3.3.5. Lysin induction impaired *Mtb* viability during mouse infection

To evaluate the impact of lysin on *Mtb* during *in vivo* infection, we challenged C57BL/6 mice with the dual lysin strain and fed them with doxy food to induce lysin during (day 14) and after (day 28) the establishment of infection. A control group of mice were treated with isoniazid and pyrazinamide starting on day 28, which have been shown to effectively clear *Mtb* infection *in vivo* (Figure 3.5 A). We found that *Mtb* failed to establish and maintain infection in lungs and spleens when lysin was induced (Figure 3.5 B and C). Consistent with decreasing bacterial load in the lungs, we also observed improved pulmonary pathology in doxy-treated mice (Figure 3.5 D).

Furthermore, we measured the cytokine levels in the lungs of infected mice using multiplex ELISA, which allowed simultaneous detection of multiple cytokines. On day 42, the Chemokine (C-C motif) ligand 5 (CCL5) levels in the doxy day 14 group and antibiotics day 28 group were five-fold lower than those in untreated mice and the doxy day 28 group. Of note, the bacterial loads of the doxy day 14 group and antibiotics day 28 group were also lower. On day 60, the CCL5 level in the doxy day 28 group declined to about 20% of that in untreated mice, coinciding with a tenfold reduction in CFU (Figure 3.5 E). The same pattern was also seen for IL-12 p40, indicating the levels of pro-inflammatory cytokine production mainly reflect the bacterial burden in the host (Figure 3.5 F). Although lysis induction resulted in clearance of infection *in vivo*, we did not observed enhanced cytokine production associated with inducible lysis. It is possible that lysis induced a transient upregulation of pro-inflammatory cytokines, but the levels waned overtime. We plan to collect more samples during the early stage of infection, which may provide better

chance to detect the difference. We are now performing re-challenge experiments to determine the efficacy of the vaccine candidate against subsequent *Mtb* infection.

Figure 3.5 Lysin induction impaired *Mtb* viability during infection.

(A) Schematic of the mouse infection experiment. Mice were infected with D29-L5 dual lysin strains. Mice received doxy-containing food starting on day 14 or day 28 or not at all. Another group of mice received isoniazid and pyrazinamide in drinking water from day 28. (B and C) Quantification of bacterial loads in lungs (B) and spleens (C) of C56BL/6 mice infected with D29-L5-Lys. Data are means ± SD of four mice per group. The limit of detection was 4 CFU per organ and is indicated by the dashed line. (D) Gross pathology of lungs from infected mice. Lungs were isolated on day 84 post infection. (E and F) CCL5 and IL-12 p40 levels in the lung homogenates of infected mice measured by multiplex ELISA. Data are means ± SD of three mice per group.

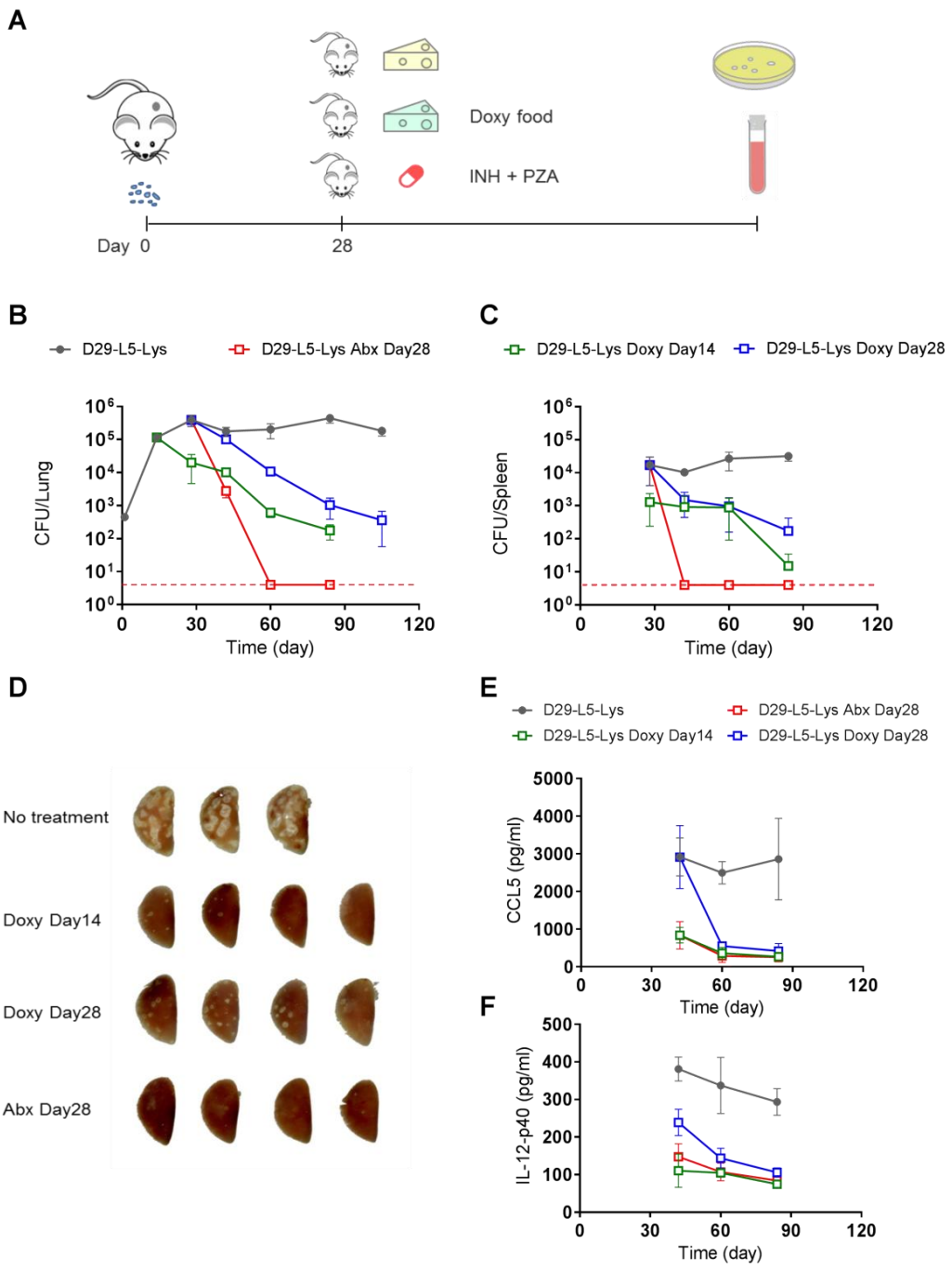
A
Doxy food
INH + PZA
Day 0
28
B
D29-L5-Lys
D29-L5-Lys Abx Day28
CFU/Lung
Time (day)
C
D29-L5-Lys Doxy Day14
D29-L5-Lys Doxy Day28
CFU/Spleen
Time (day)
D
No treatment
Doxy Day14
Doxy Day28
Abx Day28
E
D29-L5-Lys
D29-L5-Lys Abx Day28
D29-L5-Lys Doxy Day14
D29-L5-Lys Doxy Day28
CCL5 (pg/ml)
Time (day)
F
IL-12-p40 (pg/ml)
Time (day)

3.3.6. The Tet repressor sequence is frequently mutated in the escape mutants of D29-L5 dual lysin strains

Our ultimate goal is to develop an inducible lysis TB vaccine for human use. Nevertheless, our current work is mainly proof-of-concept study, as all the work was performed in the background of a virulent strain H37Rv. If the inducible lysin strain confers good protection in animal models, we will consider developing it into a human vaccine strain. In that scenario, safety stands out as the foremost concern. Ideally, the vaccine strain should be sterilized *in vivo* by lysin induction or in combination with other killing mechanisms. The existence of a high frequency of non-inducible mutant or suppressor population may compromise the efficacy of the inducible lysis system. Therefore, a better understanding of the escape mechanisms is not only of scientific importance, but will also help us improve the vaccine candidate by rational design.

To identify the suppressor mutations, we sequenced the lysin plasmid regions of 10 suppressor mutants of the integrase-containing dual lysin strain (D29-L5-Lys) and 16 mutants of the integrase-free strain (D29-L5-Lys-ni), all of which were selected on antibiotics and atc plates to prevent plasmid loss. We found one mutation in each of the individual suppressor strains in the lysin plasmid regions we sequenced. Among the 10 mutants of D29-L5-Lys, seven of them harbor mutations and one contains a short deletion in the TetR sequence (Figure 3.6 A and B). These mutations (TetR-H64Y, H100R, L131R, H333R) interfere with atc binding to TetR and abolish its ability to induce conformational changes (Muller et al., 1995). These types of mutations can function in a dominant-negative way, because the mutated TetR will replace wt

TetR and keep transcription repressed even in the presence of atc. Therefore, a mutation in one lysin plasmid can abrogate lysin induction from both plasmids. We also identified two suppressors with a single amino acid change in one of the two lysin genes. It remains unclear how these lysin mutations affect the enzymatic functions.

Similarly, we found point mutations in the TetR region in 15 suppressors of D29-L5-Lys-ni (n=16), 10 of which have mutations that affect atc binding to TetR (Figure 3.6 C). The others contain G143R and G376R mutation, which represent a different escape mechanism (Figure 3.6 D). Glycine 143 and 376 sit at the dimer interface of TetR, and mutations to arginine convert TetR into a non-inducible state (Muller et al., 1995). There is also one suppressor from D29-L5-Lys-ni with a deletion in the TetR sequence.

Our sequencing data for the 26 suppressor mutants identified the TetR region as the most frequently mutated sequence; 92.3% of the suppressors harbored mutations or deletion in the TetR region (Figure 3.6 E). The distribution of mutation mechanisms does not dramatically differ between D29-L5-Lys or D29-L5-Lys-ni, with mutations that abolish atc binding to TetR (TetR-H64Y, H100R, L131R, H333R) being the predominant type (Figure 3.6 F). These atc binding mutants can function as dominant mutations, so one mutation can inactivate lysin induction from multiple plasmids with the same regulatory system. Our data highlights the need to incorporate independent regulatory systems and killing mechanisms to decrease escape mutant frequency when designing inducible lysis vaccines for human use.

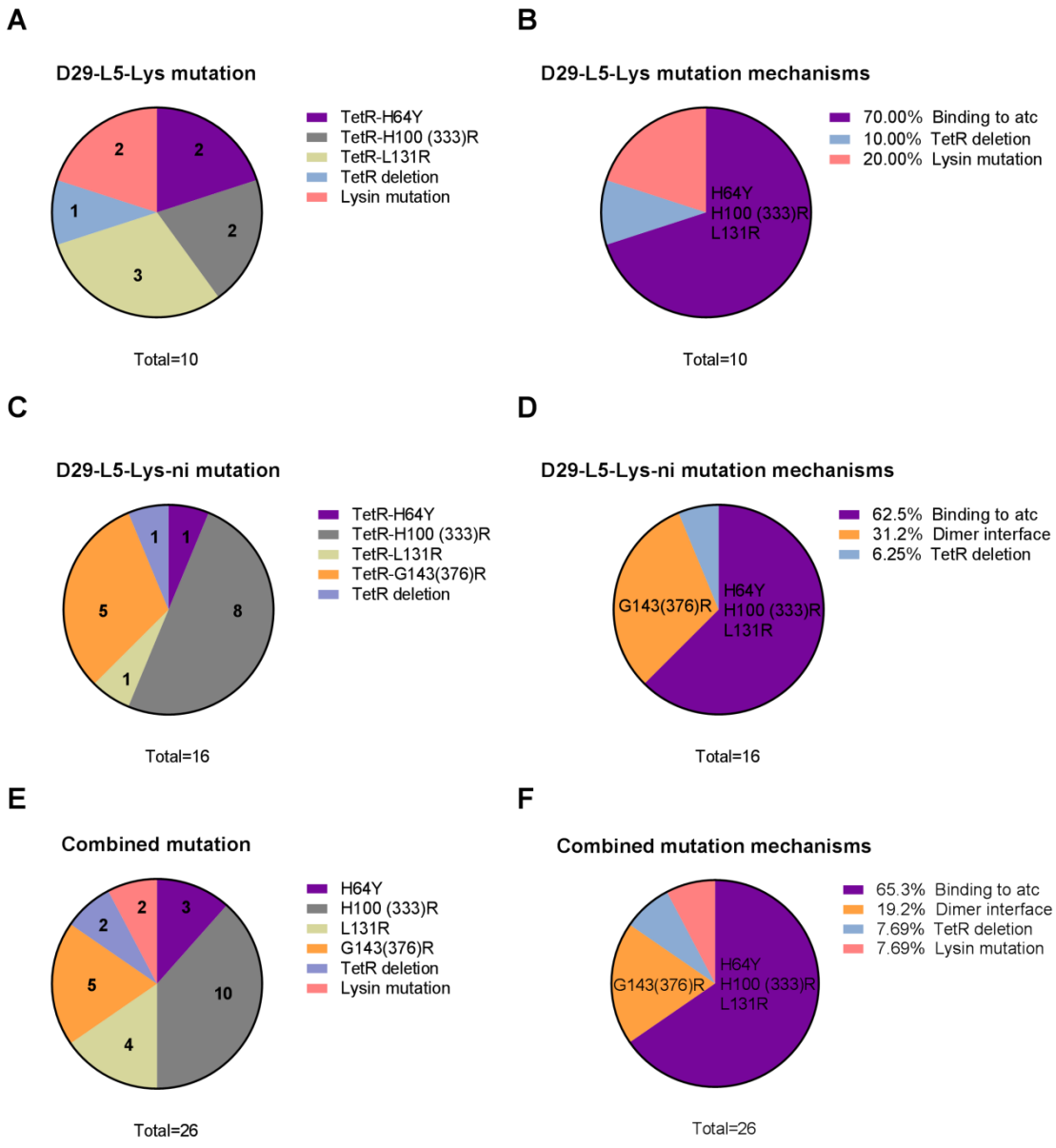

Figure 3.6 Tet repressor sequence is frequently mutated in D29-L5 dual lysin escape mutants.

Mutation sites and possible mechanisms identified in the escape mutants of integrase-containing D29-L5 dual lysin strains (A and B), integrase-free dual lysin strains (C and D) or combined (E and F). Numbers in (A), (C) and (E) correspond to the number of strains found with the indicated type of mutation.

The sequencing of D29-L5-Lys-ni mutants was performed by Joshua B. Wallach.

3.4. Discussion

3.4.1. Construction of a new type of TB vaccine candidate – inducible lysis strains

TB vaccine development has been hampered by the incomplete understanding of protective immunity against TB, the lack of surrogate biomarkers and the absence of animal models that predict vaccine efficacy. Although it remains unclear what immunological pathways constitute the portfolio that is sufficient to confer protection, studies have revealed the lack of important virulence factors in BCG-based vaccine candidates, insufficient antigen presentation and suboptimal DC activation as factors contributing to undesirable protection (Egen et al., 2011; Grace and Ernst, 2016; Griffiths et al., 2016; Pym et al., 2003).

To overcome these limitations, we generated *Mtb*-based inducible lysis strains, which contain the virulence factors that are likely important for vaccine protection and are able to release a sufficient amount of antigens upon lysin induction. The strains were constructed by site-specific integration of lysin plasmid into the *Mtb* genome mediated by integrases. This system has been widely used to generate stable recombinants in mycobacteria species, and usually no continual selection is required due to chromosomal integration of the plasmids (Lee et al., 1991). In contrast to previous reports, we observed a high frequency of plasmid loss in integrase-containing single lysin strains caused by integrase-mediated reverse recombination. The high toxicity of lysins may impose a strong pressure for bacteria to expel the lysin plasmids, and may explain the discrepancy between our observation and previous reports. Interestingly, adding an additional copy of integrase-containing lysin

plasmid reduces the plasmid loss frequency as effectively as the removal of integrase, possibly because the likelihood to simultaneously losing both plasmids is rare. Dual lysin strains with or without integrase behaved similarly in most of the *in vitro* and *ex vivo* assays, and were exempted from plasmid loss. However, we believe that the integrase-free version may provide an advantage for *in vivo* mouse infection where the experiments usually take months and continuous selection is not feasible.

Although the relatively low suppressor frequency (10^{-5} ~10^{-6}) in the dual lysin strains does not interfere with most microbiological assays, even *in vivo* mouse infection, it is far from desirable for a human vaccine. We sequenced the lysin plasmid regions of 26 suppressors to understand the escape mechanisms, with the ultimate goal to improve the design and deliver an inducible lysis vaccine for human use. We only found one mutation for each individual strain we sequenced. TetR was identified as the most frequently mutated region in the suppressors; 84.6% suppressors contain point mutations and 7.69% have deletion in the TetR sequence. Mutations that abolish atc binding to TetR can act in a dominant-negative manner. It takes only one mutation of this type in one lysin plasmid to abrogate lysin induction from multiple lysin plasmids with the same regulatory systems. Other suppression mechanisms include mutations at dimer interface of TetR that convert it into a non-inducible state (Muller et al., 1995). We also found point mutations in lysin genes that cause single amino acid change (not premature termination codon). However, how one lysin point mutation in one plasmid disrupts the functions of both lysin cassettes remains unclear. It is possible that the mutant lysins lose the catalytic activity, but can still bind to the substrates and prevent access of

active lysins. It should also be noted that we only sequenced the lysin plasmids region on the chromosome. Therefore we cannot exclude the possibility that the mutations truly responsible for the non-inducible/suppressor phenotype lie in the region yet to be sequenced.

Considering that most of the mutations occur in the TetR region and dominant-negative mutations are the primary suppression mechanism, it is critical to include other independent regulatory systems and killing mechanisms. For example, we can introduce the inducible lysis system (integrase-free version) to auxotroph *Mtb* strains or combine with other toxins to improve the safety.

3.4.2. Lysin induction causes lytic death in both replicating and non-replicating *Mtb*

The lysin system is composed of lysin A, lysin B and holin. The LysA proteins are extensively modular enzymes that hydrolyze peptidoglycan, with N-terminus catalytic domains and C-terminus cell wall binding domains which determine the substrate specificity (Hatfull et al., 2006). Lysin A enzymes have highly diverse activities, containing combinations of amidase, glycosidase and peptidase motifs (Payne and Hatfull, 2012). Bioinformatics analysis identified a GH19 (glycoside hydrolase) domain and a N4 domain (possible amidase) in D29 lysin A, while L5 lysin A only contains a N4 domain (Payne and Hatfull, 2012). Lysin B enzymes cleave the linkage of mycolic acids to the arabinogalactan layer and release free mycolic acid (Payne et al., 2009). Holins coordinate the lysis by allowing these enzymes to pass through the cell membrane (Wang et al., 2000). However, D29 or L5 Lysin A alone enables lysis of *M.smegmatis*, suggesting holin-independent lysis in some Lysin A

proteins and also their functional diversity (Payne and Hatfull, 2012; Pohane et al., 2014). The activities of these enzymes in *Mtb* are relatively undefined. To achieve effective lysis, we included both the holin and endolysins of D29 and L5 phages in constructing the inducible lysis strains. Consistent with the requirement of cell wall synthesis in actively dividing bacteria, lysins rapidly killed replicating *Mtb*. Interestingly, lysin expression caused lytic death in non-replicating *Mtb* as well, indicating that latent *Mtb* has to maintain cell wall integrity and thus is vulnerable to lysin killing. In non-replicating conditions, we observed decreased viability long before detectable lysis, suggesting that lysis is preceded by bacterial death.

3.4.3. Inducible lysis killed *Mtb* and enhanced protective cytokine production *ex vivo* in macrophages and *in vivo* during mouse infection

Lysin induction restricted *Mtb* growth inside macrophages and elicited robust production of protective cytokines, including IL-12 p40, TNF-a and IL-6. Mice lacking IL-12 p40, the shared subunit of IL12 and IL-23, are highly susceptible to *Mtb* infection (Cooper et al., 2002; Feng et al., 2005; Holscher et al., 2001). IL-12 initiates and promotes differentiation of Th1 cells, a critical player in adaptive immunity against *Mtb* infection (Feng et al., 2005; Khader et al., 2006). IL-23 has been implicated in mediating protective responses after vaccination, although it is dispensable for controlling *Mtb* infection (Khader et al., 2007). The protective role of TNF has also been well-established. Mice lacking TNF fail to control infection (Flynn et al., 1995). Its importance is further supported by the observation that use of TNF neutralizing antibodies to treat rheumatoid arthritis results in latent TB reactivation (Keane et al., 2001). IL-6 can antagonize the differentiation of regulatory T cells, which

delay the onset of protective immune responses in the context of TB infection (Kimura and Kishimoto, 2010; Scott-Browne et al., 2007; Shafiani et al., 2010). In contrast to lytic death, we didn't observe enhanced production of protective cytokines in macrophages when *Mtb* was killed by rifampicin treatment, indicating bacterial death alone was not sufficient to boost the cytokine production. It also highlights that the mechanisms of how *Mtb* or the vaccine strain are cleared may play a role in shaping the protective immune response, in addition to the well-documented factors like the antigens, adjuvants and routes of immunization.

The increased production of IL-12 p40, TNF-a and IL-6 upon inducible lysis represents a signature of myeloid cell activation and points to a potential better protection conferred by the inducible lysis strains. How inducible lysis activates the host immune system remains an open question. Considering that the direct targets of lysin are cell wall associated components, particularly peptidoglycan, it is tempting to speculate that TLR2/ MyD88-dependent or NOD-2-dependent pathways are involved sensing *Mtb* lysis. Mycobacterial lipoproteins activate myeloid cells via TLR2 to produce pro-inflammatory cytokines such as TNF (Hertz et al., 2001). Mice lacking the downstream adaptor protein MyD88 quickly succumb to infection and display markedly decreased levels of IL-12, TNF, and Th1 cytokines (Scanga et al., 2004). In light of the accumulating evidence that supports phagosomal escape of *Mtb*, cytosolic immune sensors may play an important role as well (Simeone et al., 2012; Simeone et al., 2015; van der Wel et al., 2007). NOD-2 is a cytoplasmic pattern-recognition receptor implicated in sensing bacterial peptidoglycan-derived molecules. The unique modification of mycobacterial peptidoglycan (N-glycolylated muramyldipeptide) makes it a highly effective agonist for

NOD2 (Coulombe et al., 2009). NOD2 has been shown to mediate the optimal production of IL-12p40, TNF and IL-6 in response to *Mtb*, however the susceptibility of NOD2-deficient mice to *Mtb* infection was not universally observed (Divangahi et al., 2008; Gandotra et al., 2007). In addition to disrupted cell wall, the intracellular contents were also released upon inducible lysis. Therefore, other innate immune pathways, such as phagosomal and cytosolic DNA sensing pathways, may be engaged as well. Cytosolic *Mtb* DNA was found to activate host DNA sensor, cyclic GMP-AMP synthase (cGAS) and the adaptor protein stimulator of interferon genes (STING), and thereby target bacteria for autophagy (Collins et al., 2015; Manzanillo et al., 2012; Wassermann et al., 2015; Watson et al., 2015; Watson et al., 2012). Probing the immune sensors using genetic knockout mice will not only broaden our knowledge on how the immune system senses and reacts to bacterial lysis, but also help identify the host population that will benefit most from inducible lysis vaccines in the long run.

Although inducible lysis killed *Mtb* infection *in vivo*, we did not detect enhanced production of protective cytokines by using multiplex ELSA. Instead, the cytokine levels were largely determined by the bacterial load even after lysin induction, similar to the observations in some groups using *Mtb* and pneumococcal pneumonia infection models (Goodsmith et al., 2015; Witzenrath et al., 2009). In contrast, other groups found that lysin infusion via the bloodstream induced pro-inflammatory cytokine production in a *Streptococcus pneumonia* endocarditis rat model, which peaked at six hours post lysin administration and went back to basal levels after 24 hours (Entenza et al., 2005; Pastagia et al., 2013). The discrepancy may be related to animal

species, disease models and method of dosing. It is also likely that inducible lysis may cause a transient upregulation of these cytokines as in the case of the endocarditis rat model, but the inflammation resolved before we harvested the tissues. If we sample more frequently at early stages upon inducible lysis, we may be able to detect the difference. Moreover, the results can be affected by the detection methods as well. Multiplex ELISA measures an average level of a cytokine in the lung homogenate, while the majority of cells in lungs are non-immune cells. Switching to methods with higher sensitivity like RNA-seq or single-cell level analysis like FACS staining of may improve the detection.

3.5. Future directions

With the establishment and verification of the inducible lysin system *in vitro* and during infection, we can address many new questions. First, it will be interesting to identify the exact immune sensors in macrophages that respond to inducible lysis using genetic knockout mice. This will also help understand the molecular nature (DNA, RNA or bacterial cell wall) of the lysis-induced signals that enhance the immune response.

Second, most of our *ex vivo* work was performed with BMDM, because macrophages are the preferred cell type for *Mtb* to reside and replicate inside the lung. However, the priming and activation of *Mtb*-specific CD4 T cells depends on DCs (Bhatt et al., 2004; Khader et al., 2006; Samstein et al., 2013). Recent studies also showed that pulmonary delivery of activated DCs can accelerate T cell activation and improve protection in vaccinated mice (Griffiths et al., 2016). Therefore, it may be more physiologically relevant to

study the impact of inducible lysis on DC activation status and production of inflammatory cytokines, in particular those involved in priming T cells like IL-12.

Third, we are conducting re-challenge experiments to determine if the inducible lysis strains protect against subsequent *Mtb* infection. The bacterial loads, lung pathology, survival and lung functions will be compared between unvaccinated mice and mice vaccinated by inducible lysis strains or BCG. We are also trying to sample more frequently during the early stage upon vaccination with more sensitive methods, hoping to detect the early induction of protective cytokines. However, it may be more relevant to measure the protective memory response at the end of vaccination and early expansion of immune cells after re-challenge. Experiments include measuring the antigen-specific IFN-γ or other cytokine release from *in vitro*–stimulated splenocytes isolated from vaccinated mice. Some reports suggest that multifunctionality, defined by the ability to simultaneously produce multiple cytokines (mostly IFN-γ, TNF and IL-2) or multiple effector molecules, as a marker of protective CD8 T cells and possibly CD4 T cells as well (Caccamo et al., 2006; Darrah et al., 2007; Derrick et al., 2011). We may be able to better understand the protection upon inducible lysis by analyzing the single, double and multiple cytokine producers among CD8 and CD4 T cells. It will also be informative to directly profile the memory T cell populations in the vaccinated hosts, especially the tissue-resident memory T cells which have been recently appreciated as a favorable target for efficacious vaccination (Gebhardt et al., 2009; Perdomo et al., 2016).

Lastly, if the inducible lysis strain outperforms BCG and current TB vaccine candidates in TB animal models, we will improve its safety toward human use

by incorporating other independent regulatory and killing mechanisms. For example, we are considering introducing the inducible lysis system to auxotroph *Mtb* strains that require supplementation of unnatural amino acid for survival. Alternatively, applying this system to generate better and safer BCG-based priming vaccines may represent another attractive option.

3.6. Materials and Methods

Strains, media and culture conditions

Wild type *Mtb* (H37Rv) and the inducible lysis strains were grown in Middlebrook 7H9 medium supplemented with 0.2% glycerol, 0.05% Tween-80, 0.5% BSA, 0.2% dextrose and 0.085% NaCl or on Middlebrook 7H10 agar containing OADC (Becton Dickinson and Company) and 0.5% glycerol.

Construction of inducible lysis strains

To generate the integrase-containing single lysin strains (D29-Lys or L5-Lys), we first transformed wild type *Mtb* H37Rv with an attL5-site integration plasmid expressing either D29 or L5 phage lysin under the control of the promoter Pmyc1tetO. To generate the integrase-containing dual lysin strain (D29-L5-Lys), we also introduced a copy of L5 phage lysin integrated to the tweety site of the D29 single lysin strain. Integrase-free single and dual lysin strains were generated in a similar manner, except that these lysin plasmids did not contain integrases and were not capable of genome integration. Instead, integrases were transiently introduced to *Mtb* by co-transformation of integrase-

expressing plasmids with the integrase-free lysin plasmids. Corresponding antibiotics were added for selection when passaging the inducible lysis strains. 25 μg/ml kanamycin for D29-Lys or L5-Lys; 25 μg/ml kanamycin and 20 μg/ml streptomycin for D20-L5-Lys; 25 μg/ml zeocin for D29-Lys-ni or L5-Lys-ni; 25 μg/ml kanamycin and 25 μg/ml zeocin for D20-L5-Lys-ni. 1ug/ml atc was added to for lysin induction in all the inducible lysin strains.

Suppressor rate estimation

The suppressor rate was defined as the number of colonies recovered from plates containing atc or plates containing atc and corresponding antibiotics, divided by the numbers of colonies obtained from 7H10 plates. The colony numbers were determined 3 weeks after plating.

Bone marrow derived macrophage infection

Bone marrow derived macrophages were harvested and differentiated as previously described (Goodsmith et al., 2015; Vandal et al., 2008). Cells were seeded at 2.5 $x10^5$ /mL and infected at the indicated multiplicity of infection (MOI) with a single cell suspension of log-phase *Mtb* culture 24 hours later. We then washed the monolayers with PBS 4 hours post-infection to remove extracellular bacteria. When indicated, 1ug/ml atc or 1ug/ml rifampicin was added to the media after PBS washing. Cell were lysed with 0.5% Triton X-100 and bacteria were enumerated bacteria by plating serial dilutions on 7H10 plates. We replaced the media with fresh ones after 3 days.

Mouse infections

We infected female C57BL/6 mice (Jackson Laboratory) using an inhalation exposure system (Glas-Col) with mid-log phase *Mtb* to deliver approximately 200 bacilli per mouse. Mice received doxycycline containing mouse chow (2,000 ppm; Research Diets) starting at the indicated time-points. The antibiotics-treated group received 125ug/ml isoniazid and 15g/L pyrazinamide delivered in the drinking water. Lungs and spleens were homogenized in PBS, serially diluted and plated on 7H10 charcoal-containing agar to quantify CFU.

Measurement of cytokine production *ex vivo* and *in vivo*

For measuring cytokine production by macrophages *ex vivo*, macrophages were infected at a MOI of 5 as described above. Culture supernatant was collected 24 hr or 72 hr post infection, and passed through a 0.22 μm filter. The cytokine levels were quantified using BD OptEIA ELISA kits for mouse IL-6 or IL-12p40 (BD Biosciences) or Biolegend ELISA kit for TNF-a according to the manufacturer's instructions. For measuring cytokine levels *in vivo*, the lungs from infected mice were bead-beat to homogenize. We then passed the lung homogenate through a 0.22 μm filter and assayed with Mouse 9-Plex ProcartaPlex Immunoassay kit (Thermo Fisher) according to the manufacturer's instructions. The multiplex plate was analyzed with MAGPIX luminex instruments.

References

Aagaard, C., Hoang, T., Dietrich, J., Cardona, P.J., Izzo, A., Dolganov, G., Schoolnik, G.K., Cassidy, J.P., Billeskov, R., and Andersen, P. (2011). A multistage tuberculosis vaccine that confers efficient protection before and after exposure. Nat Med *17*, 189-194.

Akif, M., Khare, G., Tyagi, A.K., Mande, S.C., and Sardesai, A.A. (2008). Functional studies of multiple thioredoxins from Mycobacterium tuberculosis. J Bacteriol *190*, 7087-7095.

Akif, M., Suhre, K., Verma, C., and Mande, S.C. (2005). Conformational flexibility of Mycobacterium tuberculosis thioredoxin reductase: crystal structure and normal-mode analysis. Acta Crystallogr D Biol Crystallogr *61*, 1603-1611.

Andersen, P., Askgaard, D., Ljungqvist, L., Bennedsen, J., and Heron, I. (1991). Proteins released from Mycobacterium tuberculosis during growth. Infect Immun *59*, 1905-1910.

Arbues, A., Aguilo, J.I., Gonzalo-Asensio, J., Marinova, D., Uranga, S., Puentes, E., Fernandez, C., Parra, A., Cardona, P.J., Vilaplana, C.*, et al.* (2013). Construction, characterization and preclinical evaluation of *MTB*VAC, the first live-attenuated M. tuberculosis-based vaccine to enter clinical trials. Vaccine *31*, 4867-4873.

Aronson, N.E., Santosham, M., Comstock, G.W., Howard, R.S., Moulton, L.H., Rhoades, E.R., and Harrison, L.H. (2004). Long-term efficacy of BCG vaccine in American Indians and Alaska Natives: A 60-year follow-up study. JAMA *291*, 2086-2091.

Attarian, R., Bennie, C., Bach, H., and Av-Gay, Y. (2009). Glutathione disulfide and S-nitrosoglutathione detoxification by Mycobacterium tuberculosis thioredoxin system. FEBS Lett *583*, 3215-3220.

Babu, S., Bhat, S.Q., Kumar, N.P., Jayantasri, S., Rukmani, S., Kumaran, P., Gopi, P.G., Kolappan, C., Kumaraswami, V., and Nutman, T.B. (2009). Human type 1 and 17 responses in latent tuberculosis are modulated by coincident filarial infection through cytotoxic T lymphocyte antigen-4 and programmed death-1. J Infect Dis *200*, 288-298.

Barry, C.E., 3rd, Boshoff, H.I., Dartois, V., Dick, T., Ehrt, S., Flynn, J., Schnappinger, D., Wilkinson, R.J., and Young, D. (2009). The spectrum of latent tuberculosis: rethinking the biology and intervention strategies. Nat Rev Microbiol *7*, 845-855.

Behar, S.M., Dascher, C.C., Grusby, M.J., Wang, C.R., and Brenner, M.B. (1999). Susceptibility of mice deficient in CD1D or TAP1 to infection with Mycobacterium tuberculosis. J Exp Med *189*, 1973-1980.

Behr, M.A., Wilson, M.A., Gill, W.P., Salamon, H., Schoolnik, G.K., Rane, S., and Small, P.M. (1999). Comparative genomics of BCG vaccines by whole-genome DNA microarray. Science *284*, 1520-1523.

Berry, M.P., Graham, C.M., McNab, F.W., Xu, Z., Bloch, S.A., Oni, T., Wilkinson, K.A., Banchereau, R., Skinner, J., Wilkinson, R.J.*, et al.* (2010). An interferon-inducible neutrophil-driven blood transcriptional signature in human tuberculosis. Nature *466*, 973-977.

Betts, J.C., Lukey, P.T., Robb, L.C., McAdam, R.A., and Duncan, K. (2002). Evaluation of a nutrient starvation model of Mycobacterium tuberculosis persistence by gene and protein expression profiling. Mol Microbiol *43*, 717-731.

Bhat, S.A., Singh, N., Trivedi, A., Kansal, P., Gupta, P., and Kumar, A. (2012). The mechanism of redox sensing in Mycobacterium tuberculosis. Free Radic Biol Med *53*, 1625-1641.

Bhatt, K., Hickman, S.P., and Salgame, P. (2004). Cutting edge: a new approach to modeling early lung immunity in murine tuberculosis. J Immunol *172*, 2748-2751.

Botha, T., and Ryffel, B. (2002). Reactivation of latent tuberculosis by an inhibitor of inducible nitric oxide synthase in an aerosol murine model. Immunology *107*, 350-357.

Botha, T., and Ryffel, B. (2003). Reactivation of latent tuberculosis infection in TNF-deficient mice. J Immunol *171*, 3110-3118.

Brandt, L., Feino Cunha, J., Weinreich Olsen, A., Chilima, B., Hirsch, P., Appelberg, R., and Andersen, P. (2002). Failure of the Mycobacterium bovis BCG vaccine: some species of environmental mycobacteria block multiplication of BCG and induction of protective immunity to tuberculosis. Infect Immun *70*, 672-678.

Braunstein, M., Espinosa, B.J., Chan, J., Belisle, J.T., and Jacobs, W.R., Jr. (2003). SecA2 functions in the secretion of superoxide dismutase A and in the virulence of Mycobacterium tuberculosis. Mol Microbiol *48*, 453-464.

Brosch, R., Gordon, S.V., Garnier, T., Eiglmeier, K., Frigui, W., Valenti, P., Dos Santos, S., Duthoy, S., Lacroix, C., Garcia-Pelayo, C.*, et al.* (2007). Genome plasticity of BCG and impact on vaccine efficacy. Proc Natl Acad Sci U S A *104*, 5596-5601.

Bryk, R., Griffin, P., and Nathan, C. (2000). Peroxynitrite reductase activity of bacterial peroxiredoxins. Nature *407*, 211-215.

Bryk, R., Lima, C.D., Erdjument-Bromage, H., Tempst, P., and Nathan, C. (2002). Metabolic enzymes of mycobacteria linked to antioxidant defense by a thioredoxin-like protein. Science *295*, 1073-1077.

Buchmeier, N.A., Newton, G.L., and Fahey, R.C. (2006). A mycothiol synthase mutant of Mycobacterium tuberculosis has an altered thiol-disulfide content and limited tolerance to stress. J Bacteriol *188*, 6245-6252.

Bustamante, J., Arias, A.A., Vogt, G., Picard, C., Galicia, L.B., Prando, C., Grant, A.V., Marchal, C.C., Hubeau, M., Chapgier, A.*, et al.* (2011). Germline CYBB mutations that selectively affect macrophages in kindreds with X-linked predisposition to tuberculous mycobacterial disease. Nat Immunol *12*, 213-221.

Caccamo, N., Guggino, G., Meraviglia, S., Gelsomino, G., Di Carlo, P., Titone, L., Bocchino, M., Galati, D., Matarese, A., Nouta, J.*, et al.* (2009). Analysis of Mycobacterium tuberculosis-specific CD8 T-cells in patients with active tuberculosis and in individuals with latent infection. PLoS One *4*, e5528.

Caccamo, N., Meraviglia, S., La Mendola, C., Guggino, G., Dieli, F., and Salerno, A. (2006). Phenotypical and functional analysis of memory and effector human CD8 T cells specific for mycobacterial antigens. J Immunol *177*, 1780-1785.

Cambier, C.J., Takaki, K.K., Larson, R.P., Hernandez, R.E., Tobin, D.M., Urdahl, K.B., Cosma, C.L., and Ramakrishnan, L. (2014). Mycobacteria manipulate macrophage recruitment through coordinated use of membrane lipids. Nature *505*, 218-222.

Carmel-Harel, O., and Storz, G. (2000). Roles of the glutathione- and thioredoxin-dependent reduction systems in the Escherichia coli and

saccharomyces cerevisiae responses to oxidative stress. Annu Rev Microbiol *54*, 439-461.

Casanova, J.L., Abel, L., and Quintana-Murci, L. (2013). Immunology taught by human genetics. Cold Spring Harb Symp Quant Biol *78*, 157-172.

Chan, J., Tanaka, K., Carroll, D., Flynn, J., and Bloom, B.R. (1995). Effects of nitric oxide synthase inhibitors on murine infection with Mycobacterium tuberculosis. Infect Immun *63*, 736-740.

Chan, J., Xing, Y., Magliozzo, R.S., and Bloom, B.R. (1992). Killing of virulent Mycobacterium tuberculosis by reactive nitrogen intermediates produced by activated murine macrophages. J Exp Med *175*, 1111-1122.

Chen, L., Xie, Q.W., and Nathan, C. (1998). Alkyl hydroperoxide reductase subunit C (AhpC) protects bacterial and human cells against reactive nitrogen intermediates. Mol Cell *1*, 795-805.

Choi, H.S., Rai, P.R., Chu, H.W., Cool, C., and Chan, E.D. (2002). Analysis of nitric oxide synthase and nitrotyrosine expression in human pulmonary tuberculosis. Am J Respir Crit Care Med *166*, 178-186.

Colditz, G.A., Berkey, C.S., Mosteller, F., Brewer, T.F., Wilson, M.E., Burdick, E., and Fineberg, H.V. (1995). The efficacy of bacillus Calmette-Guerin vaccination of newborns and infants in the prevention of tuberculosis: meta-analyses of the published literature. Pediatrics *96*, 29-35.

Colditz, G.A., Brewer, T.F., Berkey, C.S., Wilson, M.E., Burdick, E., Fineberg, H.V., and Mosteller, F. (1994). Efficacy of BCG vaccine in the prevention of tuberculosis. Meta-analysis of the published literature. JAMA *271*, 698-702.

Collins, A.C., Cai, H., Li, T., Franco, L.H., Li, X.D., Nair, V.R., Scharn, C.R., Stamm, C.E., Levine, B., Chen, Z.J.*, et al.* (2015). Cyclic GMP-AMP Synthase Is an Innate Immune DNA Sensor for Mycobacterium tuberculosis. Cell Host Microbe *17*, 820-828.

Comas, I., Coscolla, M., Luo, T., Borrell, S., Holt, K.E., Kato-Maeda, M., Parkhill, J., Malla, B., Berg, S., Thwaites, G.*, et al.* (2013). Out-of-Africa migration and Neolithic coexpansion of Mycobacterium tuberculosis with modern humans. Nat Genet *45*, 1176-1182.

Cooper, A.M., Dalton, D.K., Stewart, T.A., Griffin, J.P., Russell, D.G., and Orme, I.M. (1993). Disseminated tuberculosis in interferon gamma gene-disrupted mice. J Exp Med *178*, 2243-2247.

Cooper, A.M., Kipnis, A., Turner, J., Magram, J., Ferrante, J., and Orme, I.M. (2002). Mice lacking bioactive IL-12 can generate protective, antigen-specific cellular responses to mycobacterial infection only if the IL-12 p40 subunit is present. J Immunol *168*, 1322-1327.

Cooper, A.M., Magram, J., Ferrante, J., and Orme, I.M. (1997). Interleukin 12 (IL-12) is crucial to the development of protective immunity in mice intravenously infected with mycobacterium tuberculosis. J Exp Med *186*, 39-45.

Cooper, A.M., Segal, B.H., Frank, A.A., Holland, S.M., and Orme, I.M. (2000). Transient loss of resistance to pulmonary tuberculosis in p47(phox-/-) mice. Infect Immun *68*, 1231-1234.

Coulombe, F., Divangahi, M., Veyrier, F., de Leseleuc, L., Gleason, J.L., Yang, Y., Kelliher, M.A., Pandey, A.K., Sassetti, C.M., Reed, M.B.*, et al.* (2009). Increased NOD2-mediated recognition of N-glycolyl muramyl dipeptide. J Exp Med *206*, 1709-1716.

Cruz, A., Fraga, A.G., Fountain, J.J., Rangel-Moreno, J., Torrado, E., Saraiva, M., Pereira, D.R., Randall, T.D., Pedrosa, J., Cooper, A.M.*, et al.* (2010). Pathological role of interleukin 17 in mice subjected to repeated BCG vaccination after infection with Mycobacterium tuberculosis. J Exp Med *207*, 1609-1616.

Daniel, T.M. (2006). The history of tuberculosis. Respir Med *100*, 1862-1870.

Darrah, P.A., Patel, D.T., De Luca, P.M., Lindsay, R.W., Davey, D.F., Flynn, B.J., Hoff, S.T., Andersen, P., Reed, S.G., Morris, S.L.*, et al.* (2007). Multifunctional TH1 cells define a correlate of vaccine-mediated protection against Leishmania major. Nat Med *13*, 843-850.

Davis, J.M., and Ramakrishnan, L. (2009). The role of the granuloma in expansion and dissemination of early tuberculous infection. Cell *136*, 37-49.

Derrick, S.C., Yabe, I.M., Yang, A., and Morris, S.L. (2011). Vaccine-induced anti-tuberculosis protective immunity in mice correlates with the magnitude and quality of multifunctional CD4 T cells. Vaccine *29*, 2902-2909.

Desel, C., Dorhoi, A., Bandermann, S., Grode, L., Eisele, B., and Kaufmann, S.H. (2011). Recombinant BCG DeltaureC hly+ induces superior protection over parental BCG by stimulating a balanced combination of type 1 and type 17 cytokine responses. J Infect Dis *204*, 1573-1584.

Divangahi, M., Desjardins, D., Nunes-Alves, C., Remold, H.G., and Behar, S.M. (2010). Eicosanoid pathways regulate adaptive immunity to Mycobacterium tuberculosis. Nat Immunol *11*, 751-758.

Divangahi, M., Mostowy, S., Coulombe, F., Kozak, R., Guillot, L., Veyrier, F., Kobayashi, K.S., Flavell, R.A., Gros, P., and Behr, M.A. (2008). NOD2-deficient mice have impaired resistance to Mycobacterium tuberculosis infection through defective innate and adaptive immunity. J Immunol *181*, 7157-7165.

Dussurget, O., Stewart, G., Neyrolles, O., Pescher, P., Young, D., and Marchal, G. (2001). Role of Mycobacterium tuberculosis copper-zinc superoxide dismutase. Infect Immun *69*, 529-533.

Edwards, K.M., Cynamon, M.H., Voladri, R.K., Hager, C.C., DeStefano, M.S., Tham, K.T., Lakey, D.L., Bochan, M.R., and Kernodle, D.S. (2001). Iron-cofactored superoxide dismutase inhibits host responses to Mycobacterium tuberculosis. Am J Respir Crit Care Med *164*, 2213-2219.

Egen, J.G., Rothfuchs, A.G., Feng, C.G., Horwitz, M.A., Sher, A., and Germain, R.N. (2011). Intravital imaging reveals limited antigen presentation and T cell effector function in mycobacterial granulomas. Immunity *34*, 807-819.

Entenza, J.M., Loeffler, J.M., Grandgirard, D., Fischetti, V.A., and Moreillon, P. (2005). Therapeutic effects of bacteriophage Cpl-1 lysin against Streptococcus pneumoniae endocarditis in rats. Antimicrob Agents Chemother *49*, 4789-4792.

Eum, S.Y., Kong, J.H., Hong, M.S., Lee, Y.J., Kim, J.H., Hwang, S.H., Cho, S.N., Via, L.E., and Barry, C.E., 3rd (2010). Neutrophils are the predominant infected phagocytic cells in the airways of patients with active pulmonary TB. Chest *137*, 122-128.

Farinacci, M., Weber, S., and Kaufmann, S.H. (2012). The recombinant tuberculosis vaccine rBCG DeltaureC::hly(+) induces apoptotic vesicles for improved priming of CD4(+) and CD8(+) T cells. Vaccine *30*, 7608-7614.

Favrot, L., Grzegorzewicz, A.E., Lajiness, D.H., Marvin, R.K., Boucau, J., Isailovic, D., Jackson, M., and Ronning, D.R. (2013). Mechanism of inhibition of Mycobacterium tuberculosis antigen 85 by ebselen. Nat Commun *4*, 2748.

Favrot, L., Lajiness, D.H., and Ronning, D.R. (2014). Inactivation of the Mycobacterium tuberculosis antigen 85 complex by covalent, allosteric inhibitors. J Biol Chem *289*, 25031-25040.

Feng, C.G., Jankovic, D., Kullberg, M., Cheever, A., Scanga, C.A., Hieny, S., Caspar, P., Yap, G.S., and Sher, A. (2005). Maintenance of pulmonary Th1 effector function in chronic tuberculosis requires persistent IL-12 production. J Immunol *174*, 4185-4192.

Firmani, M.A., and Riley, L.W. (2002). Reactive nitrogen intermediates have a bacteriostatic effect on Mycobacterium tuberculosis in vitro. J Clin Microbiol *40*, 3162-3166.

Flynn, J.L., Chan, J., Triebold, K.J., Dalton, D.K., Stewart, T.A., and Bloom, B.R. (1993). An essential role for interferon gamma in resistance to Mycobacterium tuberculosis infection. J Exp Med *178*, 2249-2254.

Flynn, J.L., Goldstein, M.M., Chan, J., Triebold, K.J., Pfeffer, K., Lowenstein, C.J., Schreiber, R., Mak, T.W., and Bloom, B.R. (1995). Tumor necrosis factor-alpha is required in the protective immune response against Mycobacterium tuberculosis in mice. Immunity *2*, 561-572.

Flynn, J.L., Goldstein, M.M., Triebold, K.J., Koller, B., and Bloom, B.R. (1992). Major histocompatibility complex class I-restricted T cells are required for resistance to Mycobacterium tuberculosis infection. Proc Natl Acad Sci U S A *89*, 12013-12017.

Gallegos, A.M., Pamer, E.G., and Glickman, M.S. (2008). Delayed protection by ESAT-6-specific effector CD4+ T cells after airborne M. tuberculosis infection. J Exp Med *205*, 2359-2368.

Gallegos, A.M., van Heijst, J.W., Samstein, M., Su, X., Pamer, E.G., and Glickman, M.S. (2011). A gamma interferon independent mechanism of CD4 T cell mediated control of M. tuberculosis infection in vivo. PLoS Pathog *7*, e1002052.

Gandotra, S., Jang, S., Murray, P.J., Salgame, P., and Ehrt, S. (2007). Nucleotide-binding oligomerization domain protein 2-deficient mice control infection with Mycobacterium tuberculosis. Infect Immun *75*, 5127-5134.

Garcon, N., and Van Mechelen, M. (2011). Recent clinical experience with vaccines using MPL- and QS-21-containing adjuvant systems. Expert Rev Vaccines *10*, 471-486.

Gebhardt, T., Wakim, L.M., Eidsmo, L., Reading, P.C., Heath, W.R., and Carbone, F.R. (2009). Memory T cells in nonlymphoid tissue that provide enhanced local immunity during infection with herpes simplex virus. Nat Immunol *10*, 524-530.

Gold, M.C., Cerri, S., Smyk-Pearson, S., Cansler, M.E., Vogt, T.M., Delepine, J., Winata, E., Swarbrick, G.M., Chua, W.J., Yu, Y.Y.*, et al.* (2010). Human mucosal associated invariant T cells detect bacterially infected cells. PLoS Biol *8*, e1000407.

Goodsmith, N., Guo, X.V., Vandal, O.H., Vaubourgeix, J., Wang, R., Botella, H., Song, S., Bhatt, K., Liba, A., Salgame, P.*, et al.* (2015). Disruption of an M. tuberculosis membrane protein causes a magnesium-dependent cell division defect and failure to persist in mice. PLoS Pathog *11*, e1004645.

Grace, P.S., and Ernst, J.D. (2016). Suboptimal Antigen Presentation Contributes to Virulence of Mycobacterium tuberculosis In Vivo. J Immunol *196*, 357-364.

Green, A.M., Difazio, R., and Flynn, J.L. (2013). IFN-gamma from CD4 T cells is essential for host survival and enhances CD8 T cell function during Mycobacterium tuberculosis infection. J Immunol *190*, 270-277.

Griffiths, K.L., Ahmed, M., Das, S., Gopal, R., Horne, W., Connell, T.D., Moynihan, K.D., Kolls, J.K., Irvine, D.J., Artyomov, M.N.*, et al.* (2016). Targeting dendritic cells to accelerate T-cell activation overcomes a bottleneck in tuberculosis vaccine efficacy. Nat Commun *7*, 13894.

Grode, L., Seiler, P., Baumann, S., Hess, J., Brinkmann, V., Nasser Eddine, A., Mann, P., Goosmann, C., Bandermann, S., Smith, D.*, et al.* (2005). Increased vaccine efficacy against tuberculosis of recombinant Mycobacterium bovis bacille Calmette-Guerin mutants that secrete listeriolysin. J Clin Invest *115*, 2472-2479.

Gromer, S., Arscott, L.D., Williams, C.H., Jr., Schirmer, R.H., and Becker, K. (1998). Human placenta thioredoxin reductase. Isolation of the selenoenzyme, steady state kinetics, and inhibition by therapeutic gold compounds. J Biol Chem *273*, 20096-20101.

Han, S., Kim, K., Kim, H., Kwon, J., Lee, Y.H., Lee, C.K., Song, Y., Lee, S.J., Ha, N., and Kim, K. (2008). Auranofin inhibits overproduction of pro-inflammatory cytokines, cyclooxygenase expression and PGE2 production in macrophages. Arch Pharm Res *31*, 67-74.

Harbut, M.B., Vilcheze, C., Luo, X., Hensler, M.E., Guo, H., Yang, B., Chatterjee, A.K., Nizet, V., Jacobs, W.R., Jr., Schultz, P.G.*, et al.* (2015). Auranofin exerts broad-spectrum bactericidal activities by targeting thiol-redox homeostasis. Proc Natl Acad Sci U S A *112*, 4453-4458.

Hatfull, G.F., Pedulla, M.L., Jacobs-Sera, D., Cichon, P.M., Foley, A., Ford, M.E., Gonda, R.M., Houtz, J.M., Hryckowian, A.J., Kelchner, V.A.*, et al.* (2006). Exploring the mycobacteriophage metaproteome: phage genomics as an educational platform. PLoS Genet *2*, e92.

Hatzios, S.K., and Bertozzi, C.R. (2011). The regulation of sulfur metabolism in Mycobacterium tuberculosis. PLoS Pathog *7*, e1002036.

Hatzios, S.K., Schelle, M.W., Newton, G.L., Sogi, K.M., Holsclaw, C.M., Fahey, R.C., and Bertozzi, C.R. (2011). The Mycobacterium tuberculosis CysQ phosphatase modulates the biosynthesis of sulfated glycolipids and bacterial growth. Bioorg Med Chem Lett *21*, 4956-4959.

Hertz, C.J., Kiertscher, S.M., Godowski, P.J., Bouis, D.A., Norgard, M.V., Roth, M.D., and Modlin, R.L. (2001). Microbial lipopeptides stimulate dendritic cell maturation via Toll-like receptor 2. J Immunol *166*, 2444-2450.

Heym, B., Alzari, P.M., Honore, N., and Cole, S.T. (1995). Missense mutations in the catalase-peroxidase gene, katG, are associated with isoniazid resistance in Mycobacterium tuberculosis. Mol Microbiol *15*, 235-245.

Hillas, P.J., del Alba, F.S., Oyarzabal, J., Wilks, A., and Ortiz De Montellano, P.R. (2000). The AhpC and AhpD antioxidant defense system of Mycobacterium tuberculosis. J Biol Chem *275*, 18801-18809.

Holscher, C., Atkinson, R.A., Arendse, B., Brown, N., Myburgh, E., Alber, G., and Brombacher, F. (2001). A protective and agonistic function of IL-12p40 in mycobacterial infection. J Immunol *167*, 6957-6966.

Horwitz, M.A., Harth, G., Dillon, B.J., and Maslesa-Galic, S. (2000). Recombinant bacillus calmette-guerin (BCG) vaccines expressing the Mycobacterium tuberculosis 30-kDa major secretory protein induce greater

protective immunity against tuberculosis than conventional BCG vaccines in a highly susceptible animal model. Proc Natl Acad Sci U S A *97*, 13853-13858.

Imlay, J.A. (2013). The molecular mechanisms and physiological consequences of oxidative stress: lessons from a model bacterium. Nat Rev Microbiol *11*, 443-454.

Jaeger, T., Budde, H., Flohe, L., Menge, U., Singh, M., Trujillo, M., and Radi, R. (2004). Multiple thioredoxin-mediated routes to detoxify hydroperoxides in Mycobacterium tuberculosis. Arch Biochem Biophys *423*, 182-191.

Jeon, K.I., Jeong, J.Y., and Jue, D.M. (2000). Thiol-reactive metal compounds inhibit NF-kappa B activation by blocking I kappa B kinase. J Immunol *164*, 5981-5989.

Jung, Y.J., LaCourse, R., Ryan, L., and North, R.J. (2002). Virulent but not avirulent Mycobacterium tuberculosis can evade the growth inhibitory action of a T helper 1-dependent, nitric oxide Synthase 2-independent defense in mice. J Exp Med *196*, 991-998.

Kagina, B.M., Abel, B., Scriba, T.J., Hughes, E.J., Keyser, A., Soares, A., Gamieldien, H., Sidibana, M., Hatherill, M., Gelderbloem, S.*, et al.* (2010). Specific T cell frequency and cytokine expression profile do not correlate with protection against tuberculosis after bacillus Calmette-Guerin vaccination of newborns. Am J Respir Crit Care Med *182*, 1073-1079.

Kashangura, R., Sena, E.S., Young, T., and Garner, P. (2015). Effects of MVA85A vaccine on tuberculosis challenge in animals: systematic review. Int J Epidemiol *44*, 1970-1981.

Kaushik, A., Makkar, N., Pandey, P., Parrish, N., Singh, U., and Lamichhane, G. (2015). Carbapenems and Rifampin Exhibit Synergy against Mycobacterium tuberculosis and Mycobacterium abscessus. Antimicrob Agents Chemother *59*, 6561-6567.

Keane, J., Gershon, S., Wise, R.P., Mirabile-Levens, E., Kasznica, J., Schwieterman, W.D., Siegel, J.N., and Braun, M.M. (2001). Tuberculosis associated with infliximab, a tumor necrosis factor alpha-neutralizing agent. N Engl J Med *345*, 1098-1104.

Khader, S.A., Bell, G.K., Pearl, J.E., Fountain, J.J., Rangel-Moreno, J., Cilley, G.E., Shen, F., Eaton, S.M., Gaffen, S.L., Swain, S.L.*, et al.* (2007). IL-23 and IL-17 in the establishment of protective pulmonary CD4+ T cell responses

after vaccination and during Mycobacterium tuberculosis challenge. Nat Immunol *8*, 369-377.

Khader, S.A., Partida-Sanchez, S., Bell, G., Jelley-Gibbs, D.M., Swain, S., Pearl, J.E., Ghilardi, N., Desauvage, F.J., Lund, F.E., and Cooper, A.M. (2006). Interleukin 12p40 is required for dendritic cell migration and T cell priming after Mycobacterium tuberculosis infection. J Exp Med *203*, 1805-1815.

Kim, J.H., O'Brien, K.M., Sharma, R., Boshoff, H.I., Rehren, G., Chakraborty, S., Wallach, J.B., Monteleone, M., Wilson, D.J., Aldrich, C.C.*, et al.* (2013). A genetic strategy to identify targets for the development of drugs that prevent bacterial persistence. Proc Natl Acad Sci U S A *110*, 19095-19100.

Kimmey, J.M., Huynh, J.P., Weiss, L.A., Park, S., Kambal, A., Debnath, J., Virgin, H.W., and Stallings, C.L. (2015). Unique role for ATG5 in neutrophil-mediated immunopathology during M. tuberculosis infection. Nature *528*, 565-569.

Kimura, A., and Kishimoto, T. (2010). IL-6: regulator of Treg/Th17 balance. Eur J Immunol *40*, 1830-1835.

Koul, A., Arnoult, E., Lounis, N., Guillemont, J., and Andries, K. (2011). The challenge of new drug discovery for tuberculosis. Nature *469*, 483-490.

Kumar, A., Farhana, A., Guidry, L., Saini, V., Hondalus, M., and Steyn, A.J. (2011). Redox homeostasis in mycobacteria: the key to tuberculosis control? Expert Rev Mol Med *13*, e39.

Kumar, P., Arora, K., Lloyd, J.R., Lee, I.Y., Nair, V., Fischer, E., Boshoff, H.I., and Barry, C.E., 3rd (2012). Meropenem inhibits D,D-carboxypeptidase activity in Mycobacterium tuberculosis. Mol Microbiol *86*, 367-381.

Lamichhane, G. (2011). Novel targets in M. tuberculosis: search for new drugs. Trends Mol Med *17*, 25-33.

Larsen, M.H., Biermann, K., Chen, B., Hsu, T., Sambandamurthy, V.K., Lackner, A.A., Aye, P.P., Didier, P., Huang, D., Shao, L.*, et al.* (2009). Efficacy and safety of live attenuated persistent and rapidly cleared Mycobacterium tuberculosis vaccine candidates in non-human primates. Vaccine *27*, 4709-4717.

Lee, M.H., and Hatfull, G.F. (1993). Mycobacteriophage L5 integrase-mediated site-specific integration in vitro. J Bacteriol *175*, 6836-6841.

Lee, M.H., Pascopella, L., Jacobs, W.R., Jr., and Hatfull, G.F. (1991). Site-specific integration of mycobacteriophage L5: integration-proficient vectors for Mycobacterium smegmatis, Mycobacterium tuberculosis, and bacille Calmette-Guerin. Proc Natl Acad Sci U S A *88*, 3111-3115.

Leemans, J.C., Juffermans, N.P., Florquin, S., van Rooijen, N., Vervoordeldonk, M.J., Verbon, A., van Deventer, S.J., and van der Poll, T. (2001). Depletion of alveolar macrophages exerts protective effects in pulmonary tuberculosis in mice. J Immunol *166*, 4604-4611.

Leimane, V., Riekstina, V., Holtz, T.H., Zarovska, E., Skripconoka, V., Thorpe, L.E., Laserson, K.F., and Wells, C.D. (2005). Clinical outcome of individualised treatment of multidrug-resistant tuberculosis in Latvia: a retrospective cohort study. Lancet *365*, 318-326.

Lin, P.L., Dietrich, J., Tan, E., Abalos, R.M., Burgos, J., Bigbee, C., Bigbee, M., Milk, L., Gideon, H.P., Rodgers, M.*, et al.* (2012). The multistage vaccine H56 boosts the effects of BCG to protect cynomolgus macaques against active tuberculosis and reactivation of latent Mycobacterium tuberculosis infection. J Clin Invest *122*, 303-314.

Lin, P.L., and Flynn, J.L. (2015). CD8 T cells and Mycobacterium tuberculosis infection. Semin Immunopathol *37*, 239-249.

Liu, N., Li, X., Huang, H., Zhao, C., Liao, S., Yang, C., Liu, S., Song, W., Lu, X., Lan, X.*, et al.* (2014). Clinically used antirheumatic agent auranofin is a proteasomal deubiquitinase inhibitor and inhibits tumor growth. Oncotarget *5*, 5453-5471.

Lu, J., and Holmgren, A. (2014). The thioredoxin antioxidant system. Free Radic Biol Med *66*, 75-87.

Lu, J., Vlamis-Gardikas, A., Kandasamy, K., Zhao, R., Gustafsson, T.N., Engstrand, L., Hoffner, S., Engman, L., and Holmgren, A. (2013). Inhibition of bacterial thioredoxin reductase: an antibiotic mechanism targeting bacteria lacking glutathione. FASEB J *27*, 1394-1403.

MacMicking, J.D., North, R.J., LaCourse, R., Mudgett, J.S., Shah, S.K., and Nathan, C.F. (1997). Identification of nitric oxide synthase as a protective locus against tuberculosis. Proc Natl Acad Sci U S A *94*, 5243-5248.

Madeira, J.M., Gibson, D.L., Kean, W.F., and Klegeris, A. (2012). The biological activity of auranofin: implications for novel treatment of diseases. Inflammopharmacology *20*, 297-306.

Manzanillo, P.S., Shiloh, M.U., Portnoy, D.A., and Cox, J.S. (2012). Mycobacterium tuberculosis activates the DNA-dependent cytosolic surveillance pathway within macrophages. Cell Host Microbe *11*, 469-480.

Martin, C., Williams, A., Hernandez-Pando, R., Cardona, P.J., Gormley, E., Bordat, Y., Soto, C.Y., Clark, S.O., Hatch, G.J., Aguilar, D.*, et al.* (2006). The live Mycobacterium tuberculosis phoP mutant strain is more attenuated than BCG and confers protective immunity against tuberculosis in mice and guinea pigs. Vaccine *24*, 3408-3419.

Martineau, A.R., Newton, S.M., Wilkinson, K.A., Kampmann, B., Hall, B.M., Nawroly, N., Packe, G.E., Davidson, R.N., Griffiths, C.J., and Wilkinson, R.J. (2007). Neutrophil-mediated innate immune resistance to mycobacteria. J Clin Invest *117*, 1988-1994.

McCune, R.M., Feldmann, F.M., Lambert, H.P., and McDermott, W. (1966a). Microbial persistence. I. The capacity of tubercle bacilli to survive sterilization in mouse tissues. J Exp Med *123*, 445-468.

McCune, R.M., Feldmann, F.M., and McDermott, W. (1966b). Microbial persistence. II. Characteristics of the sterile state of tubercle bacilli. J Exp Med *123*, 469-486.

McCune, R.M., Jr., McDermott, W., and Tompsett, R. (1956). The fate of Mycobacterium tuberculosis in mouse tissues as determined by the microbial enumeration technique. II. The conversion of tuberculous infection to the latent state by the administration of pyrazinamide and a companion drug. J Exp Med *104*, 763-802.

McCune, R.M., Jr., and Tompsett, R. (1956). Fate of Mycobacterium tuberculosis in mouse tissues as determined by the microbial enumeration technique. I. The persistence of drug-susceptible tubercle bacilli in the tissues despite prolonged antimicrobial therapy. J Exp Med *104*, 737-762.

McShane, H., Pathan, A.A., Sander, C.R., Keating, S.M., Gilbert, S.C., Huygen, K., Fletcher, H.A., and Hill, A.V. (2004). Recombinant modified vaccinia virus Ankara expressing antigen 85A boosts BCG-primed and naturally acquired antimycobacterial immunity in humans. Nat Med *10*, 1240-1244.

Mirabelli, C.K., Johnson, R.K., Sung, C.M., Faucette, L., Muirhead, K., and Crooke, S.T. (1985). Evaluation of the in vivo antitumor activity and in vitro cytotoxic properties of auranofin, a coordinated gold compound, in murine tumor models. Cancer Res *45*, 32-39.

Mishra, B.B., Lovewell, R.R., Olive, A.J., Zhang, G., Wang, W., Eugenin, E., Smith, C.M., Phuah, J.Y., Long, J.E., Dubuke, M.L.*, et al.* (2017). Nitric oxide prevents a pathogen-permissive granulocytic inflammation during tuberculosis. Nat Microbiol *2*, 17072.

Mishra, B.B., Rathinam, V.A., Martens, G.W., Martinot, A.J., Kornfeld, H., Fitzgerald, K.A., and Sassetti, C.M. (2013). Nitric oxide controls the immunopathology of tuberculosis by inhibiting NLRP3 inflammasome-dependent processing of IL-1beta. Nat Immunol *14*, 52-60.

Mogues, T., Goodrich, M.E., Ryan, L., LaCourse, R., and North, R.J. (2001). The relative importance of T cell subsets in immunity and immunopathology of airborne Mycobacterium tuberculosis infection in mice. J Exp Med *193*, 271-280.

Moliva, J.I., Turner, J., and Torrelles, J.B. (2017). Immune Responses to Bacillus Calmette-Guerin Vaccination: Why Do They Fail to Protect against Mycobacterium tuberculosis? Front Immunol *8*, 407.

Moncada, S., Palmer, R.M., and Higgs, E.A. (1991). Nitric oxide: physiology, pathophysiology, and pharmacology. Pharmacol Rev *43*, 109-142.

Muller, G., Hecht, B., Helbl, V., Hinrichs, W., Saenger, W., and Hillen, W. (1995). Characterization of non-inducible Tet repressor mutants suggests conformational changes necessary for induction. Nat Struct Biol *2*, 693-703.

Nambi, S., Long, J.E., Mishra, B.B., Baker, R., Murphy, K.C., Olive, A.J., Nguyen, H.P., Shaffer, S.A., and Sassetti, C.M. (2015). The Oxidative Stress Network of Mycobacterium tuberculosis Reveals Coordination between Radical Detoxification Systems. Cell Host Microbe *17*, 829-837.

Nandi, B., and Behar, S.M. (2011). Regulation of neutrophils by interferon-gamma limits lung inflammation during tuberculosis infection. J Exp Med *208*, 2251-2262.

Nathan, C. (2002). Inducible nitric oxide synthase in the tuberculous human lung. Am J Respir Crit Care Med *166*, 130-131.

Nathan, C., and Barry, C.E., 3rd (2015). TB drug development: immunology at the table. Immunol Rev *264*, 308-318.

Nathan, C., and Ding, A. (2010). SnapShot: Reactive Oxygen Intermediates (ROI). Cell *140*, 951-951 e952.

Nerlich, A.G., Haas, C.J., Zink, A., Szeimies, U., and Hagedorn, H.G. (1997). Molecular evidence for tuberculosis in an ancient Egyptian mummy. Lancet *350*, 1404.

Newton, G.L., Arnold, K., Price, M.S., Sherrill, C., Delcardayre, S.B., Aharonowitz, Y., Cohen, G., Davies, J., Fahey, R.C., and Davis, C. (1996). Distribution of thiols in microorganisms: mycothiol is a major thiol in most actinomycetes. J Bacteriol *178*, 1990-1995.

Ng, V.H., Cox, J.S., Sousa, A.O., MacMicking, J.D., and McKinney, J.D. (2004). Role of KatG catalase-peroxidase in mycobacterial pathogenesis: countering the phagocyte oxidative burst. Mol Microbiol *52*, 1291-1302.

Nguipdop-Djomo, P., Heldal, E., Rodrigues, L.C., Abubakar, I., and Mangtani, P. (2016). Duration of BCG protection against tuberculosis and change in effectiveness with time since vaccination in Norway: a retrospective population-based cohort study. Lancet Infect Dis *16*, 219-226.

Nicholson, S., Bonecini-Almeida Mda, G., Lapa e Silva, J.R., Nathan, C., Xie, Q.W., Mumford, R., Weidner, J.R., Calaycay, J., Geng, J., Boechat, N.*, et al.* (1996). Inducible nitric oxide synthase in pulmonary alveolar macrophages from patients with tuberculosis. J Exp Med *183*, 2293-2302.

Nordlund, P., and Reichard, P. (2006). Ribonucleotide reductases. Annu Rev Biochem *75*, 681-706.

Okada, S., Markle, J.G., Deenick, E.K., Mele, F., Averbuch, D., Lagos, M., Alzahrani, M., Al-Muhsen, S., Halwani, R., Ma, C.S.*, et al.* (2015). IMMUNODEFICIENCIES. Impairment of immunity to Candida and Mycobacterium in humans with bi-allelic RORC mutations. Science *349*, 606-613.

Okamoto Yoshida, Y., Umemura, M., Yahagi, A., O'Brien, R.L., Ikuta, K., Kishihara, K., Hara, H., Nakae, S., Iwakura, Y., and Matsuzaki, G. (2010). Essential role of IL-17A in the formation of a mycobacterial infection-induced granuloma in the lung. J Immunol *184*, 4414-4422.

Ostash, B., and Walker, S. (2005). Bacterial transglycosylase inhibitors. Curr Opin Chem Biol *9*, 459-466.

Ottenhoff, T.H., Doherty, T.M., van Dissel, J.T., Bang, P., Lingnau, K., Kromann, I., and Andersen, P. (2010). First in humans: a new molecularly defined vaccine shows excellent safety and strong induction of long-lived Mycobacterium tuberculosis-specific Th1-cell like responses. Hum Vaccin *6*, 1007-1015.

Ottenhoff, T.H., and Kaufmann, S.H. (2012). Vaccines against tuberculosis: where are we and where do we need to go? PLoS Pathog *8*, e1002607.

Pai, M., Behr, M.A., Dowdy, D., Dheda, K., Divangahi, M., Boehme, C.C., Ginsberg, A., Swaminathan, S., Spigelman, M., Getahun, H.*, et al.* (2016). Tuberculosis. Nat Rev Dis Primers *2*, 16076.

Paritala, H., and Carroll, K.S. (2013). New targets and inhibitors of mycobacterial sulfur metabolism. Infect Disord Drug Targets *13*, 85-115.

Pastagia, M., Schuch, R., Fischetti, V.A., and Huang, D.B. (2013). Lysins: the arrival of pathogen-directed anti-infectives. J Med Microbiol *62*, 1506-1516.

Patel, R.P., McAndrew, J., Sellak, H., White, C.R., Jo, H., Freeman, B.A., and Darley-Usmar, V.M. (1999). Biological aspects of reactive nitrogen species. Biochim Biophys Acta *1411*, 385-400.

Payne, K., Sun, Q., Sacchettini, J., and Hatfull, G.F. (2009). Mycobacteriophage Lysin B is a novel mycolylarabinogalactan esterase. Mol Microbiol *73*, 367-381.

Payne, K.M., and Hatfull, G.F. (2012). Mycobacteriophage endolysins: diverse and modular enzymes with multiple catalytic activities. PLoS One *7*, e34052.

Penn-Nicholson, A., Geldenhuys, H., Burny, W., van der Most, R., Day, C.L., Jongert, E., Moris, P., Hatherill, M., Ofori-Anyinam, O., Hanekom, W.*, et al.* (2015). Safety and immunogenicity of candidate vaccine M72/AS01E in adolescents in a TB endemic setting. Vaccine *33*, 4025-4034.

Perdomo, C., Zedler, U., Kuhl, A.A., Lozza, L., Saikali, P., Sander, L.E., Vogelzang, A., Kaufmann, S.H., and Kupz, A. (2016). Mucosal BCG Vaccination Induces Protective Lung-Resident Memory T Cell Populations against Tuberculosis. MBio *7*.

Piddington, D.L., Fang, F.C., Laessig, T., Cooper, A.M., Orme, I.M., and Buchmeier, N.A. (2001). Cu,Zn superoxide dismutase of Mycobacterium tuberculosis contributes to survival in activated macrophages that are generating an oxidative burst. Infect Immun *69*, 4980-4987.

Pohane, A.A., Joshi, H., and Jain, V. (2014). Molecular dissection of phage endolysin: an interdomain interaction confers host specificity in Lysin A of Mycobacterium phage D29. J Biol Chem *289*, 12085-12095.

Potian, J.A., Rafi, W., Bhatt, K., McBride, A., Gause, W.C., and Salgame, P. (2011). Preexisting helminth infection induces inhibition of innate pulmonary anti-tuberculosis defense by engaging the IL-4 receptor pathway. J Exp Med *208*, 1863-1874.

Prinz, W.A., Aslund, F., Holmgren, A., and Beckwith, J. (1997). The role of the thioredoxin and glutaredoxin pathways in reducing protein disulfide bonds in the Escherichia coli cytoplasm. J Biol Chem *272*, 15661-15667.

Puckett, S., Trujillo, C., Eoh, H., Marrero, J., Spencer, J., Jackson, M., Schnappinger, D., Rhee, K., and Ehrt, S. (2014). Inactivation of fructose-1,6-bisphosphate aldolase prevents optimal co-catabolism of glycolytic and gluconeogenic carbon substrates in Mycobacterium tuberculosis. PLoS Pathog *10*, e1004144.

Pym, A.S., Brodin, P., Majlessi, L., Brosch, R., Demangel, C., Williams, A., Griffiths, K.E., Marchal, G., Leclerc, C., and Cole, S.T. (2003). Recombinant BCG exporting ESAT-6 confers enhanced protection against tuberculosis. Nat Med *9*, 533-539.

Ralph, A.P., Waramori, G., Pontororing, G.J., Kenangalem, E., Wiguna, A., Tjitra, E., Sandjaja, Lolong, D.B., Yeo, T.W., Chatfield, M.D*., et al.* (2013a). L-arginine and vitamin D adjunctive therapies in pulmonary tuberculosis: a randomised, double-blind, placebo-controlled trial. PLoS One *8*, e70032.

Ralph, A.P., Yeo, T.W., Salome, C.M., Waramori, G., Pontororing, G.J., Kenangalem, E., Sandjaja, Tjitra, E., Lumb, R., Maguire, G.P*., et al.* (2013b). Impaired pulmonary nitric oxide bioavailability in pulmonary tuberculosis: association with disease severity and delayed mycobacterial clearance with treatment. J Infect Dis *208*, 616-626.

Rawat, M., Newton, G.L., Ko, M., Martinez, G.J., Fahey, R.C., and Av-Gay, Y. (2002). Mycothiol-deficient Mycobacterium smegmatis mutants are

hypersensitive to alkylating agents, free radicals, and antibiotics. Antimicrob Agents Chemother *46*, 3348-3355.

Reiley, W.W., Calayag, M.D., Wittmer, S.T., Huntington, J.L., Pearl, J.E., Fountain, J.J., Martino, C.A., Roberts, A.D., Cooper, A.M., Winslow, G.M.*, et al.* (2008). ESAT-6-specific CD4 T cell responses to aerosol Mycobacterium tuberculosis infection are initiated in the mediastinal lymph nodes. Proc Natl Acad Sci U S A *105*, 10961-10966.

Resende Co, T., Hirsch, C.S., Toossi, Z., Dietze, R., and Ribeiro-Rodrigues, R. (2007). Intestinal helminth co-infection has a negative impact on both anti-Mycobacterium tuberculosis immunity and clinical response to tuberculosis therapy. Clin Exp Immunol *147*, 45-52.

Ritz, D., Patel, H., Doan, B., Zheng, M., Aslund, F., Storz, G., and Beckwith, J. (2000). Thioredoxin 2 is involved in the oxidative stress response in Escherichia coli. J Biol Chem *275*, 2505-2512.

Rothchild, A.C., Jayaraman, P., Nunes-Alves, C., and Behar, S.M. (2014). iNKT cell production of GM-CSF controls Mycobacterium tuberculosis. PLoS Pathog *10*, e1003805.

Roy, A., Eisenhut, M., Harris, R.J., Rodrigues, L.C., Sridhar, S., Habermann, S., Snell, L., Mangtani, P., Adetifa, I., Lalvani, A.*, et al.* (2014). Effect of BCG vaccination against Mycobacterium tuberculosis infection in children: systematic review and meta-analysis. BMJ *349*, g4643.

Saini, V., Cumming, B.M., Guidry, L., Lamprecht, D.A., Adamson, J.H., Reddy, V.P., Chinta, K.C., Mazorodze, J.H., Glasgow, J.N., Richard-Greenblatt, M.*, et al.* (2016). Ergothioneine Maintains Redox and Bioenergetic Homeostasis Essential for Drug Susceptibility and Virulence of Mycobacterium tuberculosis. Cell Rep *14*, 572-585.

Salo, W.L., Aufderheide, A.C., Buikstra, J., and Holcomb, T.A. (1994). Identification of Mycobacterium tuberculosis DNA in a pre-Columbian Peruvian mummy. Proc Natl Acad Sci U S A *91*, 2091-2094.

Sambandamurthy, V.K., Derrick, S.C., Hsu, T., Chen, B., Larsen, M.H., Jalapathy, K.V., Chen, M., Kim, J., Porcelli, S.A., Chan, J.*, et al.* (2006). Mycobacterium tuberculosis DeltaRD1 DeltapanCD: a safe and limited replicating mutant strain that protects immunocompetent and immunocompromised mice against experimental tuberculosis. Vaccine *24*, 6309-6320.

Sambandamurthy, V.K., Wang, X., Chen, B., Russell, R.G., Derrick, S., Collins, F.M., Morris, S.L., and Jacobs, W.R., Jr. (2002). A pantothenate auxotroph of Mycobacterium tuberculosis is highly attenuated and protects mice against tuberculosis. Nat Med *8*, 1171-1174.

Samstein, M., Schreiber, H.A., Leiner, I.M., Susac, B., Glickman, M.S., and Pamer, E.G. (2013). Essential yet limited role for CCR2(+) inflammatory monocytes during Mycobacterium tuberculosis-specific T cell priming. Elife *2*, e01086.

Sassetti, C.M., Boyd, D.H., and Rubin, E.J. (2003). Genes required for mycobacterial growth defined by high density mutagenesis. Mol Microbiol *48*, 77-84.

Satti, I., Meyer, J., Harris, S.A., Manjaly Thomas, Z.R., Griffiths, K., Antrobus, R.D., Rowland, R., Ramon, R.L., Smith, M., Sheehan, S.*, et al.* (2014). Safety and immunogenicity of a candidate tuberculosis vaccine MVA85A delivered by aerosol in BCG-vaccinated healthy adults: a phase 1, double-blind, randomised controlled trial. Lancet Infect Dis *14*, 939-946.

Scanga, C.A., Bafica, A., Feng, C.G., Cheever, A.W., Hieny, S., and Sher, A. (2004). MyD88-deficient mice display a profound loss in resistance to Mycobacterium tuberculosis associated with partially impaired Th1 cytokine and nitric oxide synthase 2 expression. Infect Immun *72*, 2400-2404.

Scanga, C.A., Mohan, V.P., Joseph, H., Yu, K., Chan, J., and Flynn, J.L. (1999). Reactivation of latent tuberculosis: variations on the Cornell murine model. Infect Immun *67*, 4531-4538.

Schaberg, T., Rebhan, K., and Lode, H. (1996). Risk factors for side-effects of isoniazid, rifampin and pyrazinamide in patients hospitalized for pulmonary tuberculosis. Eur Respir J *9*, 2026-2030.

Schaible, U.E., Winau, F., Sieling, P.A., Fischer, K., Collins, H.L., Hagens, K., Modlin, R.L., Brinkmann, V., and Kaufmann, S.H. (2003). Apoptosis facilitates antigen presentation to T lymphocytes through MHC-I and CD1 in tuberculosis. Nat Med *9*, 1039-1046.

Schnappinger, D., O'Brien, K.M., and Ehrt, S. (2015). Construction of conditional knockdown mutants in mycobacteria. Methods Mol Biol *1285*, 151-175.

Schon, T., Elias, D., Moges, F., Melese, E., Tessema, T., Stendahl, O., Britton, S., and Sundqvist, T. (2003). Arginine as an adjuvant to chemotherapy improves clinical outcome in active tuberculosis. Eur Respir J *21*, 483-488.

Scott-Browne, J.P., Shafiani, S., Tucker-Heard, G., Ishida-Tsubota, K., Fontenot, J.D., Rudensky, A.Y., Bevan, M.J., and Urdahl, K.B. (2007). Expansion and function of Foxp3-expressing T regulatory cells during tuberculosis. J Exp Med *204*, 2159-2169.

Senaratne, R.H., De Silva, A.D., Williams, S.J., Mougous, J.D., Reader, J.R., Zhang, T., Chan, S., Sidders, B., Lee, D.H., Chan, J.*, et al.* (2006). 5'-Adenosinephosphosulphate reductase (CysH) protects Mycobacterium tuberculosis against free radicals during chronic infection phase in mice. Mol Microbiol *59*, 1744-1753.

Shafiani, S., Tucker-Heard, G., Kariyone, A., Takatsu, K., and Urdahl, K.B. (2010). Pathogen-specific regulatory T cells delay the arrival of effector T cells in the lung during early tuberculosis. J Exp Med *207*, 1409-1420.

Simeone, R., Bobard, A., Lippmann, J., Bitter, W., Majlessi, L., Brosch, R., and Enninga, J. (2012). Phagosomal rupture by Mycobacterium tuberculosis results in toxicity and host cell death. PLoS Pathog *8*, e1002507.

Simeone, R., Sayes, F., Song, O., Groschel, M.I., Brodin, P., Brosch, R., and Majlessi, L. (2015). Cytosolic access of Mycobacterium tuberculosis: critical impact of phagosomal acidification control and demonstration of occurrence in vivo. PLoS Pathog *11*, e1004650.

Singh, A., Crossman, D.K., Mai, D., Guidry, L., Voskuil, M.I., Renfrow, M.B., and Steyn, A.J. (2009). Mycobacterium tuberculosis WhiB3 maintains redox homeostasis by regulating virulence lipid anabolism to modulate macrophage response. PLoS Pathog *5*, e1000545.

Sousa, A.O., Mazzaccaro, R.J., Russell, R.G., Lee, F.K., Turner, O.C., Hong, S., Van Kaer, L., and Bloom, B.R. (2000). Relative contributions of distinct MHC class I-dependent cell populations in protection to tuberculosis infection in mice. Proc Natl Acad Sci U S A *97*, 4204-4208.

Springer, B., Master, S., Sander, P., Zahrt, T., McFalone, M., Song, J., Papavinasasundaram, K.G., Colston, M.J., Boettger, E., and Deretic, V. (2001). Silencing of oxidative stress response in Mycobacterium tuberculosis: expression patterns of ahpC in virulent and avirulent strains and effect of ahpC inactivation. Infect Immun *69*, 5967-5973.

Stenger, S., Hanson, D.A., Teitelbaum, R., Dewan, P., Niazi, K.R., Froelich, C.J., Ganz, T., Thoma-Uszynski, S., Melian, A., Bogdan, C.*, et al.* (1998). An antimicrobial activity of cytolytic T cells mediated by granulysin. Science *282*, 121-125.

Stewart, G.R., Boussinesq, M., Coulson, T., Elson, L., Nutman, T., and Bradley, J.E. (1999). Onchocerciasis modulates the immune response to mycobacterial antigens. Clin Exp Immunol *117*, 517-523.

Tameris, M.D., Hatherill, M., Landry, B.S., Scriba, T.J., Snowden, M.A., Lockhart, S., Shea, J.E., McClain, J.B., Hussey, G.D., Hanekom, W.A.*, et al.* (2013). Safety and efficacy of MVA85A, a new tuberculosis vaccine, in infants previously vaccinated with BCG: a randomised, placebo-controlled phase 2b trial. Lancet *381*, 1021-1028.

Tang, S., Yao, L., Hao, X., Liu, Y., Zeng, L., Liu, G., Li, M., Li, F., Wu, M., Zhu, Y.*, et al.* (2015). Clofazimine for the treatment of multidrug-resistant tuberculosis: prospective, multicenter, randomized controlled study in China. Clin Infect Dis *60*, 1361-1367.

Thangamani, S., Mohammad, H., Abushahba, M.F., Sobreira, T.J., Hedrick, V.E., Paul, L.N., and Seleem, M.N. (2016). Antibacterial activity and mechanism of action of auranofin against multi-drug resistant bacterial pathogens. Sci Rep *6*, 22571.

Thwaites, G.E., van Toorn, R., and Schoeman, J. (2013). Tuberculous meningitis: more questions, still too few answers. Lancet Neurol *12*, 999-1010.

Torrents, E. (2014). Ribonucleotide reductases: essential enzymes for bacterial life. Front Cell Infect Microbiol *4*, 52.

Trivedi, A., Singh, N., Bhat, S.A., Gupta, P., and Kumar, A. (2012). Redox biology of tuberculosis pathogenesis. Adv Microb Physiol *60*, 263-324.

Trunz, B.B., Fine, P., and Dye, C. (2006). Effect of BCG vaccination on childhood tuberculous meningitis and miliary tuberculosis worldwide: a meta-analysis and assessment of cost-effectiveness. Lancet *367*, 1173-1180.

Tullius, M.V., Harth, G., Maslesa-Galic, S., Dillon, B.J., and Horwitz, M.A. (2008). A Replication-Limited Recombinant Mycobacterium bovis BCG vaccine against tuberculosis designed for human immunodeficiency virus-positive persons is safer and more efficacious than BCG. Infect Immun *76*, 5200-5214.

Ung, K.S., and Av-Gay, Y. (2006). Mycothiol-dependent mycobacterial response to oxidative stress. FEBS Lett *580*, 2712-2716.

van der Wel, N., Hava, D., Houben, D., Fluitsma, D., van Zon, M., Pierson, J., Brenner, M., and Peters, P.J. (2007). M. tuberculosis and M. leprae translocate from the phagolysosome to the cytosol in myeloid cells. Cell *129*, 1287-1298.

van Dissel, J.T., Soonawala, D., Joosten, S.A., Prins, C., Arend, S.M., Bang, P., Tingskov, P.N., Lingnau, K., Nouta, J., Hoff, S.T.*, et al.* (2011). Ag85B-ESAT-6 adjuvanted with IC31(R) promotes strong and long-lived Mycobacterium tuberculosis specific T cell responses in volunteers with previous BCG vaccination or tuberculosis infection. Vaccine *29*, 2100-2109.

van Pinxteren, L.A., Cassidy, J.P., Smedegaard, B.H., Agger, E.M., and Andersen, P. (2000). Control of latent Mycobacterium tuberculosis infection is dependent on CD8 T cells. Eur J Immunol *30*, 3689-3698.

Vandal, O.H., Pierini, L.M., Schnappinger, D., Nathan, C.F., and Ehrt, S. (2008). A membrane protein preserves intrabacterial pH in intraphagosomal Mycobacterium tuberculosis. Nat Med *14*, 849-854.

Vilcheze, C., Av-Gay, Y., Attarian, R., Liu, Z., Hazbon, M.H., Colangeli, R., Chen, B., Liu, W., Alland, D., Sacchettini, J.C.*, et al.* (2008). Mycothiol biosynthesis is essential for ethionamide susceptibility in Mycobacterium tuberculosis. Mol Microbiol *69*, 1316-1329.

Voskuil, M.I., Visconti, K.C., and Schoolnik, G.K. (2004). Mycobacterium tuberculosis gene expression during adaptation to stationary phase and low-oxygen dormancy. Tuberculosis (Edinb) *84*, 218-227.

Waksman, S.A. (1964). The conquest of tuberculosis (Berkeley,: University of California Press).

Wang, I.N., Smith, D.L., and Young, R. (2000). Holins: the protein clocks of bacteriophage infections. Annu Rev Microbiol *54*, 799-825.

Wassermann, R., Gulen, M.F., Sala, C., Perin, S.G., Lou, Y., Rybniker, J., Schmid-Burgk, J.L., Schmidt, T., Hornung, V., Cole, S.T.*, et al.* (2015). Mycobacterium tuberculosis Differentially Activates cGAS- and Inflammasome-Dependent Intracellular Immune Responses through ESX-1. Cell Host Microbe *17*, 799-810.

Waters, W.R., Palmer, M.V., Nonnecke, B.J., Thacker, T.C., Scherer, C.F., Estes, D.M., Jacobs, W.R., Jr., Glatman-Freedman, A., and Larsen, M.H. (2007). Failure of a Mycobacterium tuberculosis DeltaRD1 DeltapanCD double deletion mutant in a neonatal calf aerosol M. bovis challenge model: comparisons to responses elicited by M. bovis bacille Calmette Guerin. Vaccine *25*, 7832-7840.

Watson, R.O., Bell, S.L., MacDuff, D.A., Kimmey, J.M., Diner, E.J., Olivas, J., Vance, R.E., Stallings, C.L., Virgin, H.W., and Cox, J.S. (2015). The Cytosolic Sensor cGAS Detects Mycobacterium tuberculosis DNA to Induce Type I Interferons and Activate Autophagy. Cell Host Microbe *17*, 811-819.

Watson, R.O., Manzanillo, P.S., and Cox, J.S. (2012). Extracellular M. tuberculosis DNA targets bacteria for autophagy by activating the host DNA-sensing pathway. Cell *150*, 803-815.

Wengenack, N.L., Jensen, M.P., Rusnak, F., and Stern, M.K. (1999). Mycobacterium tuberculosis KatG is a peroxynitritase. Biochem Biophys Res Commun *256*, 485-487.

Wieles, B., Ottenhoff, T.H., Steenwijk, T.M., Franken, K.L., de Vries, R.R., and Langermans, J.A. (1997). Increased intracellular survival of Mycobacterium smegmatis containing the Mycobacterium leprae thioredoxin-thioredoxin reductase gene. Infect Immun *65*, 2537-2541.

Williams, C.H., Arscott, L.D., Muller, S., Lennon, B.W., Ludwig, M.L., Wang, P.F., Veine, D.M., Becker, K., and Schirmer, R.H. (2000). Thioredoxin reductase two modes of catalysis have evolved. Eur J Biochem *267*, 6110-6117.

Wilson, L.G. (2005). Commentary: Medicine, population, and tuberculosis. Int J Epidemiol *34*, 521-524.

Winau, F., Weber, S., Sad, S., de Diego, J., Hoops, S.L., Breiden, B., Sandhoff, K., Brinkmann, V., Kaufmann, S.H., and Schaible, U.E. (2006). Apoptotic vesicles crossprime CD8 T cells and protect against tuberculosis. Immunity *24*, 105-117.

Witzenrath, M., Schmeck, B., Doehn, J.M., Tschernig, T., Zahlten, J., Loeffler, J.M., Zemlin, M., Muller, H., Gutbier, B., Schutte, H.*, et al.* (2009). Systemic use of the endolysin Cpl-1 rescues mice with fatal pneumococcal pneumonia. Crit Care Med *37*, 642-649.

Wolf, A.J., Desvignes, L., Linas, B., Banaiee, N., Tamura, T., Takatsu, K., and Ernst, J.D. (2008). Initiation of the adaptive immune response to Mycobacterium tuberculosis depends on antigen production in the local lymph node, not the lungs. J Exp Med *205*, 105-115.

World Health Organization (2016). Global tuberculosis report 2016.

Yang, C.S., Shin, D.M., Kim, K.H., Lee, Z.W., Lee, C.H., Park, S.G., Bae, Y.S., and Jo, E.K. (2009). NADPH oxidase 2 interaction with TLR2 is required for efficient innate immune responses to mycobacteria via cathelicidin expression. J Immunol *182*, 3696-3705.

Zahrt, T.C., and Deretic, V. (2002). Reactive nitrogen and oxygen intermediates and bacterial defenses: unusual adaptations in Mycobacterium tuberculosis. Antioxid Redox Signal *4*, 141-159.

Zhang, Y., Heym, B., Allen, B., Young, D., and Cole, S. (1992). The catalase-peroxidase gene and isoniazid resistance of Mycobacterium tuberculosis. Nature *358*, 591-593.

Zhang, Y., Lathigra, R., Garbe, T., Catty, D., and Young, D. (1991). Genetic analysis of superoxide dismutase, the 23 kilodalton antigen of Mycobacterium tuberculosis. Mol Microbiol *5*, 381-391.

Zhang, Y.J., Ioerger, T.R., Huttenhower, C., Long, J.E., Sassetti, C.M., Sacchettini, J.C., and Rubin, E.J. (2012). Global assessment of genomic regions required for growth in Mycobacterium tuberculosis. PLoS Pathog *8*, e1002946.

Zhang, Z., Hillas, P.J., and Ortiz de Montellano, P.R. (1999). Reduction of peroxides and dinitrobenzenes by Mycobacterium tuberculosis thioredoxin and thioredoxin reductase. Arch Biochem Biophys *363*, 19-26.

Zumla, A., Nahid, P., and Cole, S.T. (2013). Advances in the development of new tuberculosis drugs and treatment regimens. Nat Rev Drug Discov *12*, 388-404.